Politecnico di Torino

Department of Energy

Master degree in Energy and Nuclear Engineering

Master thesis

ARC reactor: Activation analysis of the liquid blanket and structural materials for the vacuum vessel

Supervisors:
Prof. Massimo Zucchetti
Prof. Dennis G. Whyte
Prof. Zachary Hartwig

Candidate:
Beatrice Bocci

April 2018

Sommario

La Fusione Nucleare è una delle più importanti fonti di energia sotto studio oggi giorno. Uno dei principali aspetti che la rendono interessante per i ricercatori è l'elevata quantità di energia che è possibile ottenere, la quale dal punto di vista ambientale è considerata un energia pulita e senza emissione di CO2. Nel corso degli anni diversi progetti di reattori a fusione sono stati presentati e sottoposti a studi, in particolare dal Plasma Science and Fusion Center, dipartimento del Massachussets Institute of Technology, è stato proposto un esempio di design innovativo: il reattore ARC, Affordable Robust Compact reactor.
Basato sulla reazione a fusione tra Deuterio e Trizio, gli aspetti innovativi che caratterizzano questo tipo di reattore riguardano le sue dimensioni, le quali confrontate con altri progetti come ITER e DEMO, sono notevolmente ridotte grazie all'utilizzo di nuovi superconduttori ad alta temperatura per il confinamento magnetico, i quali permettono di ridurre le dimensioni del reattore ottenendo al contempo campi magnetici elevati.
Lo scopo della seguente tesi è l'analisi dei materiali strutturali per il design del vacuum vessel, il quale è progettato come un elemento indipendente dal resto della struttura ed è posizionato tra il first-wall e il tank contenente il breeding blanket liquido, ovvero il sale fuso Fluorine Lithium Beryllium (FLiBe). Vista la sua posizione molto vicina alla camera in cui viene generato il plasma, esso è soggetto ad elevati flussi neutronici, i quali possono causare l'attivazione dei suoi materiali, con conseguenze sulla durata del componente stesso e successivi problemi nel suo smaltimento. Oltre ai materiali strutturali per il vacuum vessel anche il l'attivazione del FLiBe è stata analizzata, nei casi con e senza presenza di possibili impurità, e successivamente comparato ad un altra opzione di blanket liquido: Lithium Lead (PbLi). I codici utilizzati per lo studio dei materiali scelti sono: Monte Carlo N-Particle Transport code (MCNP) e FISPACT-II. Il primo è basato su un modello neutronico per ARC, il quale divide il reattore in diversi volumi e per ognuno di essi valuta il flusso neutronico a cui è sottoposto. FISPACT-II partendo dalla composizione in massa del materiale, dal flusso neutronico a cui è sottoposto e dal tempo di irraggiamento, permette di valutare la Specific Activity, la Dose Rate a contatto e il Decay Heat come funzioni del tempo dopo lo spegnimento del reattore. Dall'analisi dei materiali strutturali e dal confronto dei risultati si è cercato di trovare quello che presentasse buone proprietà meccaniche e bassa attivazione se sottoposto ad un elevato flusso neutronico. Lo studio finale della tesi è basato sull'applicazione dei processi di Isotopic Tailoring and Elemental substitution, in cui partendo dalla composizione base delle leghe studiate si elimina o si riduce la presenza di alcuni elementi o isotopi, che creano problemi per l'attivazione a lungo termine, e si analizza come variano i risultati delle simulazioni.

Abstract

Nowadays Nuclear Fusion Energy is one of the most important sources of energy that is under studied. One of the main advantages of this source of energy is related to the huge amount of energy that it can release, which is considered a clean and carbon free energy. During the last years different designs of fusion reactor were studied. At the Plasma Science and Fusion Center of the Massachussets Institute of Technology an innovative design was created: ARC, the Affordable Robust Compact reactor. It takes advantage of the fusion reaction between Deuterium and Tritium and the innovative aspect that characterizes this new design is the dimension, which is smaller than other fusion reactors, such as ITER and DEMO, thanks to the presence of High Temperature Superconductors for the magnetic confinement, that permit to decrease the dimension of the project and at the same time it can reach high value of magnetic field.
The main goal of this thesis is the low-activation analysis of possible structural materials for the creation of the vacuum vessel, which is designed as a single-piece placed between the first-wall and the tank that contains the breeding blanket, the Fluoride Lithium Beryllium molten salt (FLiBe). Due to its position, which is very close to the plasma chamber, where plasma is generated, the vacuum vessel is subjected to high value of neutron flux, that can activate its materials and cause the reduction on the lifetime of the component and problems for the decommissioning of the component.
The activation analysis was done even for the liquid breeder, FLiBe, both in the case with and without the presence of possible impurities; then it is compared with another option of liquid blanket: Lithium Lead (PbLi).
The codes that were used for the low-activation analysis are: Monte Carlo N-Particle Transport code (MCNP) and FISPACT-II. The first one is based on a neutronic model and for each component a certain neutron flux is evaluated, while the second permits to evaluate the Specific Activity, the contact Dose Rate and the Decay Heat as functions of the time after the shutdown of the plant.
In order to choose the "best" structural material for the vacuum vessel both mechanical and low-activation properties were considered and a final comparison between the previous three parameters is done.
The last chapter of the thesis is based on the application of Isotopic Tailoring and Elemental substitution methods, in which the composition of each alloy is analyzed and isotopes or elements that create problems for the low-activation are eliminated or reduced. After the modifications new simulations are done in order to see if those methods lead significant improvements in the final results.

I would like to thank my supervisors Prof. Zucchetti, Prof. Whyte and Prof. Hartwig for the wonderful opportunity and Brandon Sorbom for his help for my thesis.
The experience at the MIT was very useful for my personal growth, I could increase my knowledge about fusion and I worked with incredible people. I wish to the entire PSFC all the best for their future projects.

Contents

Chapter 1

Introduction to fusion energy

The following thesis is the result of a collaboration between the Energy department of Politecnico of Torino and the Plasma Science and Fusion Center of the Massachusetts Institute of Technology (MIT). The main goal is the low-activation analysis of the liquid blanket and possible structural materials for the design of the vacuum vessel of ARC reactor when they are subjected to the neutron flux. The main codes that were used for reaching the purpose are Monte Carlo N-particle Transport (MCNP) and FISPACT-II.

1.1 Fusion reaction

One of the main problems related to the 21st century is the climate change caused by the large amount of pollutants that are realised in the environment, so in order to face it new kinds of clean and efficient energy sources are studied and one of these is the fusion energy. The main fusion reactions are based on the interaction between Deuterium-Tritium, which are two isotopes of the Hydrogen, Deuterium-Deuterium and Deuterium-Helium-3. ARC reactor takes advantage from the first one, which is characterized by the highest probability of occurring at relatively lower temperature, compared to the other two fusion reactions.

$$D + T \rightarrow \alpha + n + 17.6MeV \tag{1.1}$$

It is an exothermic reaction, that releases 17.6 MeV of energy, which is divided between one neutron of 14.1 MeV and one alpha particle (a nucleus of Helium) of 3.5 MeV.

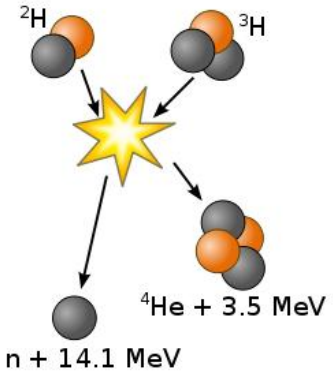

Figure 1.1: Deuterium-Tritium fusion reaction [1]

1.2 Fuel production

The Deuterium-Tritium reaction is characterised by two isotopes of Hydrogen, the first one can be obtained by water, that is abundant in nature, while the second one cannot be found in nature and its short half-life of 12.3 years [28] and its radioactivity constitute a problem for its transport, so the best solution is the production in situ. The breeding function is carried out by the blanket and for ARC's design a mixture of Fluorine-Lithium-Beryllium (FLiBe) is considered.
The presence of Lithium is fundamental for the breeding function, because from its two natural isotopes, Li^6 and Li^7, it is possible to obtain Tritium through the following reactions [2]:

$$n + Li_3^6 \rightarrow \alpha + T + n - 2.5MeV \tag{1.2}$$

$$n + Li_3^7 \rightarrow \alpha + T + 4.8MeV \tag{1.3}$$

For the evaluation of the Tritium production the parameter that is taken into account is the Tritium Breeding Ratio (TBR), which is defined as the number of Tritium produced per number of neutrons that arrive from the plasma. The formula is the following one [2]:

$$TBR = \frac{\#\text{Tritium produced}}{\#\text{neutrons from plasma}} \tag{1.4}$$

TBR must be greater than one in order to have a production of Tritium that can satisfy the request for the reactor. For reaching this goal, an enrichment of Li^6 is necessary, because it has got a cross section that permits to react with high probability with slow neutrons, while Li^7 can react with fast neutrons. In both cases Tritium is produced, but thanks to the fact that the first one is more likely to occur the enrichment of Li-6 is required and it must be at least 90%.

1.3 Plasma and tokamaks

The fusion reaction requires very high temperature, on the order of hundred millions Kelvin, in order to occur. At those temperatures atoms are completely ionized and the final "mass" of ions and electrons that is obtained is called plasma.
Plasma is an ionized gas characterised by electrons and ions that are free to move, so an important aspect for the design of a fusion reactor is related to the question : How is it possible to confine plasma?
The answer is in the using of magnetic fields, because charged particles gyrate around their lines, but not all configurations can be used for plasma confinement, so after different studies the perfect solution was found in a shaped torus called tokamak.

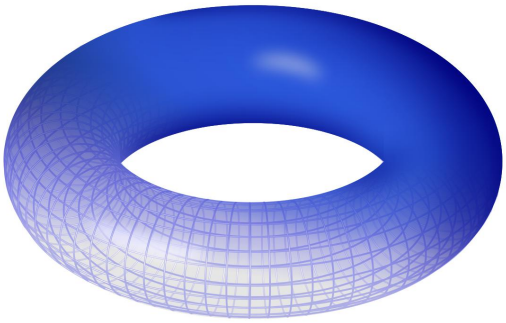

Figure 1.2: Example of torus shape for a tokamak [3]

In a tokamak magnetic field lines are both in toroidal and poloidal directions. The first one is the direction around the long way of the torus, while the second one is the direction along the short way. They are produced through the using of superconductor coils and they are used for achieving the confinement and stability of the charged particles that constitute the plasma.

Chapter 2

ARC: Affordable, Robust and Compact fusion reactor

In the following sections a brief description of ARC and its components will be done in order to understand better the parts that were analysed for the thesis (Vacuum vessel and Blanket) and why ARC can be considered a new device of a fusion reactor.

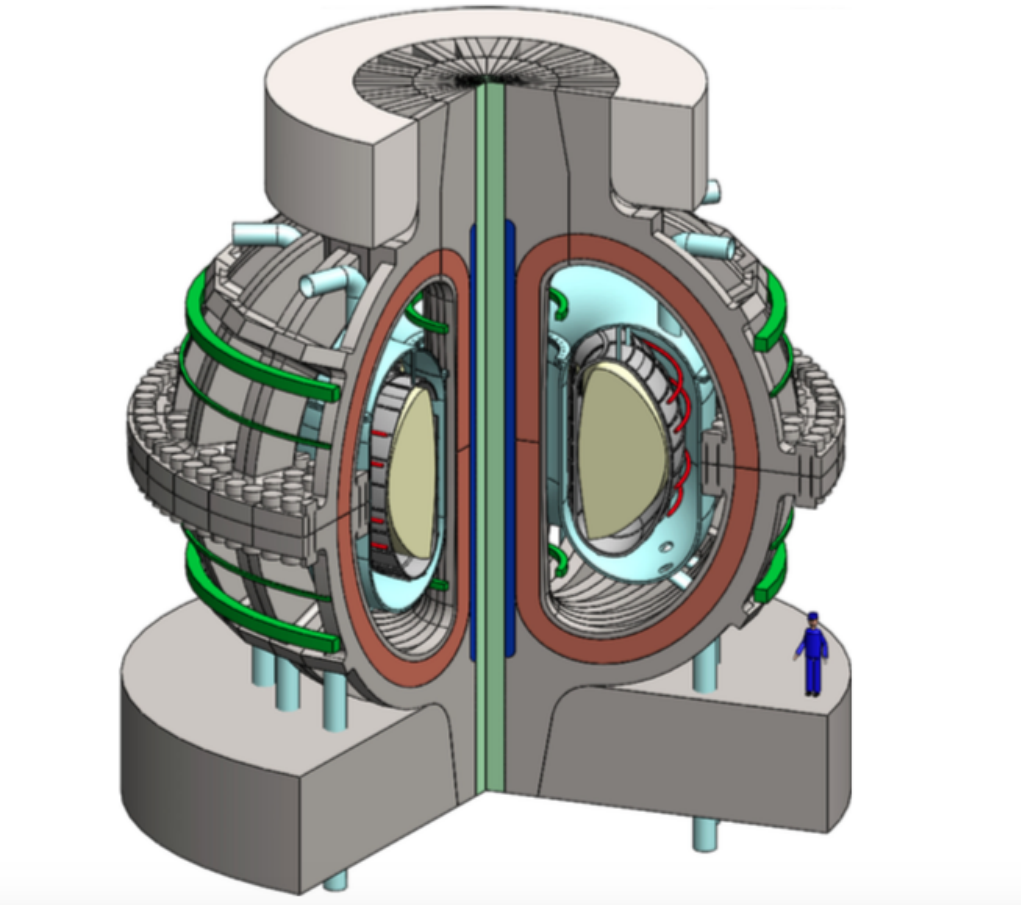

Figure 2.1: ARC reactor [4]

2.1 ARC reactor design

The Affordable Robust and Compact reactor is a tokamak designed by the researchers of the Plasma Science and Fusion Center of the Massachussets Institute of Technology. The goal of this conceptual design is to minimize the reactor size in order to reduced the cost of the plant. It is characterised by innovative details, such as the using of high temperature superconductors, that permit to obtain both high values of magnetic fields and reduce the dimensions of the tokamak, and the presence of a liquid blanket, which can be used both for the cooling and breeding functions. Another interesting aspect is the design of a single-piece vacuum vessel, that can be easily substitute after a certain period of time, and that is possible thanks to the presence of high temperature superconductors field coils that can be split in order to remove the upper part of the reactor and substitute the vacuum vessel [4].

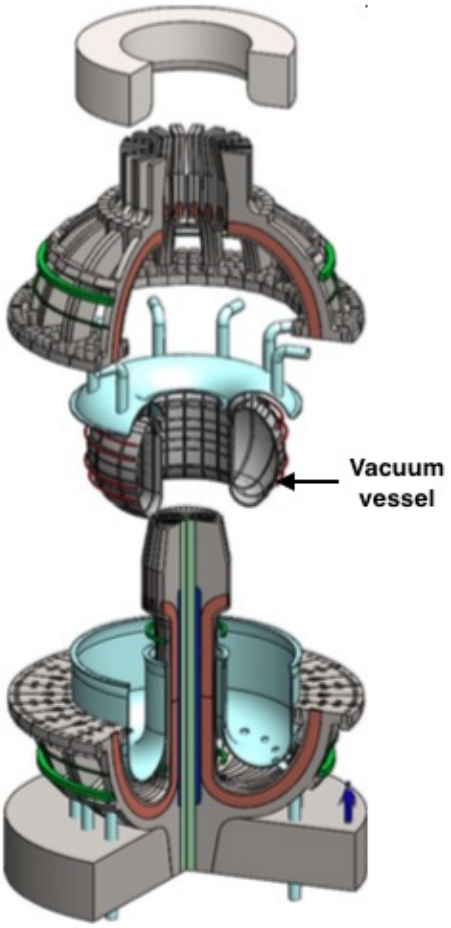

Figure 2.2: A picture of the single piece vacuum vessel [4]

The main design parameters that characterise ARC as a fusion reactor are reported in the following table:

Design parameter	Symbol	Value
Fusion power	P_f	525 MW
Total thermal power	P_{tot}	708 MW
Plant thermal efficiency	η_{elec}	0.40
Total electric power	P_e	283 MW
Net electric power	P_{net}	190 MW
LHCD coupled power	P_{LH}	25 MW
ICRF coupled power	P_{IC}	13.6 MW
Power multiplication factor	Q_e	3.0
Major radius	R_0	3.3 m
Plasma semi-minor radius	a	1.13 m
Plasma elongation	κ	1.84
Plasma volume	V_p	141 m^3
Toroidal magnetic field	B_0	9.2 T
Peak on-coil magnetic field	B_{max}	23 T
Plasma current	I_p	7.8 MA
Bootstrap fraction	f_{BS}	0.63
Tritium breeding ratio	TBR	1.1
Avg. temperature	$\langle T \rangle$	14 keV
Avg. density	$\langle n \rangle$	1.3×10^{20} m^{-3}
On-axis temperature	T_0	27 keV
On-axis density	n_0	1.8×10^{20} m^{-3}
Greenwald fraction	f_{Gr}	0.67
Toroidal beta	β_T	1.9%
Internal inductance	l_i	0.67
Normalized beta	β_N	2.59
Safety factor at $r/a = 0.95$	q_{95}	7.2
Edge safety factor	q_a	4.7
Minimum safety factor	q_{min}	3.5
Fusion power wall loading	P_f/S_b	2.5 MW/m^2
Energy confinement time	τ_E	0.64 s
H89 confinement factor	H_{89}	2.8
H98(y,2) confinement factor	$H_{98,y2}$	1.8
G89 gain factor	G_{89}	0.14

Figure 2.3: List of ARC design parameters [4]

As it is possible to see the fusion power is supposed to be 525 MW [4], which is comparable with the one that will be produced in ITER (almost 500 MW [6]), but the dimensions are smaller (Figure 2.4); the major and minor radius are respectively 3.3 m and 1.13 m in ARC [4], while for ITER are 6.2 m and 2 m [6], and the Plasma volume is 141 m3 for ARC reactor [4] and almost equal to 830 m3 in ITER [6].

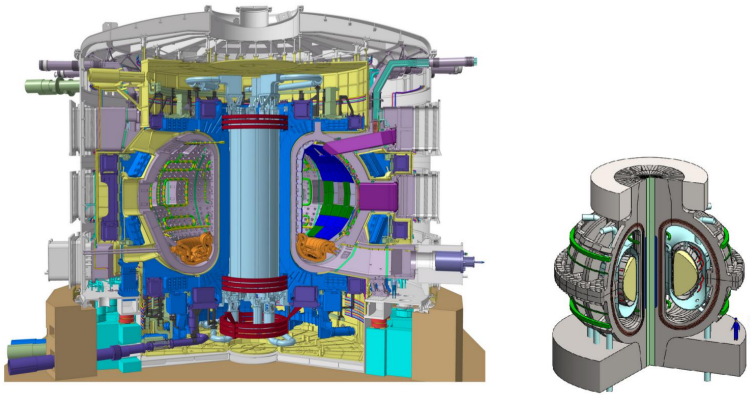

Figure 2.4: A picture created by the Plasma Science and Fusion Center of the MIT in order to compare ITER with ARC

2.2 ARC's components

The main components that characterise the design of ARC are:

- **Vacuum vessel** is a single-piece and double-walled component with the shape of a torus. It is placed between the first-wall and the tank with the breeding blanket and it contains a channel for the flowing of the liquid coolant. Its original structural material is Inconel-718, which is a Nickel based alloy characterised by high strength and corrosion resistance when it is subjected to high temperature applications. The high presence of Nickel makes the vacuum vessel prone to nuclear activation [4], which is a problem that should be solved especially for the final disposal of the component.

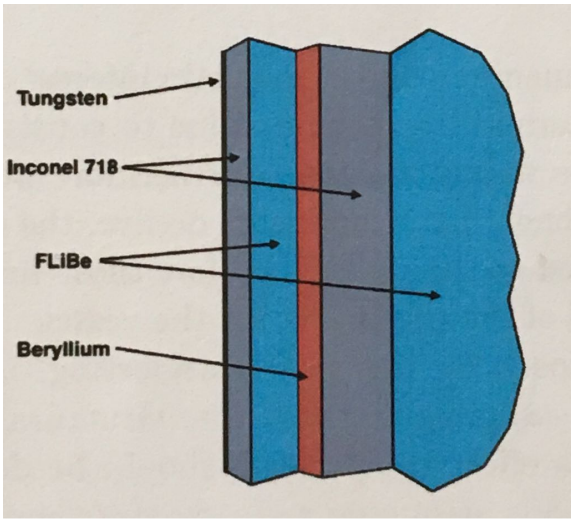

Figure 2.5: Schematic structure of vacuum vessel with first-wall and one layer of Beryllium [7]

  Beryllium is a neutron multiplier and its presence is useful in order to increase the Tritium production inside the breeder.
  Due to the position very closed to plasma's chamber, the vacuum vessel is subjected to high thermo-mechanical loads and neutron fluxes, which cause a faster deterioration of the material itself. It could be subjected to plasma disruptions, so in order to avoid problems to the entire structure of the reactor it is designed as an independent component, that can be replaced without damages to other permanent modules [4].

- **First-wall** is made with Tungsten and it is placed in the inner part of the vacuum-vessel and it faces on the plasma's chamber. It is directly subjected to high temperatures and neutron fluxes, so an important characteristic for the choice of its material is the sputtering, that is the phenomenon related to the loss of impurities from the wall when it is subjected to the interaction with the plasma charged particles. Those impurities are neutral and they don't feel the presence of the magnetic field, so when they enter in the plasma they are ionized and that process causes the loss of energy and decrease of temperature in the plasma, that could lead to the shutdown of the reactor. The presence of the divertor is the solution for the last problem.

- **Divertor** is an integrated component of the vessel and it is a solution for avoiding plasma-wall interactions phenomena. It is characterised by the presence of plates, that permit to concentrate the interactions with the plasma in a small area, then thanks to the X-shape of the magnetic field lines the path between the impurities and plasma is higher, so neutral particles can't reach the plasma easily.

- **Blanket** is important for its breeding function and in ARC a molten salt was chosen.
  The main advantage related to the using of a liquid blanket compared to a solid one is that it can satisfy both the breeding and cooling functions for the reactor.
  An innovative aspect of ARC's design is the presence of a liquid immersion blanket [4], where the percentage of solid materials is reduced and the tank is a sort of pool full of FLiBe that surrounds the entire vacuum vessel.

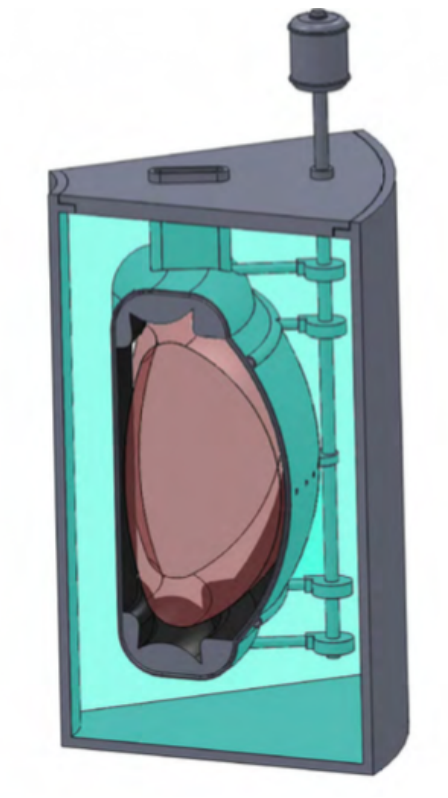

Figure 2.6: Schematic structure of the liquid immersion blanket [5]

As it was explained in the section 1.2, Tritium is the fuel for the fusion reaction and its production occurs inside the breeder. In order to be sure that enough Tritium is produced the parameter that must be controlled is the Tritium breeding ratio (TBR), which must be greater than 1 in order to sustain the entire tritium reaction cycle, in particular for ARC a TBR$\geq$ 1.1 [4] was considered in its design.

- **Cooling system** is designed in order to remove the heat produced during the operation of the reactor and avoid serious and irreparable damages to components subjected to high thermal loads. The coolant flows inside the double-walled vacuum vessel and remove the thermal energy, that will be transferred

to a turbine in order to obtain the production of electricity, which is the final aim of the fusion reactor.

- **Superconductor magnets** are extremely important for the stability and confinement of the plasma. There are three main superconductor magnets that characterize the design of a fusion reactor: Central solenoid, Toroidal field coils and Poloidal field coils. ARC reactor takes advantage of high temperature superconductor magnets, while in the case of ITER low temperature superconductors are used. The main pros related to the first ones is the possibility to reduce the dimension of the reactor and at the same time high values of magnetic fields can be produced, such as a toroidal magnetic field equals to 9.2 T [4] (Figure 2.3). Another important benefits related to the using of these kind of superconductors is the possibility to separate them for the replacement of the vacuum vessel (Figure 2.2). For the design of these modules the choice of the materials is very important, because even with the shielding of the blanket they are subjected to the neutron flux that comes from the plasma. For ARC the selected material is Rare Earth Barium Copper Oxide (REBCO), a high temperature superconductor that can work at temperature up to 80 K [4], which is higher than the one for Nb3Sn used for ITER.

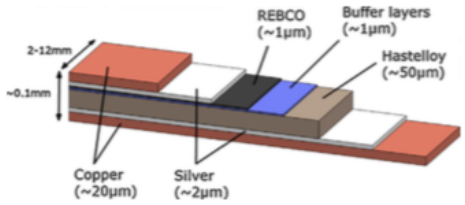

Figure 2.7: Schematic cross-section of REBCO superconductor [4]

Chapter 3

Low-activation analysis

As it was explained in the introduction, the goal of the following thesis is the selection of new feasible alloys for the design of the vacuum vessel, that must have good mechanical properties and low activation characteristics. The original material that was considered for the initial design is Inconel-718, which has got very good mechanical properties at high temperature, such as an yield stress almost equal to 1000 MPa at 900K [12] (the reference operational temperature [4]). The main problem of that alloy is related to its primary constituent, Nickel.
The neutron flux that is generated from the D-T reaction is the main responsible for the activation of the structural material of the vacuum vessel, but it is important for Tritium production and it can't be avoided, so the only possibility is the selection of specific alloys that permit to reduce that problem. Before to start the description of the activation analysis let's see the low-activation criteria that were taken into consideration for the research.

3.1 Criteria for low-activation analysis

In order to define if a material can be cleared, recycled or permanently decommissioned the criteria that were taken into account are the following ones:

- **Recycling within the nuclear industry**[9]: the reference value is 10 $[\frac{microSv}{h}]$, which is the limit below which the contact dose rate of the structural materials must decrease in order to be handled by the radiation-exposed workers.

- **Recycling outside the nuclear industry**: the value is 0.1 $[\frac{microSv}{h}]$, that is the limit value for public exposure [10].

- **Clearance Index (CI)**, which is an index that permits to verify if a material contains radioactive species above natural level and for a non-homogeneus alloy it is evaluated with the following formula [9]:

$$CI = \sum_{i=1}^{\#isotopes} \frac{A_i}{L_i} \tag{3.1}$$

  A_i and L_i are the specific activity, which is the activity per unit of mass, and the clearance limit for the i-th isotope contained in the material, which are expressed in $[\frac{Bq}{kg}]$. In order to verify if the material can be cleared and reused without any restrictions this index must be lower than 1 by 100 years of cooling after the shutdown of the reactor. In order to evaluate the clearance

index the limit values that were considered are the ones proposed by the IAEA in its report of 2004 for some main radioisotopes, which are reported in the following table [9]:

Table 3.1: Clearance limits for some nuclides encountered in fusion applications

Nuclide	**Li Bq/kg**
H3	1.00E+005
C14	1.00E+003
Na22	1.00E+002
Ca45	1.00E+005
Mn53	1.00E+005
Mn54	1.00E+002
Fe55	1.00E+006
Fe59	1.00E+003
Co58	1.00E+003
Co60	1.00E+002
Ni59	1.00E+005
Ni63	1.00E+005
Cu64	1.00E+005
Nb94	1.00E+002
Mo99	1.00E+004
Tc99	1.00E+003
Ag110m	1.00E+002
Sb125	1.00E+002
Eu152	1.00E+002
Eu154	1.00E+002
Ta182	1.00E+002
Ir192	1.00E+003
Re186	1.00E+006

- **Shallow Land Burial (SLB)** is the criteria used for the final disposal of the material, that is based on the evaluation of the waste disposal rating (WDR), which is evaluated with the following formula:

$$WDR = \sum_{i=1}^{\#isotopes} \frac{C_i}{L_i} \tag{3.2}$$

C_i is the concentration of the i-th nuclide in the waste and L_i is the concentration limit value and they are expressed in $[\frac{Bq}{cm^3}]$ [11]. It is evaluated at 100 years after the shutdown of the reactor and it must be lower than 1 in order to classify the waste as a "Low-Level waste" [29].

In Table 3.2 there is the list of the allowable limit values for long-lived nuclides, that will be considered for the evaluation of the WDR [11]:

Table 3.2: Concentration limits for WDR evaluation

Nuclide	**Li Bq/cm3**
C14	2.96E+006
Ca41	1.00E+006
Mn53	2.00E+007
Fe60	5.00E+003
Ni59	8.14E+006
Ni63	2.59E+008
Nb94	7.40E+003
Mo93	1.00E+006
Tc99	1.11E+005
Ag108m	1.00E+005
Eu150	2.00E+008
Ir192m	5.00E+004
Re186m	5.00E+005
I129	2.96E+003
Sr90	2.59E+008
Cs137	1.70E+008
Be10	4.00E+005
Al26	5.00E+003
Si32	2.00E+006
Cl36	6.00E+005
Ar39	6.00E+007
Ar42	2.60E+008
Ti44	1.00E+007
Se79	2.00E+005
Kr81	1.00E+007
Zr93	5.00E+005
Sn121m	2.60E+008
Cs135	3.00E+005
Sm151	2.00E+008
Tb158	2.00E+005
Ho166m	7.00E+003
Hf178m	2.60E+008
Pb205	1.00E+006
Bi208	5.00E+003
Bi210m	2.00E+004

For the recycling limits it is important to specify when they can be applied and the questions that should be taken into account are: Who actually uses recycled materials outside the fusion plant? Is it realistic to consider the recycling of a structural material that was exposed for years to a neutron flux? The public acceptability must be taken into account for the final answer, so for this reason it is better to consider if it can be cleared after many years of storage or the possible ways for the decommissioning of a huge quantity of radioactive material.
As regard the liquid blanket it is purified from Tritium and then it could be reused, but during the operation of the reactor it is subjected to depletion, so a part of its initial percentages of Beryllium, which is the neutron multiplier, and Lithium decrease due to neutron reactions and Tritium production, so the isotopic composition changes and there are less neutron multiplications and TBR could decreases too. In order to face this problem fresh FLiBe must be periodically added and from the economic point of view it is cheaper than substitute the entire quantity of molten salt.

3.2 Codes for activation analysis

The activation analysis was performed through the using of two different codes:

1. **Monte-Carlo N-particles transport code (MCNP)** that permits to evaluate the neutron flux, defined as $[\frac{neutrons}{cm^2 \cdot s}]$ in different regions of the reactor.

2. **FISPACT-II**, which is an activation code that calculates the specific activity, $[\frac{Bq}{kg}]$, contact dose rate, $[\frac{Sv}{h}]$, and decay heat $[\frac{kW}{kg}]$ of a material under a certain neutron flux through the using of specific libraries.

ENDF is the library that was used for the analysis, and the input data, like cross sections, were considered at the operational temperature of 900 K. The energy structure used for neutrons is "709-energy groups", with the range of neutron energy from 1.0471E-5 eV to 1.0000E+9 eV [8].The main inputs for the inventory file for FISPACT-II were the characteristics of the material, such as density, mass percentage composition, the total mass and the neutron flux (see Appendix A for the example of inventory input code file for FISPACT-II). MCNP calculation is based on a neutron model of ARC reactor, in which the main inputs are the dimensions of each region of the reactor and the mass percentage composition of each alloy that is used for the entire design. The final output file gives the results of the total mass, express in grams, the volume in cm3 and the neutron fluence, which is the total number of sources of neutrons per unit of area, for each component. In MCNP each region of the reactor is associated to a number and the ones that were considered for the study are:

1. 30: Inner part of the vacuum vessel;

2. 31: Cooling channel;

3. 34: Outer area of the vacuum vessel;

4. 40: Breeding blanket tank.

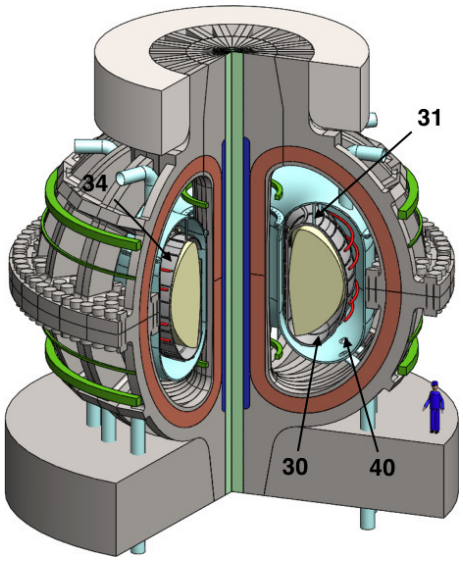

Figure 3.1: ARC's regions used for the analysis

After the evaluation through MCNP, the activation analysis can be performed with FISPACT-II and starting from the neutron fluence it is possible to obtain the neutron flux by multiplying the first one with the reaction rate equal to 1.86E+20 $[\frac{neutrons}{second}]$, which is evaluated in the following way:

$$Reaction\,rate = \frac{\frac{4}{5} \cdot P_f}{E_n} = \frac{P_n}{E_n} \tag{3.3}$$

Pf is the fusion power equals to 525 MW [4] and Pn is the neutron one, while En is the neutron energy equal to 14.1 MeV.
For this research the input neutron flux was the same for each material in order to have the same conditions for the analysis. The flux was evaluated considering the original materials of ARC reactor as inputs for MCNP: pure FLiBe as liquid blanket and Inconel-718 for the vacuum-vessel.
The final results for the neutron fluxes are 7.54E+014$\frac{neutrons}{cm^2 \cdot s}$ for the inner region of vacuum vessel, which is close to the plasma, and 5.02E+014$\frac{neutrons}{cm^2 \cdot s}$ for the region near the tank that contains the breeding blanket.
For what concern the irradiation time the expected lifetime of the vacuum vessel was considered of 2 years, then in order to have a realistic situation a pulsed mode time was used. ARC is supposed to be characterised by long pulses, which could last at least 6 months and the final goal of the design is the achievement of the steady state mode. After this step the activation analysis can be performed through FISPACT-II.

3.3 Vacuum vessel analysis: Inconel-718

The first part of the activation analysis was based on the study of Inconel-718, in order to understand if it is good or not as a low-activation material. The mass percentage composition that was considered for its study is listed in the following table [12]:

Table 3.3: Mass percentage composition of Inconel-718

Elements	**Mass % composition**
Nickel	55.00
Chromium	21.00
Iron	11.10
Niobium	5.50
Molybdenum	3.30
Titanium	0.30
Aluminium	1.15
Cobalt	1.00
Silicon	0.35
Manganese	0.35
Copper	0.80
Carbon	0.08
Phosphorus	0.015
Boron	0.006
Silicon	0.35
Sulfur	0.015

It is possible to notice the high presence of elements like Nickel, that is the primary one, Niobium and Molybdenum, which permits to do a rough evaluation of Inconel-718 and say that it will not respect the low-activation criteria, because those elements lead the production of long-lived radioactive isotopes that are activated when the material is subjected to the neutron flux. Let's see the results for the specific activity, contact dose rate and decay heat that were obtained from FISPACT-II with the conditions explained in the section 3.2. (section Tables for numerical values)

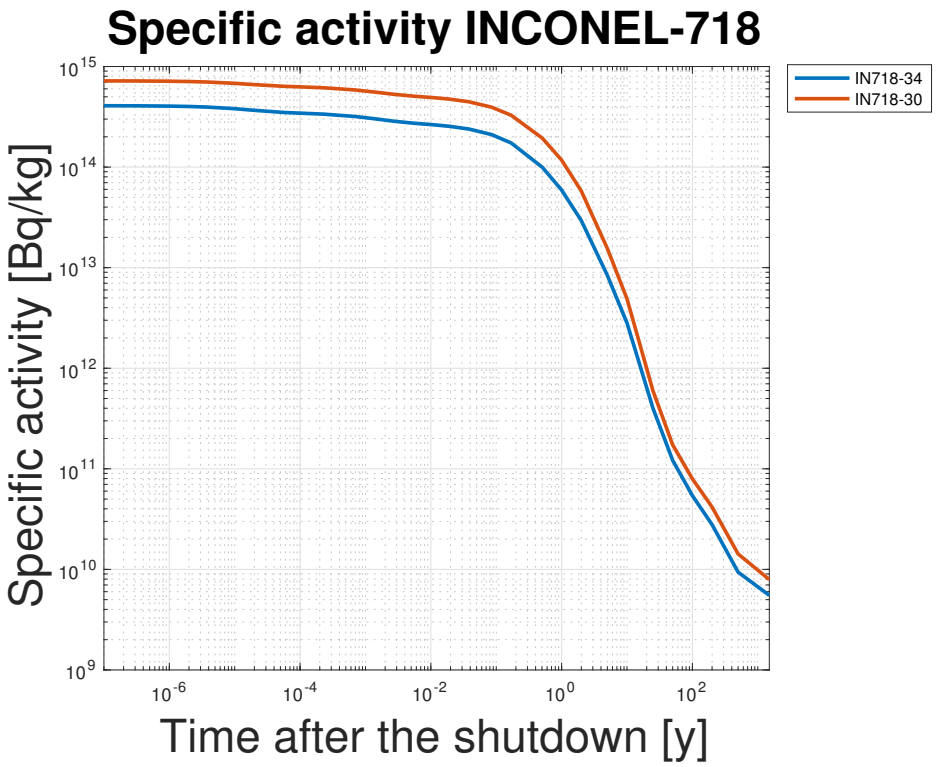

Figure 3.2: Specific activity of Inconel-718 in the inner (30) and outer (34) regions

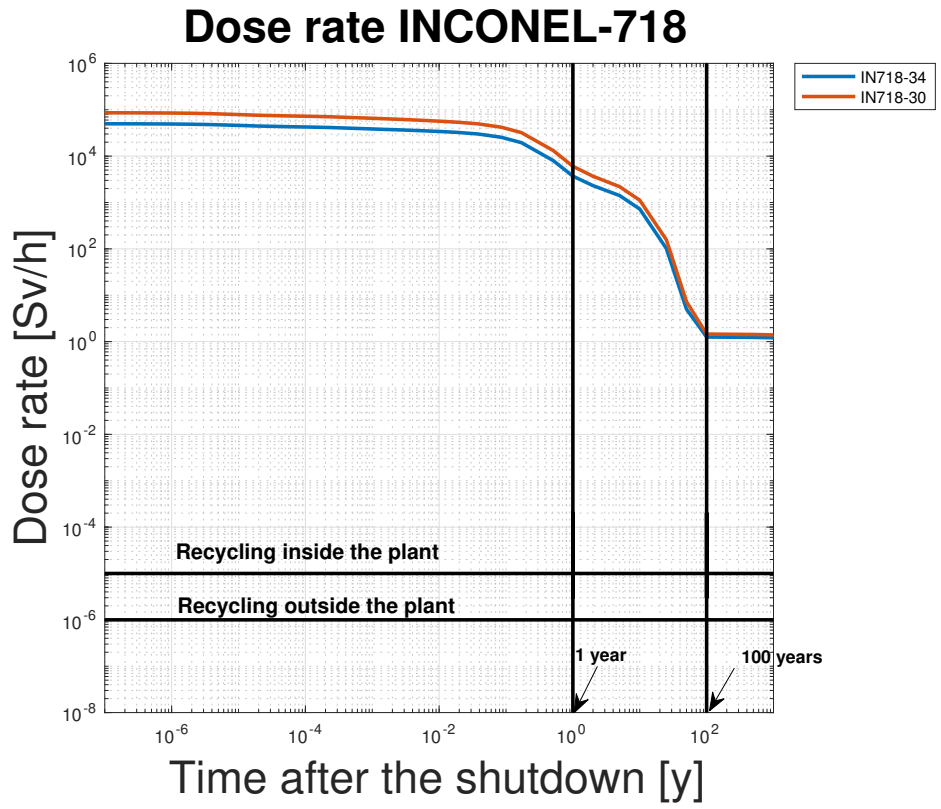

Figure 3.3: Dose rate of Inconel-718 in the inner (30) and outer (34) regions

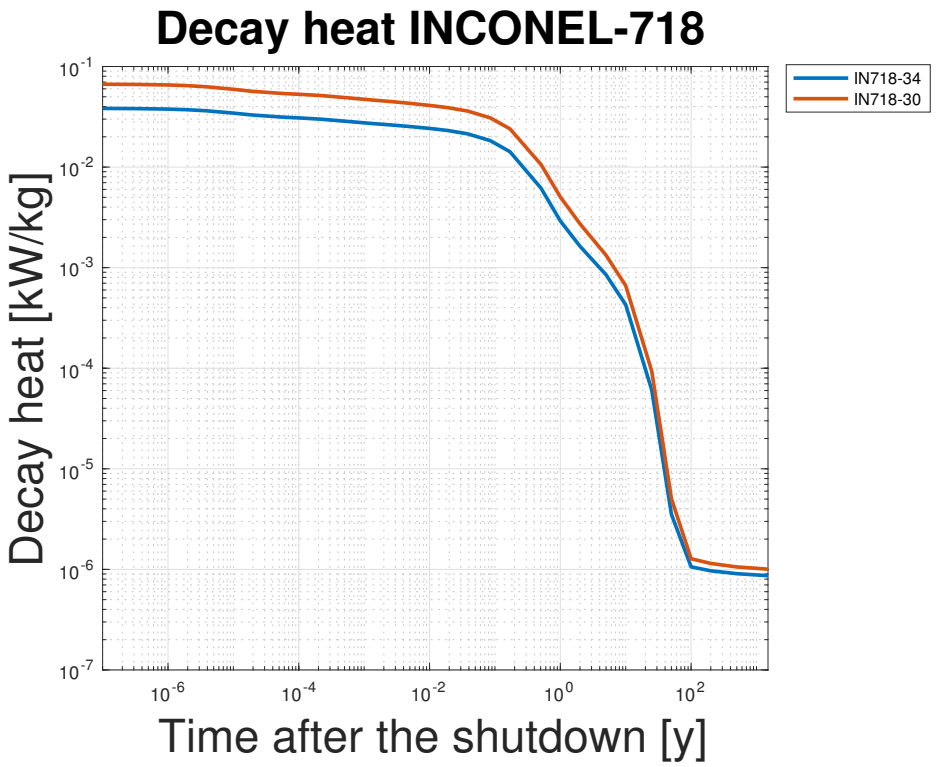

Figure 3.4: Decay heat of Inconel-718 in the inner (30) and outer (34) regions

Figure 3.3 shows the evolution in time of the contact dose rate in the inner and outer walls of the vacuum vessel and it is possible to highlight the high gap between the recycling limits and the actual values that were obtained from the activation analysis, even after 100 years from the shutdown of the reactor. This big discrepancy is mainly related to the presence of Nb-94 (half life equal 20'326 years[28]), a long lived isotope that comes from Mo-94, natural isotope of Molybdenum [22].
The decay heat immediately after the end of the operation is equal to 1.11 MW in the inner wall and 1.97 in the outer one. These values are not too high, but they decrease slow in time and this could cause problems in case of accidental scenario for the temperature evolution of the system (Chapter 6.2).
Let's see the results for the clearance and Shallow Land Burial indexes. The first one was evaluated starting from the activity of each isotopes after 100 years of storage time, that can be obtained through FISPACT-II, then it was divided by the total mass of the vacuum vessel (16.6 tonnes for the inner region and 51.4 tonnes for the outer one [4]), in order to obtain the specific activity of each isotope, that was divided by the clearance limit (Table 3.1) and the total sum was computed. The value of this index should be below the unit in order to clear and reuse the material without any restrictions. The final results for Inconel-718 are:

1. 3.81E+007 in the inner region;
2. 3.29E+007 in the outer one.

Both values are much higher than 1 and that is caused by the presence of radioactive isotopes, such as Ni-63 with half-life of 100.1 years [28], Ni-59 with half-life of 76'000 years [28], Nb-94 and Tc-99 with half-life equal 211'100 years [28], which comes from beta decay of Mo-99 [22], that is a radioactive isotopes of Molybdenum.
As regards Shallow Land Burial, the waste disposal rating was evaluated in both regions according to the procedure explained in section 3.1, but this time the concentration of the different isotopes was required, so their activities were evaluated

after 100 years from the shutdown, then they were divided by the total volume of the component, which is 2.03 m3 in the inner wall of the vacuum vessel and 6.27 m3 in the outer one [4], then the results were divided by the reference limits (Table 3.2). Finally the total sum was evaluated and the results had to be lower than 1. The final values are:

1. 4.15E+003 in the inner region;
2. 3.59E+003 in the outer one.

Even SLB criteria is not respected for the same reasons explained for the clearance index, so it is possible to confirm that it can't be directly decommissioned without any kind of interventions.
Inconel-718 is not a low-activation material and in chapter 5 Isotopic Tailoring process will be applied in order to see if the substitution of some isotopes, which cause the presence of long-lived ones, can permit to improve the results and obtain a low-activation alloy.
Inconel-718 was analysed even in the case without impurities but the final results were almost the same of the initial case, because the main problem is related to the primary and alloying elements.

3.4 Structural materials for vacuum-vessel

After having confirmed that Inconel-718 doesn't satisfy the low-activation requirements, other options of possible structural materials were chosen and analysed. The main requirements for the new alloy are:

- good mechanical properties at very high temperature, such as high value of yield stress at 900K, in order to face the high heat loads that come from the plasma;
- high melting point (greater than 1000 K);
- low activation properties.

The materials that were chosen and analysed are the following ones:

1. Vanadium-based alloy : V-15Cr-5Ti.
2. Titanium-alloy : Ti-6Al-4V.
3. Titanium-Zirconium-Molybdenum alloy (TZM).
4. Silicon Carbide (SiC), a ceramic that is supposed to be a low activation material, like the Vanadium alloy.
5. Reduced activation ferritic-martensitic (RAFM) steels: Eurofer97, that is studied for the design of DEMO reactor and the Oxide Dispersion Strenghtened (ODS) version.
6. Stainless steels 316 and 304, that are studied for fusion applications in ITER.

All the previous materials are under development for fusion applications and some of them were chosen for the presence of low-activation elements like Vanadium, Titanium and Chromium. In the following sections each of them will be analysed with and without the presence of possible undesired impurities, which come from manufacture processes, in order to understand how they influence the activation, then they will be compared with Inconel-718, in order to see which one could be a feasible choice for the construction of the vacuum-vessel.
Table 3.4 shows a comparison of the density, melting point and yield stress at 900K between Inconel-718 and the other possible options of materials.

Table 3.4: Density, range of melting temperature and yield stress at 900K of the different options of structural materials [12,13,14,15,14,21]

	Density [g/cm3]	**Melting T [K]**	**Yield stress at 900K [MPa]**
Inconel-718	8.192	1533-1609	$\simeq 980$
V-15Cr-5Ti	6.1	2153	340-350
Ti-6Al-4V	4.43	1877-1933	>800
TZM	10.22	2783-2873	635.65
SiC	3.217	3003	$\simeq 810$
Eurofer	7.798	1720-1800	$\simeq 300$
SS 316	7.96	1640-1670	112.52
SS 304	7.86	1670-1720	$\simeq 107$

3.4.1 Vanadium-based alloys

Vanadium based alloys are good candidate as structural materials for fusion applications [13], in particular V-Cr-Ti ones are characterized by the presence of Titanium the permits to increase the resistance to irradiation-induced swelling, while the presence of Chromium improves the resistance to oxidation and creep strength [13].
At the beginning of the analysis the Vanadium alloys that were chosen were V-15Cr-5Ti and V-4Cr-4Ti, but the mechanical properties of the second one weren't good enough for the design of ARC, in particular the yield stress at 900K is lower than 200 MPa [13], which made it not a feasible choice for ARC.
In this section will be shown and explained the results for the selected vanadium alloy: V-15Cr-5Ti.
Its mass percentage composition is listed in the following table [14]:

Table 3.5: Mass percentage composition of V-15Cr-5Ti with and without impurities

	V-15Cr-5Ti with impurities	**V-15Cr-5Ti without impurities**
V	80.39 %	80.5 %
Cr	14.5 %	14.5 %
Ti	5 %	5 %
N	0.0096 %	-
O	0.033 %	-
C	0.012 %	-
Si	0.04 %	-
Fe	0.02 %	-

Even if the selected Vanadium alloy hasn't got a high yield stress like Inconel-718, ARC is still a cartoon of a fusion reactor, so its design can be modified and more than one structural materials could be used for the final construction of the vacuum vessel and this particular alloy is characterised by the high percentage of Vanadium, which is considered a low-activation element that doesn't cause the production of long-lived radioactive isotopes when it interacts with neutrons.

The results of the activation analysis with FISPACT-II for Vanadium are shown in the following plots:

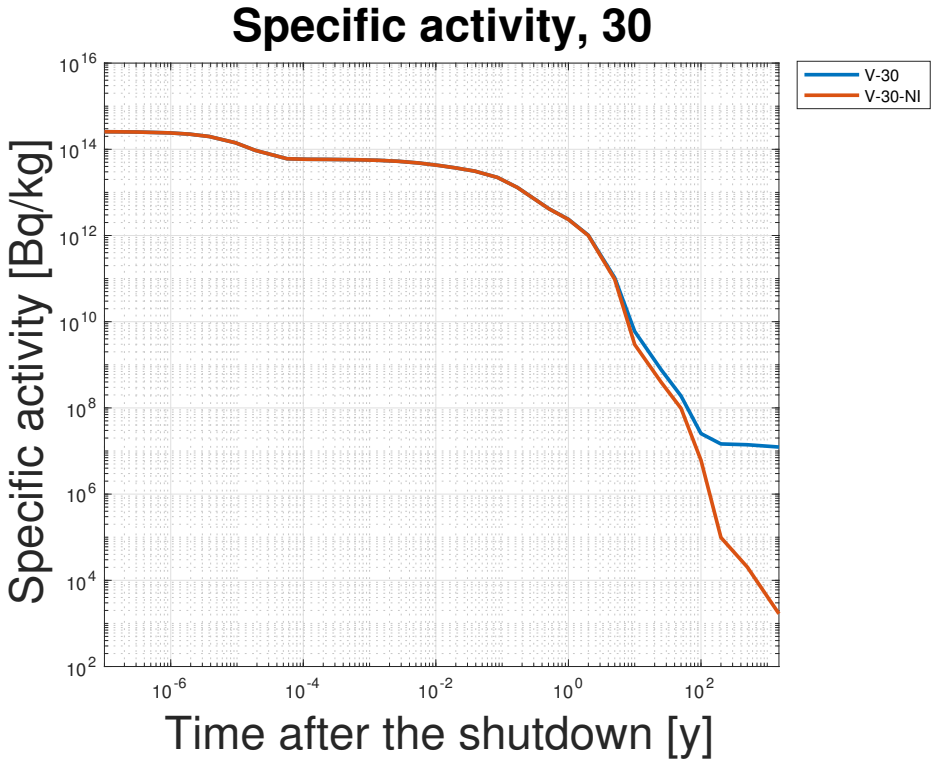

Figure 3.5: Specific activity of V-alloy in the inner vacuum vessel

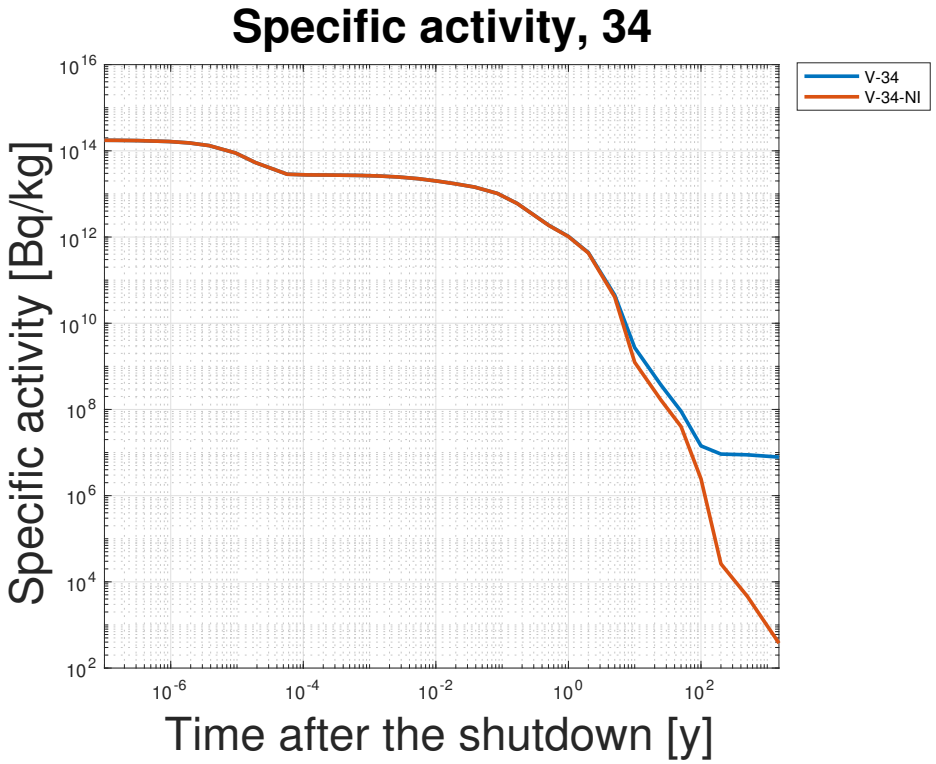

Figure 3.6: Specific activity of V-alloy in the outer vacuum vessel

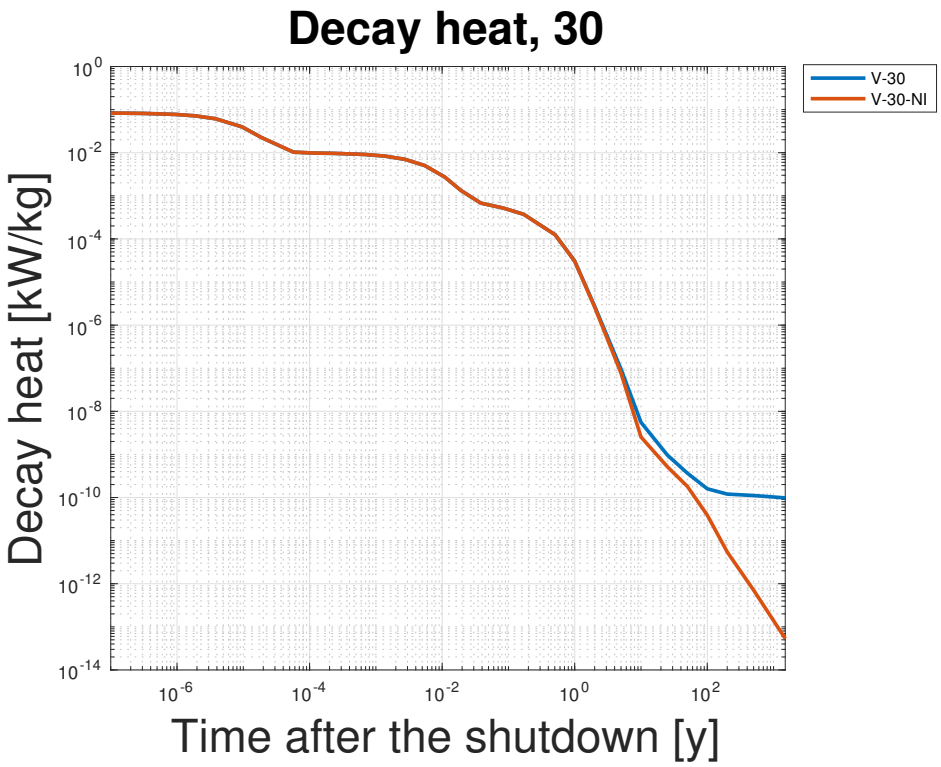

Figure 3.7: Decay heat of V-alloy in the inner vacuum vessel

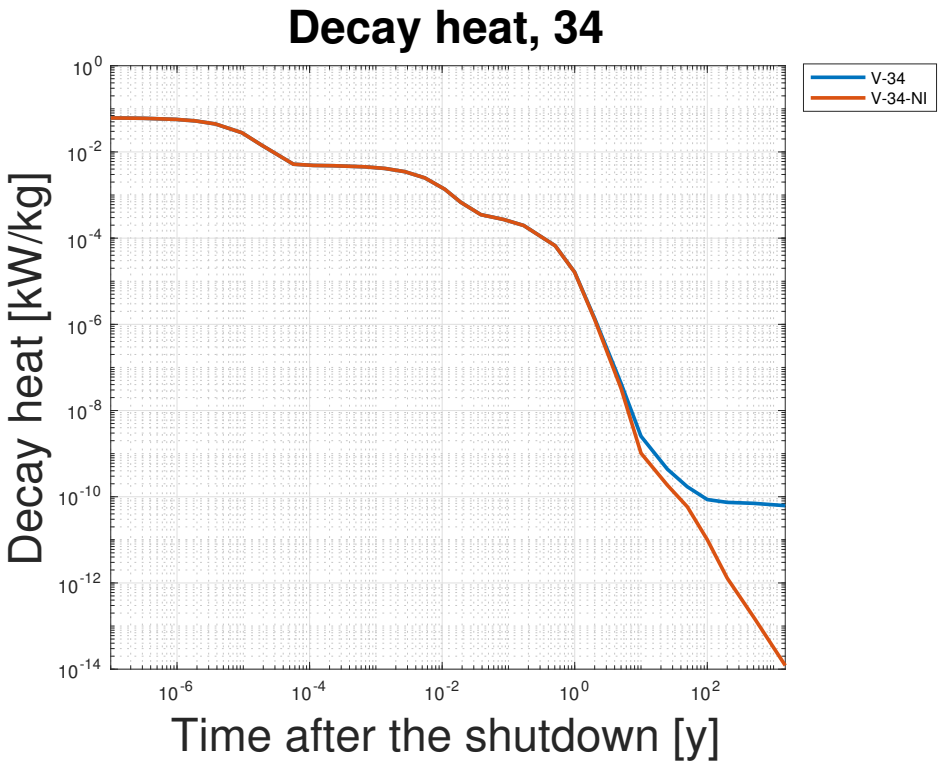

Figure 3.8: Decay heat of V-alloy in the outer vacuum vessel

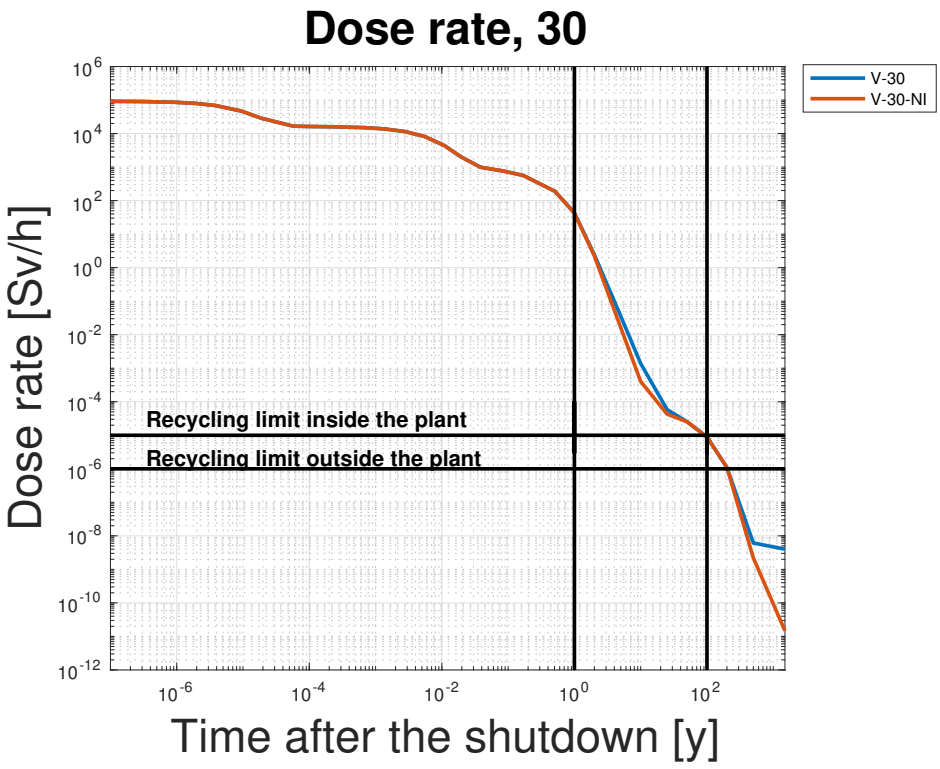

Figure 3.9: Dose rate of V-alloy in the inner vacuum vessel

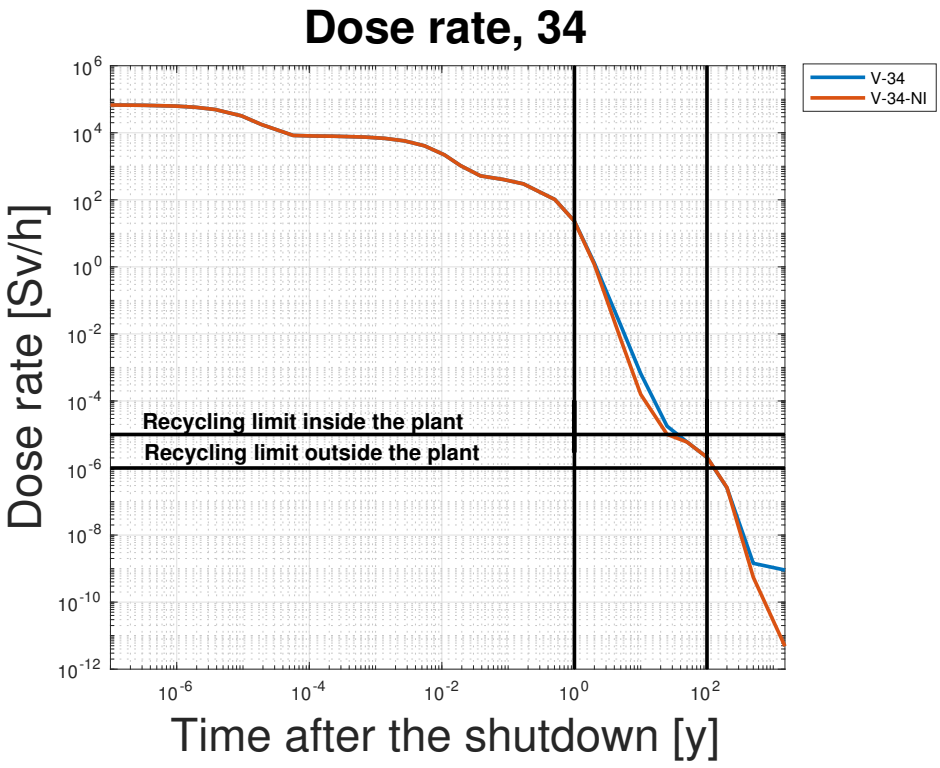

Figure 3.10: Dose rate of V-alloy in the outer vacuum vessel

The evolution of the contact dose rate shows in both regions of the vacuum vessel a rapid decrease along the period after the shutdown, and the two recycling limits are reached, both for the alloy with and without impurities, while for Inconel-718 the limits weren't reached even after 1500 years of storage.
As regards the specific activity and the decay heat, in both regions of the vacuum vessel their behaviours in time is characterized by a quicker reduction than the case of Inconel-718 (See chapter 3.5 for the final comparison) and that is connected to the presence of short-lived isotopes, thanks to the high percentage of Vanadium and Chromium. At the beginning of the time both compositions have got the same evolution of the three parameters, but then after many years it is possible to notice the achievement of lower values by the pure alloy. The improvement of the results for V-15Cr-5Ti is shown in the calculation of the low-activation criteria.
The evaluation of the clearance and SLB will be done firstly for the alloy with the presence of impurities, in order to see if they are respected or if the activation problem is related to the presence of few ppm of a particular element.

Table 3.6: Clearance and SLB indexes evaluated after 100 years of cooling time

	Clearance index after 100 years	**SLB**
V-15Cr-5Ti, with impurities, inner regions	1.48E+004	3.03E-002
V-15Cr-5Ti, with impurities, outer regions	9.33E+003	1.91E-002

The SLB criteria is respected, while the clearance index is higher than one, so in order to see which nuclides cause the high activity of Vanadium alloy, even after so many years from the shutdown, the percentage of the specific activity of each isotopes with respect the total one was evaluated at 100 years and the main results are Tritium (H-3) with a percentage of 41.23% and C-14, that influences the 57.73% of the total specific activity and its half-life is 5'708 years [28]. In particular the last one comes from N-14, which is a natural isotope of Nitrogen, through the (n,p) reaction [22]. Nitrogen is an impurity of the Vanadium alloy and even if its percentage is very low it influences the long-term high specific activity of the material.
The next step is the analysis of the alloy without the presence of impurities and the results for the clearance index and SLB are shown in the following table:

Table 3.7: Clearance and SLB indexes for V-15Cr-5Ti without the presence of impurities

	Clearance index after 100 years	**SLB**
V-15Cr-5Ti, without impurities, inner region	5.86E+001	8.19E-006
V-15Cr-5Ti, without impurities, outer region	2.41E+001	1.87E-006

The last case shows a clear decrease of the clearance index, but it is still higher than 1 due to the presence of Tritium, that contaminates the alloy and affects the final results.

3.4.2 Titanium-based alloy: Ti-6Al-4V

Titanium-based alloys are another interesting category of structural materials that are studied, thanks to their good mechanical properties, for high temperature applications. Titanium is a low-activation element, like Vanadium, and the selected alloy for the analysis is: Ti-6Al-4V.
The examination was be done both with and without the presence of impurities, like in the case of the Vanadium alloy.

Table 3.8: Mass percentage composition for Ti-6Al-4V with and without impurities [15]

	Ti-6Al-4V, with impurities	**Ti-6Al-4V, without impurities**
Ti	89.42 %	90.0 %
Al	6.0 %	6.0 %
V	4.0 %	4.0 %
Fe	0.25 %	-
C	0.08 %	-
N	0.05 %	-
O	0.2 %	-

Let's see the results from the activation analysis:

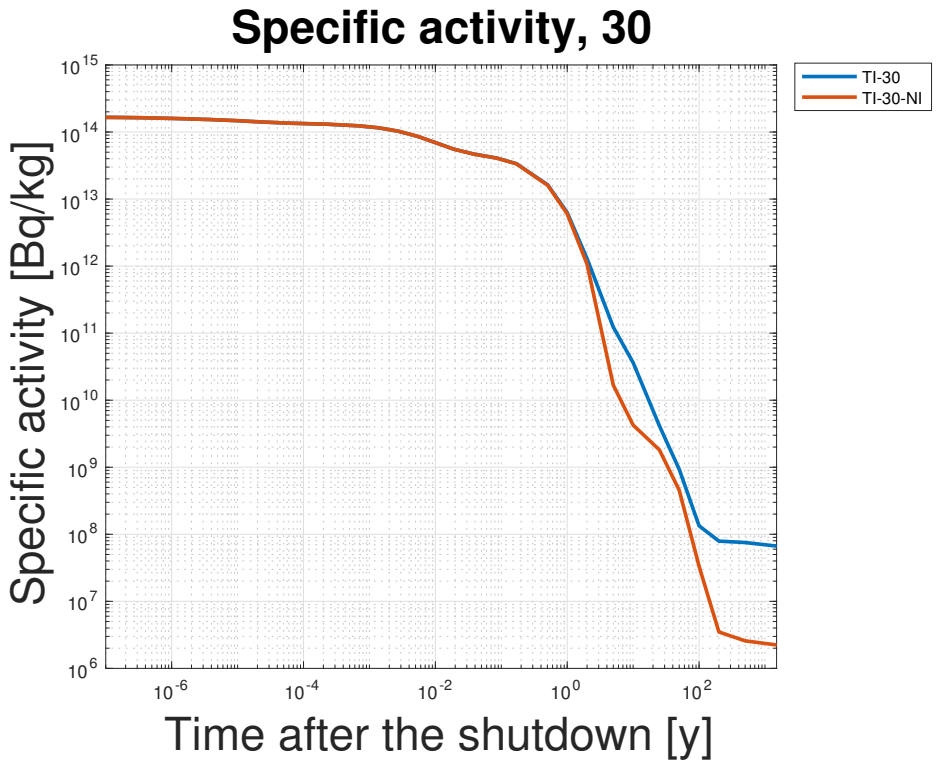

Figure 3.11: Specific activity of Ti-alloy in the inner vacuum vessel

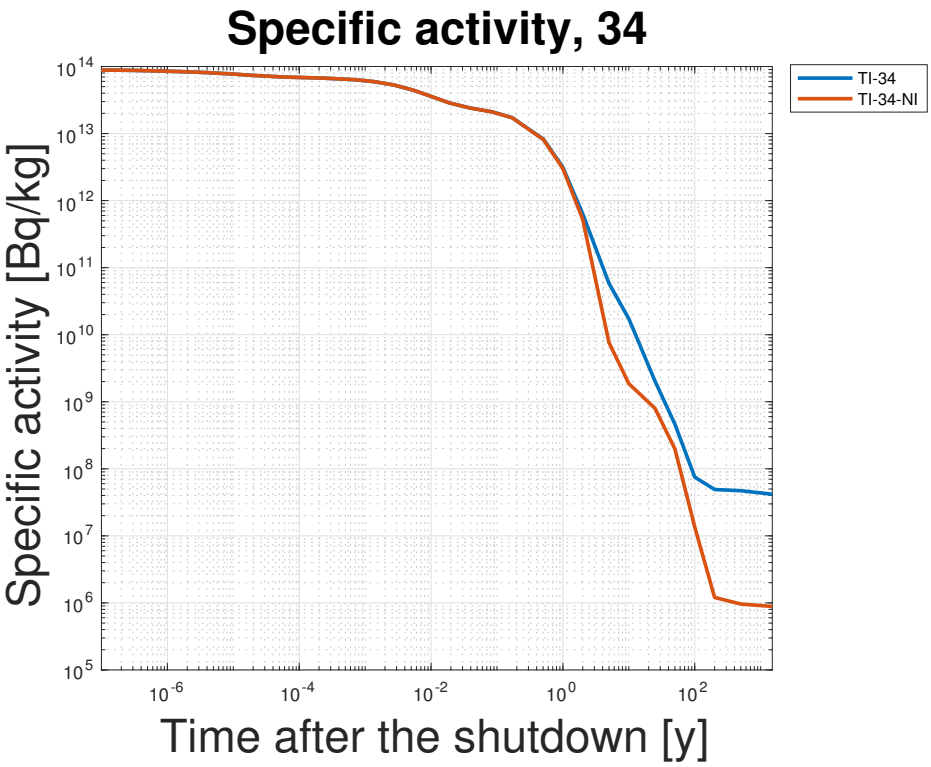

Figure 3.12: Specific activity of Ti-alloy in the outer vacuum vessel

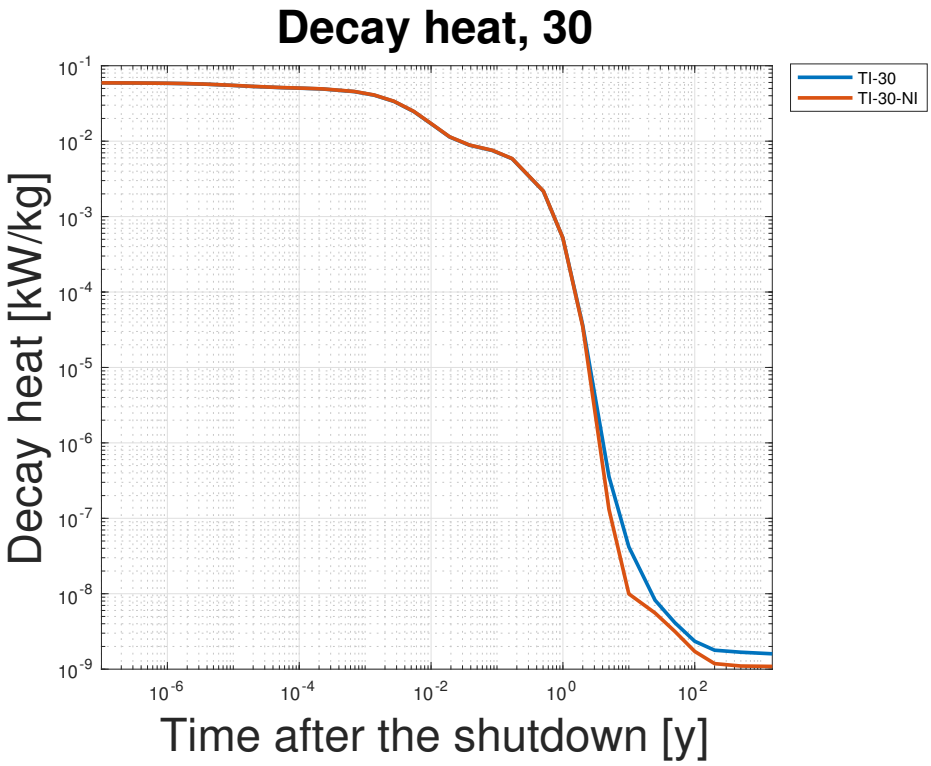

Figure 3.13: Decay heat of Ti-alloy in the inner vacuum vessel

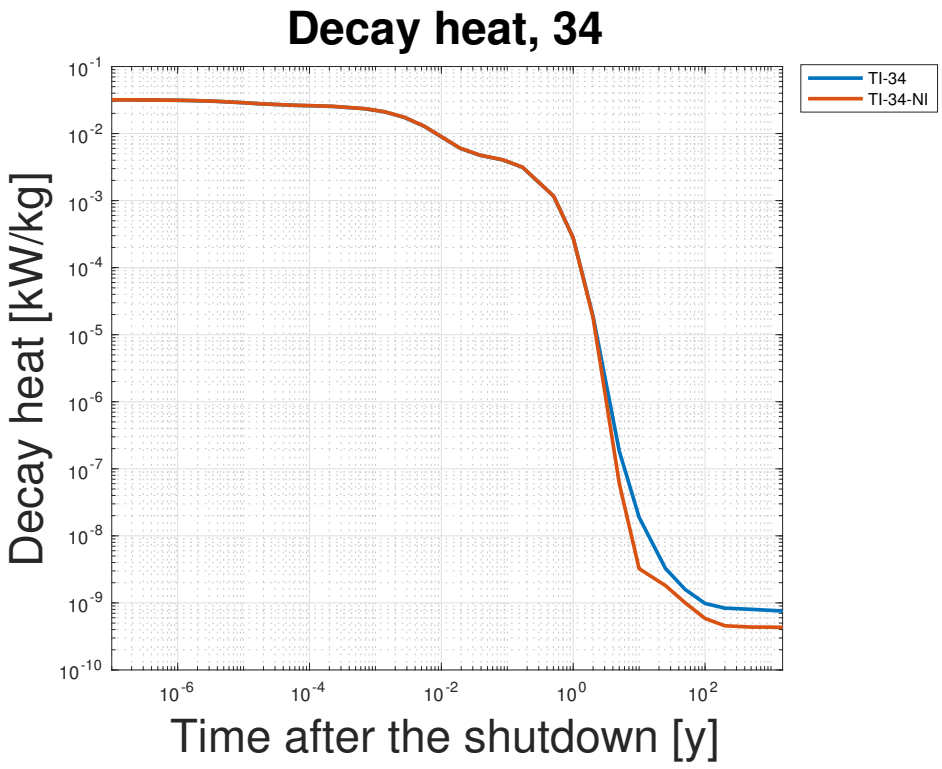

Figure 3.14: Decay heat of Ti-alloy in the outer vacuum vessel

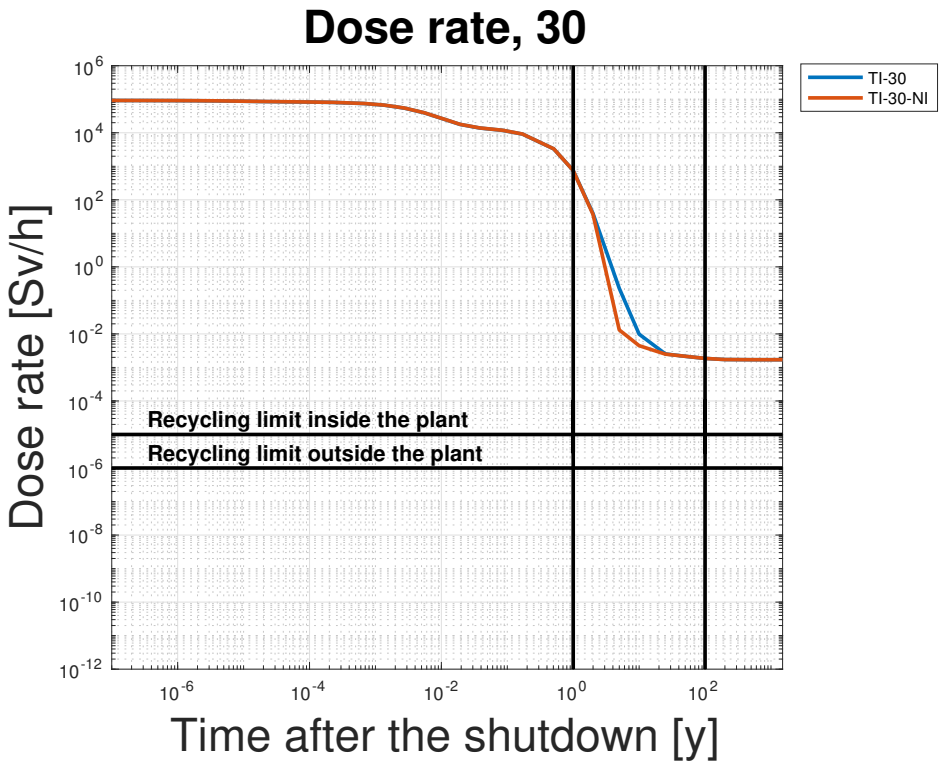

Figure 3.15: Dose rate of Ti-alloy in the inner vacuum vessel

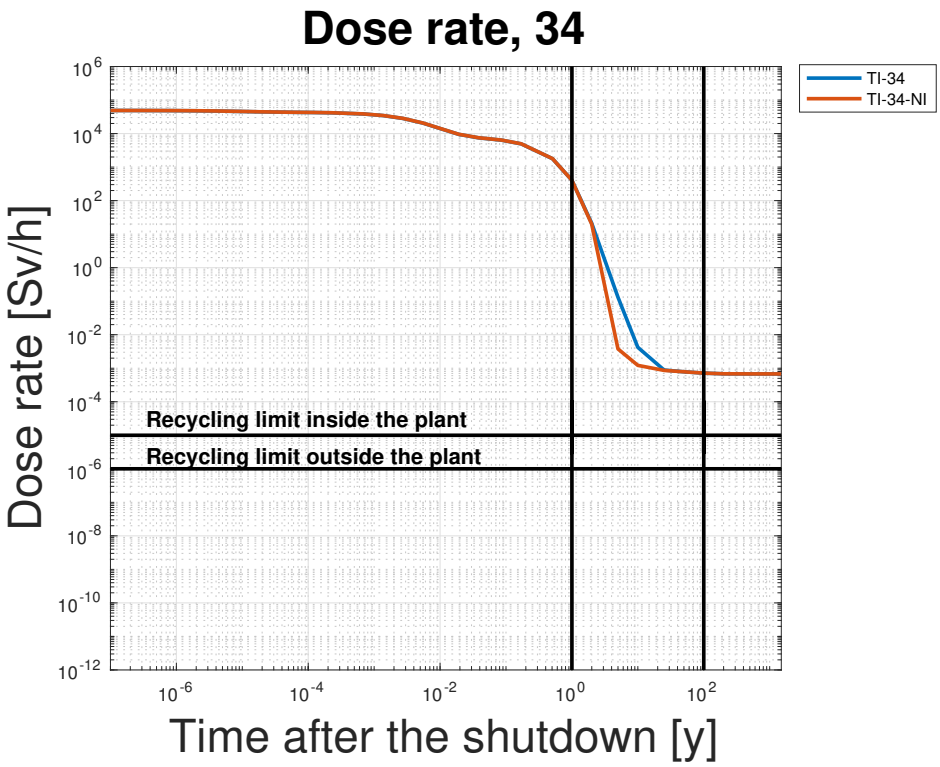

Figure 3.16: Dose rate of Ti-alloy in the outer vacuum vessel

The first thing that is possible to notice is that the contact dose rate doesn't reach the recycling limits even after 100 years from the shutdown of the reactor. The main cause is related to the long-lived isotope Al-26 (half life equal 716'641 years [28]), which comes from Al-27, the natural isotope of Aluminium, through a (n,2n) reaction [22]. Aluminium is an alloying elements, so for this reason both in the case with and without impurities the values of the contact dose rate are higher than the recycling ones.
The evolution of specific activity is faster than Inconel-718, but compared to the Vanadium-alloy it remains slower and it is possible to confirm it through the analysis of the clearance index.
For what concern the decay heat the comparison of the numerical results (see Table appendix) permitted to see that at the beginning the Titanium-alloy is characterized by lower values than Vanadium alloy, but the final evolution in time of the last one is faster (Figure 3.43).

Let's see the results of the clearance index and the waste disposal rating with the presence of possible impurities, in order to see how they influence the activation of Ti-6Al-4V:

Table 3.9: Clearance index and SLB for Ti-6Al-4V with impurities

	Clearance index after 100 years	**SLB**
Ti-6Al-4V, with impurities, inner region	7.68E+004	2.07E+000
Ti-6Al-4V, with impurities, outer region	4.87E+004	8.53E-001

SLB criteria is respected just in the outer wall of the vacuum vessel, where the neutron flux is lower, while the clearance index is greater than 1. The main long-lived radioactive isotope that causes the long activation of this Titanium-alloy is C-14, which comes from N-14 [22].
After having seen that it is related to the small percentage of Nitrogen, the analysis of the alloy without the presence of impurities was performed and the final results for the two indexes are:

Table 3.10: Clearance index and SLB for Ti-6Al-4V without impurities

	Clearance index after 100 years	**SLB**
Ti-6Al-4V, without impurities, inner region	2.65E+002	1.96E+000
Ti-6Al-4V, without impurities, outer region	1.17E+002	7.80E-001

CI and SLB for the pure alloy are lower but they still don't reach the unit and the high value of the first one is caused by the high specific activity of Tritium, while the second one is influenced by the presence of Aluminium, that can't be eliminated from the nominal composition of the material.

3.4.3 Molybdenum alloy: TZM

TZM (Titanium-Zirconium-Molybdenum) is a Molybdenum-alloy that is under study for high temperature fusion applications, but like in the case of Inconel-718 the main problem is related to the primary element, Molybdenum, which is characterized by the following natural isotopes: Mo-92, Mo-94, Mo-95, Mo-96, Mo-97, Mo-98 and Mo-100 [28]. They can develop the production of long-term isotopes through interactions with neutrons and a deeper analysis will be done in chapter 4.
The activation analysis was performed on the base of the following compositions [16]:

Table 3.11: Mass percentage composition of TZM with and without impurities

	TZM, with impurities	**TZM, without impurities**
Mo	99.369 %	99.369 %
Ti	0.5 %	0.5 %
Zr	0.08 %	0.08 %
C	0.025 %	0.025 %
O	0.025 %	0.025 %
N	0.0005 %	0.0005 %
H	0.0005 %	0.0005 %
Ag	0.0005 %	-
Al	0.001 %	-
As	0.0001 %	-
Ba	0.0002 %	-
Ca	0.0005 %	-
Cd	0.0001 %	-
Co	0.0005 %	-
Cr	0.001 %	-
Cu	0.0005 %	-
Fe	0.005 %	-
K	0.0005 %	-
Mn	0.0005 %	-
Mg	0.0005 %	-
Na	0.0005 %	-
Ni	0.0005 %	-
P	0.0005 %	-
Pb	0.0005 %	-
S	0.0005 %	-
Si	0.0005 %	-
W	0.01 %	-
Zn	0.0005 %	-

The results from FISPACT-II for both compositions are:

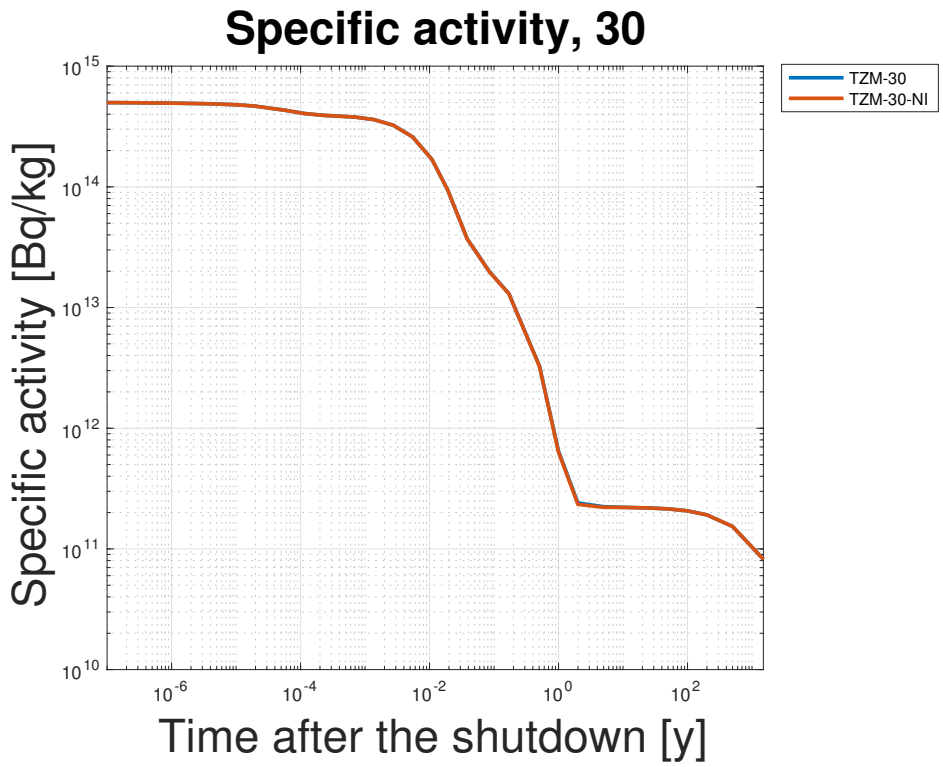

Figure 3.17: Specific activity of Mo-alloy in the inner vacuum vessel

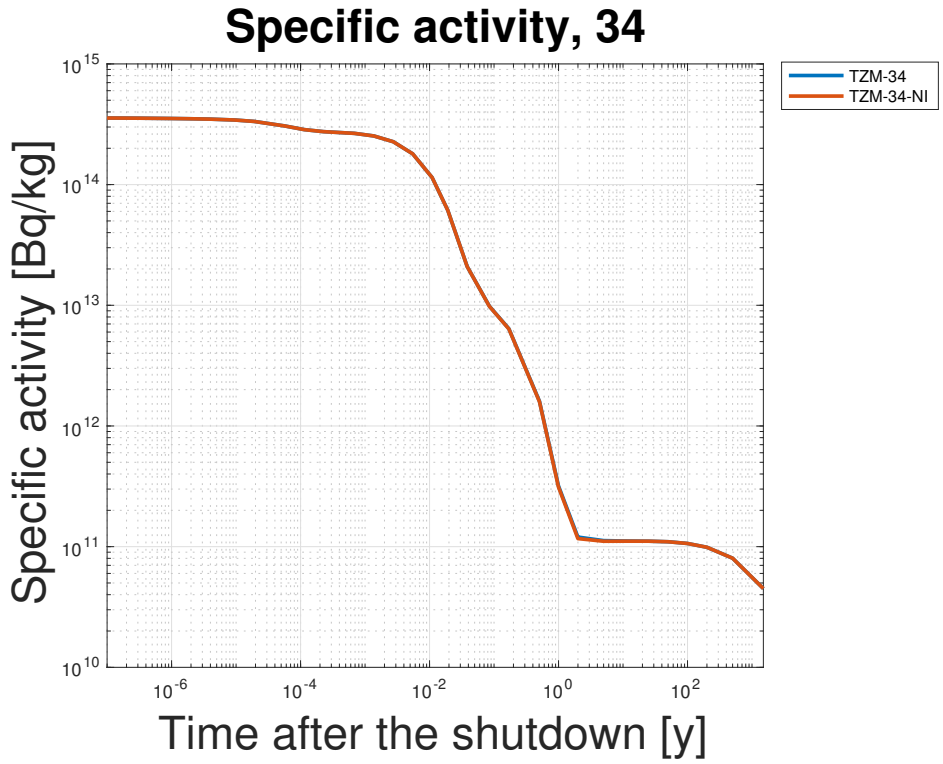

Figure 3.18: Specific activity of Mo-alloy in the outer vacuum vessel

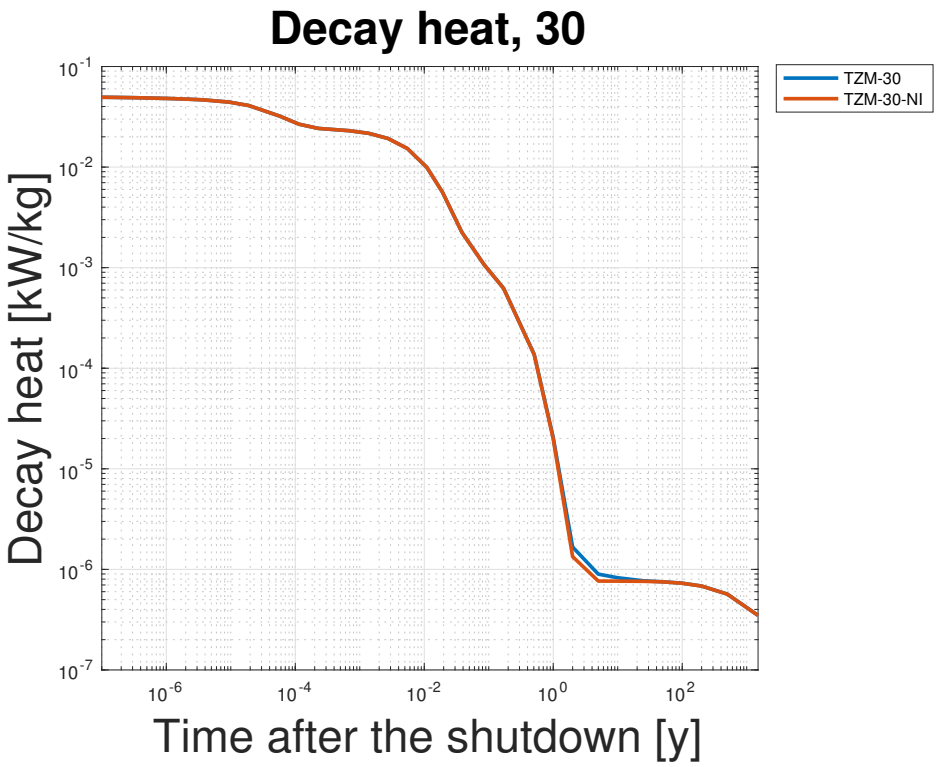

Figure 3.19: Decay heat of Mo-alloy in the inner vacuum vessel

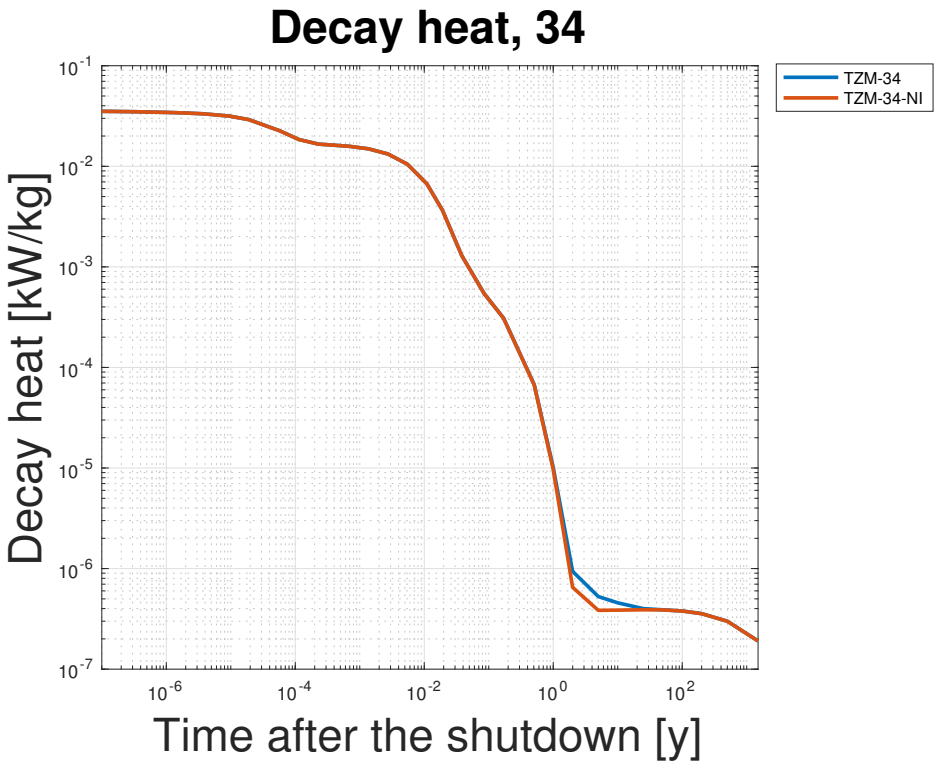

Figure 3.20: Decay heat of Mo-alloy in the outer vacuum vessel

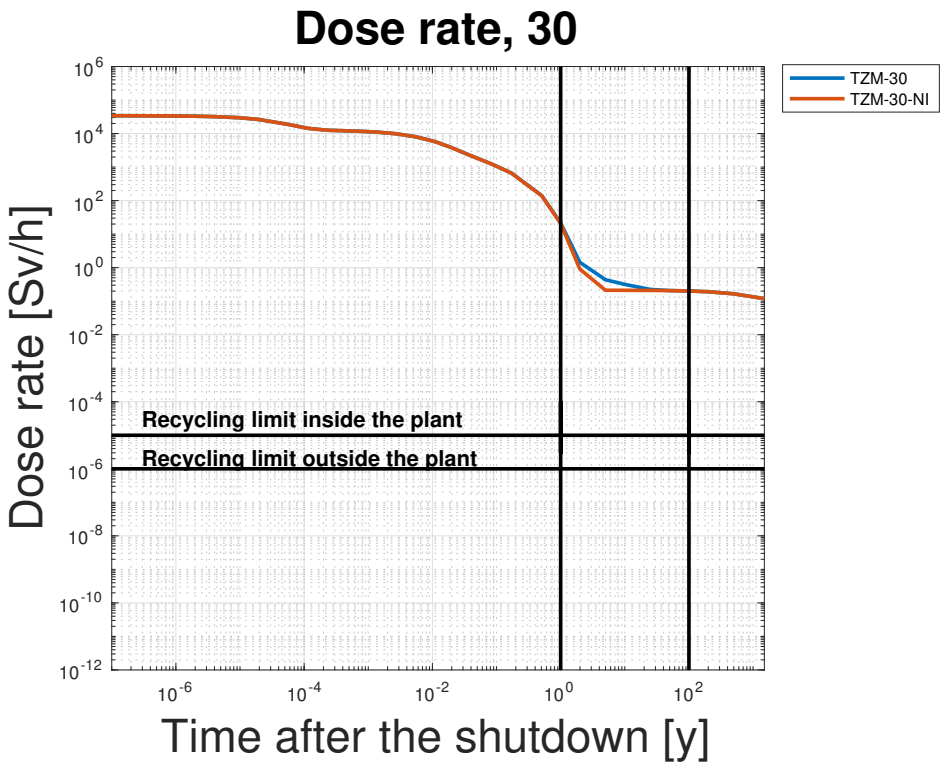

Figure 3.21: Dose rate of Mo-alloy in the inner vacuum vessel

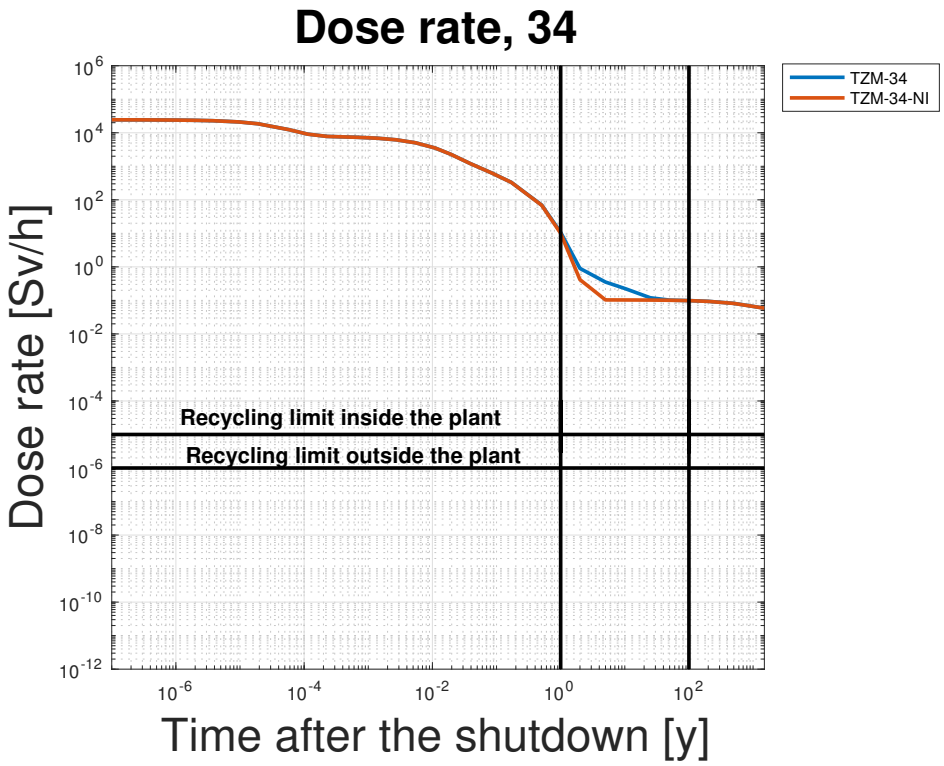

Figure 3.22: Dose rate of Mo-alloy in the outer vacuum vessel

The evolution of the three parameters is almost similar to the one of Inconel-718. The dose rate isn't able to reach the recycling limits even after thousands years from the end of the operation.
The specific activity maintains high values along the time, which is related to the presence of long-lived isotopes that come from the activation of Molybdenum.
The decay heat immediately after the shutdown is almost equal to the one of Inconel-718, and its reduction is very slow, so through the analysis of the results it is possible to confirm that TZM isn't a valid substitute for ARC's vacuum vessel, but let's see the results of the clearance index and Shallow Land Burial:

Table 3.12: Clearance and SLB indexes for TZM with and without impurities

	Clearance index after 100 years	**SLB**
TZM, with impurities, inner region	3.48E+006	7.41E+002
TZM, with impurities, outer region	1.97E+006	4.20E+002
TZM, without impurities, inner region	3.48E+006	7.41E+002
TZM, without impurities, outer region	1.97E+006	4.20E+002

Recalling that TZM is a Molybdenum alloy the analysis confirmed its high activation, in particular the clearance and waste disposal rating indexes are much higher than 1, so even for the permanently disposal the final process could require particular treatments.
The main radioactive isotopes that cause the activation of TZM are Nb-94 and Tc-99. They were considered for the final evaluation of CI and SLB criteria, which come respectively from Mo-94, through a (n,p) reaction, and Mo-98 through the following one [22]:

$$Mo^{98} + n \rightarrow \gamma + Mo^{99} \rightarrow Tc^{99} + \beta^{+} \tag{3.4}$$

In chapter 4 there will be the analysis of TZM after the application of isotopic tailoring, in which the isotopic composition of Molybdenum is modified in order to see which kind of improvements that process could lead.

3.4.4 Silicon Carbide

Silicon Carbide is a ceramic that is considered for fusion applications. The compositions analysed are [17]:

Table 3.13: Mass percentage composition of SiC with and without the presence of impurities

Elements	**Pure SiC** [%]	**SiC with impurities** [%]
C	29.95	29.95
Si	70.05	70.05
Na	-	5.00E-006
K	-	1.80E-005
Sc	-	1.30E-006
Cr	-	1.70E-006
Fe	-	4.40E-005
Co	-	1.30E-006
Ni	-	7.40E-006
Cu	-	4.80E-006
Zn	-	4.30E-006
Ga	-	5.00E-007
As	-	3.00E-007
Se	-	1.00E-007
Br	-	1.00E-007
Rb	-	1.00E-007
Sr	-	1.20E-006
Zr	-	2.34E-005
Mo	-	4.10E-006
Ag	-	2.00E-007
Cd	-	4.00E-007
In	-	1.00E-007
Sn	-	7.60E-006
Sb	-	1.00E-007
Cs	-	1.00E-007
Ba	-	4.70E-006
La	-	1.80E-006
Eu	-	1.00E-007
Tb	-	1.00E-007
Yb	-	1.00E-007
Hf	-	1.00E-007
Ta	-	1.00E-007
W	-	3.20E-006
Ir	-	1.00E-007
Pt	-	5.42E-005
Hg	-	1.00E-007
Th	-	1.00E-007
U	-	1.00E-007

Neutron studies showed that Silicon Carbide is characterised by activation level lower than the ones of metal alloys [13], but on the other side it is a ceramic and this is the first reason for which it could not be a valid and feasible substitute for the construction of a huge component like the vacuum vessel of ARC. Its brittle behaviour doesn't permit to detect a failure and the possible presence of a crack is propagated rapidly through the entire stressed region [13]. These are just some of the main disadvantages that could make SiC not a feasible choice. The results obtained from its activation analysis are:

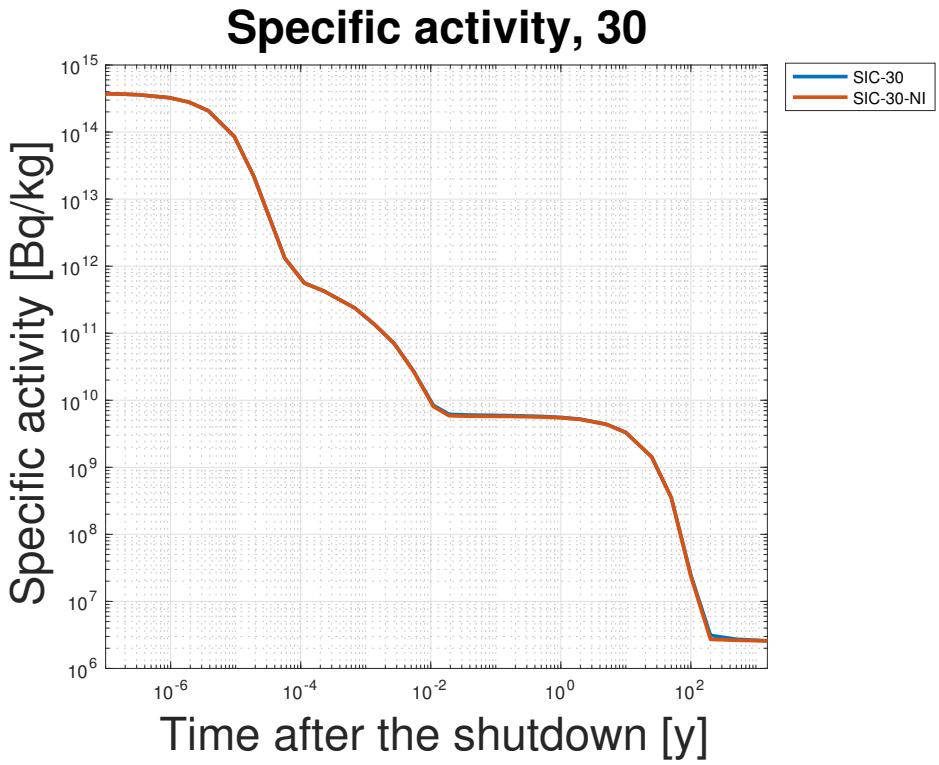

Figure 3.23: Specific activity of Silicon Carbide in the inner vacuum vessel

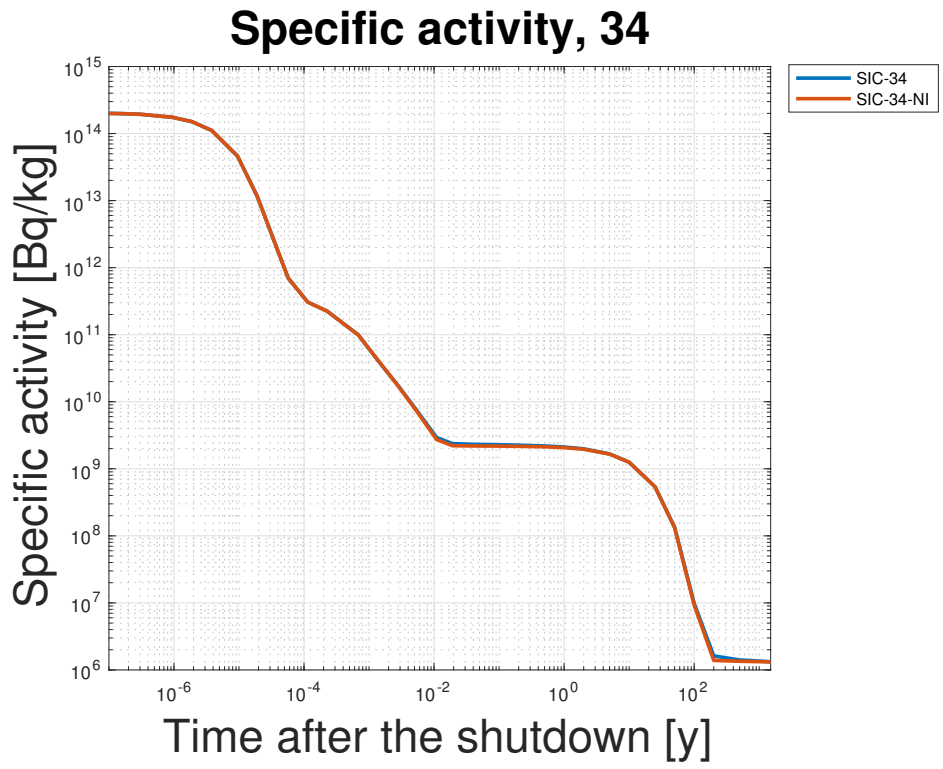

Figure 3.24: Specific activity of Silicon Carbide in the inner vacuum vessel

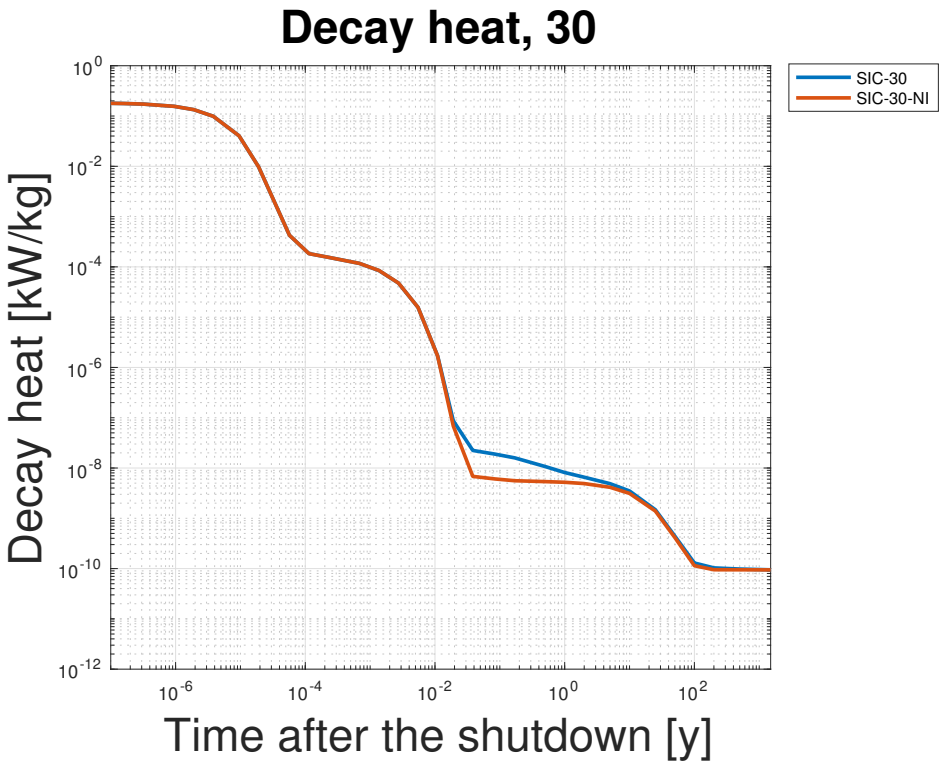

Figure 3.25: Decay heat of Silicon Carbide in the inner vacuum vessel

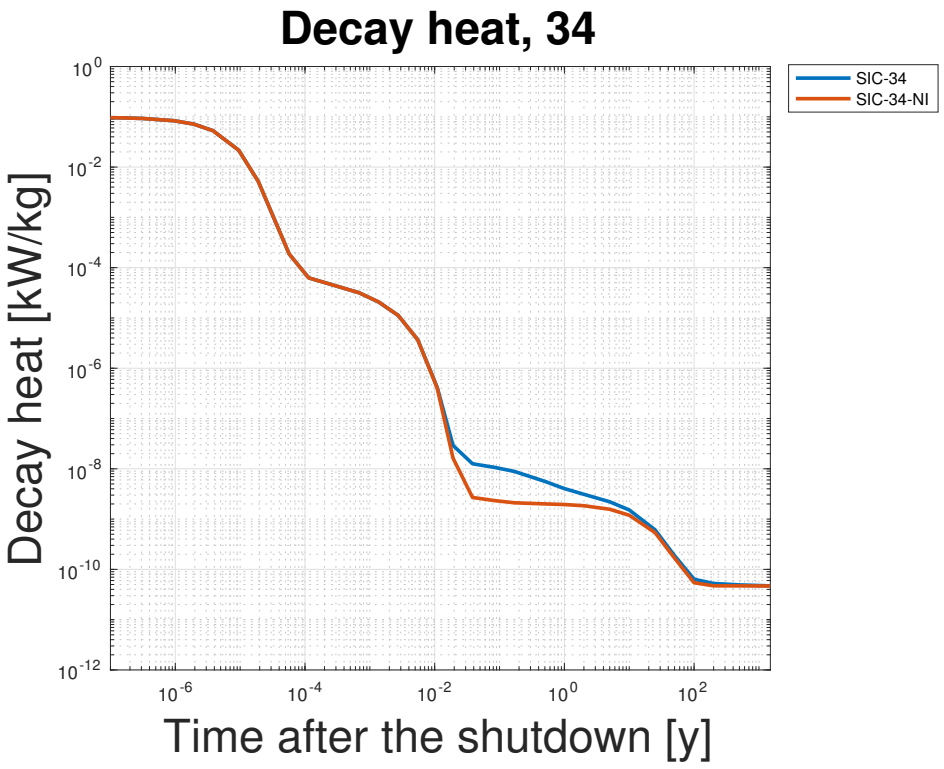

Figure 3.26: Decay heat of Silicon Carbide in the outer vacuum vessel

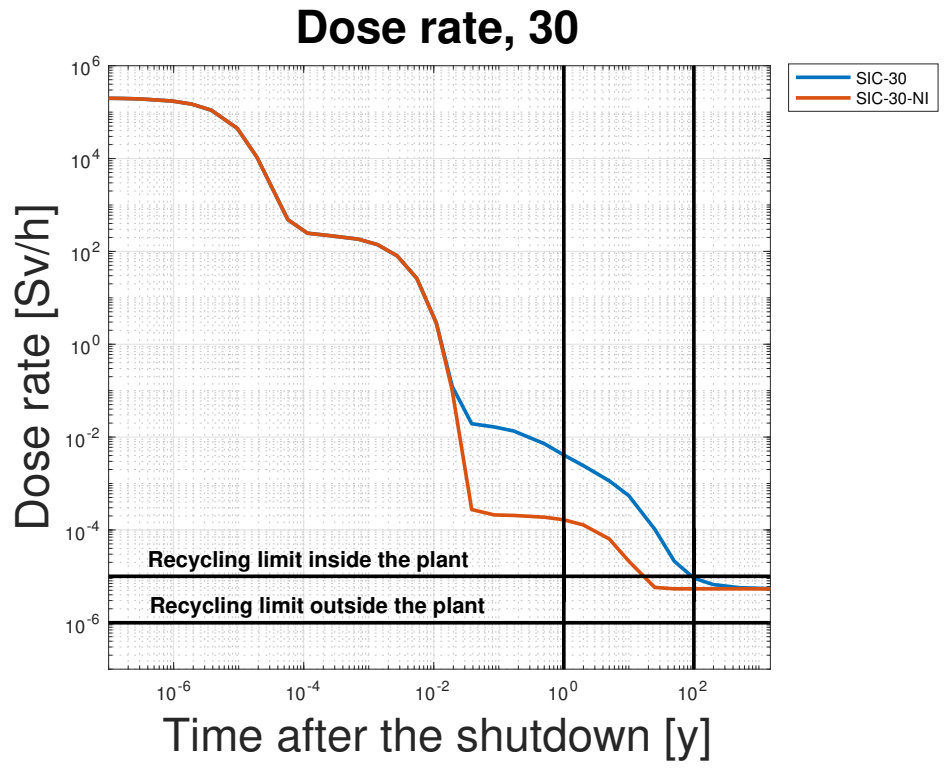

Figure 3.27: Dose rate of Silicon Carbide in the inner vacuum vessel

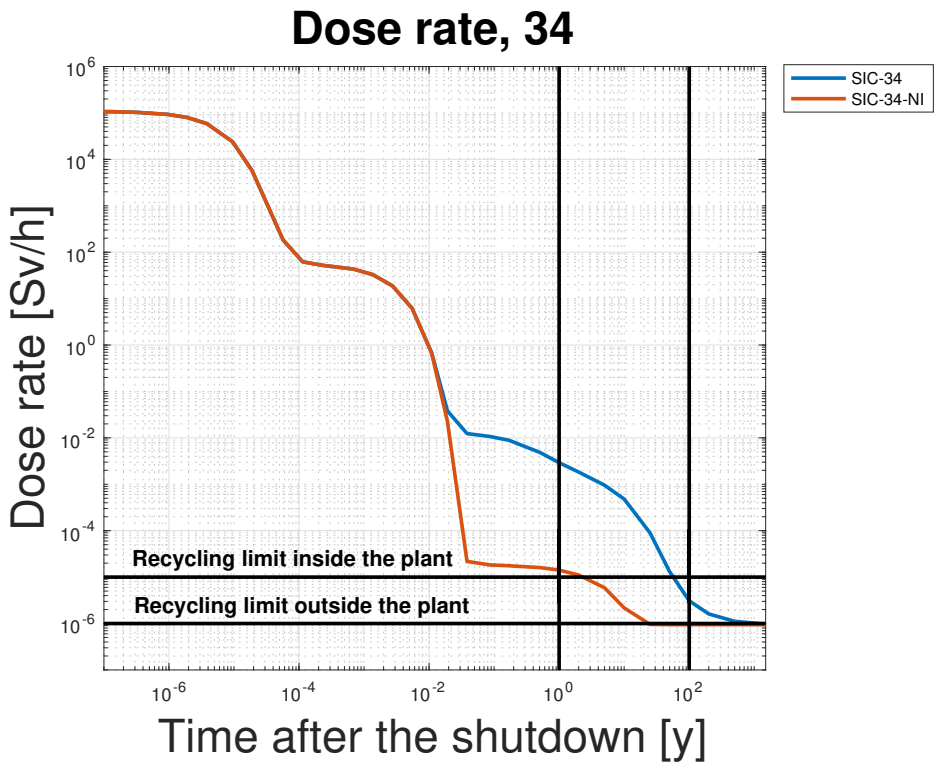

Figure 3.28: Dose rate of Silicon Carbide in the outer vacuum vessel

Silicon Carbide was the material that showed the best results from the activation analysis, each parameter was characterized by a rapid evolution in time (Figures in Chapter 3.5 permit to understand better their behaviours) , in fact it is supposed to be a low-activation material. The results obtained from the evaluation of the low-activation criteria are listed in the next table:

Table 3.14: Clearance and SLB indexes for SiC with and without the presence of impurities

	Clearance index after 100 years	**SLB**
SiC with impurities, inner region	6.91E+002	2.28E-002
SiC, without impurities, inner region	6.79E+002	2.23E-002
SiC, with impurities, outer region	3.57E+002	9.99E-003
SiC, without impurities, outer region	3.35E+002	9.77E-003

The first thing that can be noticed is that the clearance index is not respected and this is due to Tritium contamination, like in the case of Vanadium-alloy, and the presence of C-14.

Shallow Land Burial is respected and the influence of the impurities doesn't affect the final result.
As regards the recycling limits, for both the material with impurities and the pure one the limit inside the plant is reached, while the limit for the recycling outside the plant is reached just for the outer wall of the vacuum vessel in the case of pure Silicon Carbide (Figure 3.27 and 3.28).

3.4.5 RAFM: Eurofer97 and Eurofer-ODS

Reduced Activation Ferritic-Martensitic steels (RAFM) are considered the benchmark structural materials for fusion applications. The main alloys that were analysed are Eurofer 97 and Eurofer-ODS, which are under study for the design of the future DEMO reactor [18,19].

Table 3.15: Eurofer97 composition with and without impurities

	Eurofer97, with impurities	**Eurofer97, without impurities**
Cr	9.0 %	9.0 %
C	0.11 %	0.11 %
W	1.5 %	1.5%
V	0.2 %	0.2 %
Ta	0.07 %	0.07 %
B	0.001 %	0.001 %
N	0.03 %	0.03 %
O	0.01 %	0.01 %
S	0.005 %	0.005 %
Fe	88.558 %	88.664 %
Mn	0.4 %	0.4 %
P	0.005 %	0.005 %
Si	0.05 %	-
Ni	0.005 %	-
Mo	0.005 %	-
Ti	0.01 %	0.01 %
Cu	0.005 %	-
Nb	0.001 %	-
Al	0.01 %	-
Co	0.005 %	-
As	0.005 %	-
Sn	0.005 %	-
Zr	0.005 %	-
Sb	0.005 %	-

The Oxide Dispersion Strengthened (ODS) alloy is characterized by the addiction of 0.3% of Yttrium oxide (Y2O3), in order to improve the mechanical properties at high temperature operations. The weight composition is [19]: 8.92%Cr, 1.11%W, 0.193%V, 0.081%Ta, 0.408%Mn, 0.11%Si, 0.07%C, 0.192%Y and 88.92%Fe.

The results for Eurofer97, with and without possible impurities, compared with the ones for the ODS version are shown in the following plots:

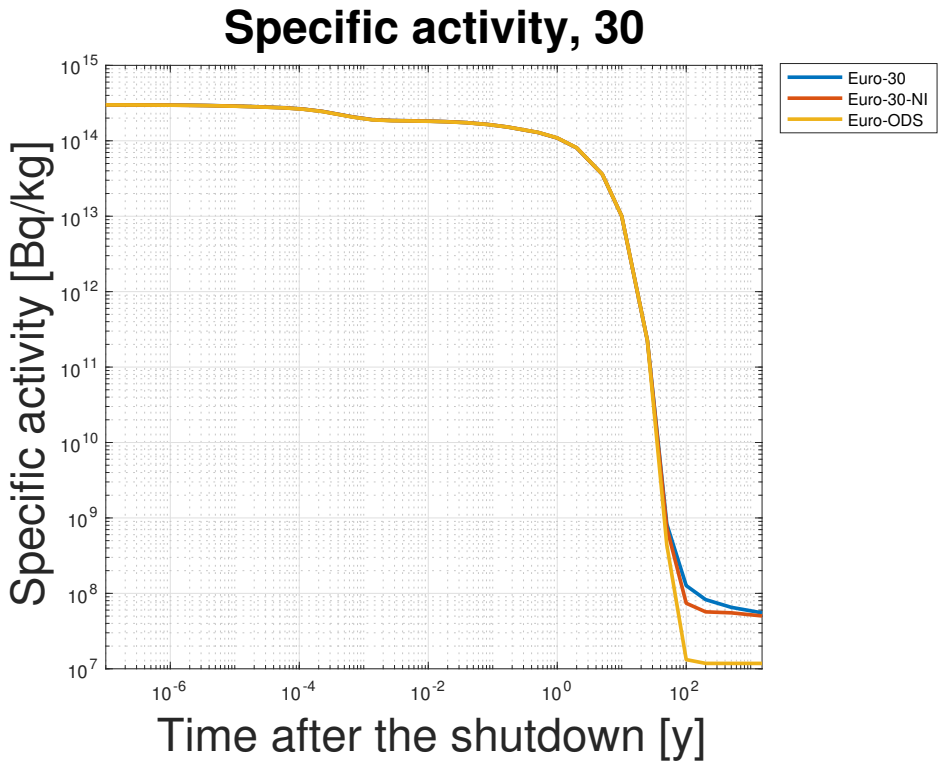

Figure 3.29: Specific activity of Eurofer97 and Eurofer-ODS in the inner vacuum vessel

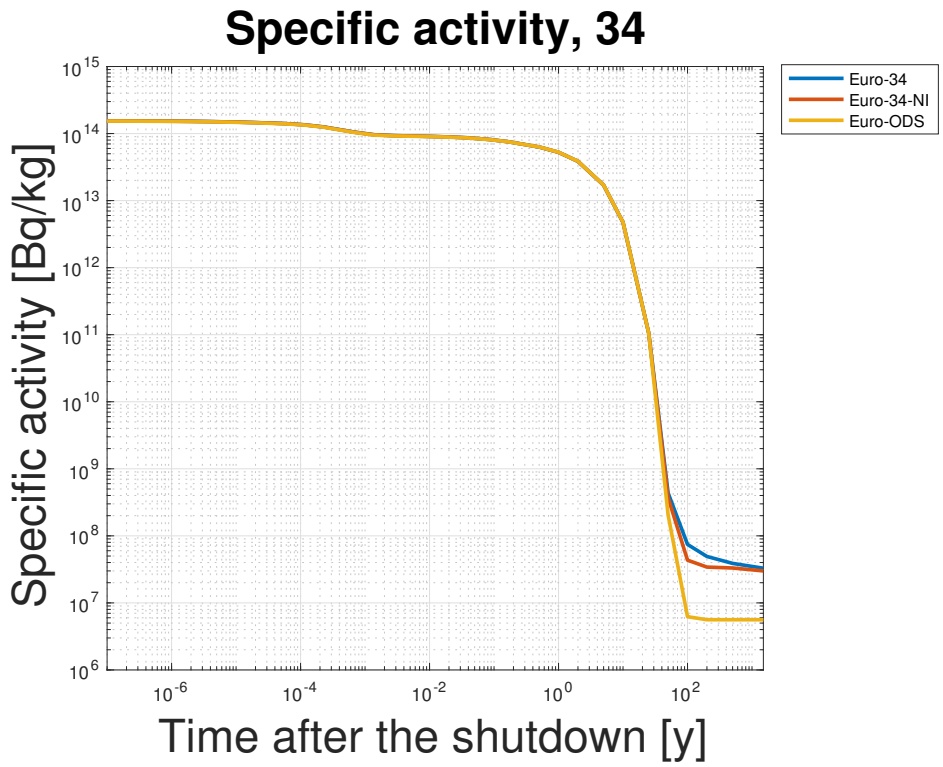

Figure 3.30: Specific activity of Eurofer97 and Eurofer-ODS in the outer vacuum vessel

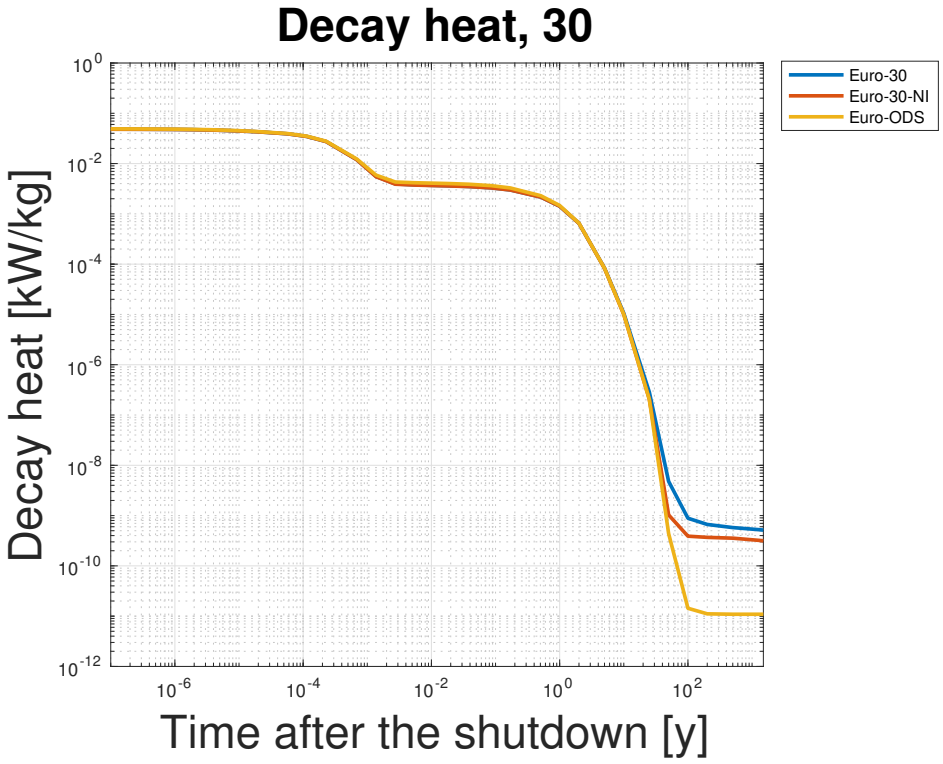

Figure 3.31: Decay heat of Eurofer97 and Eurofer-ODS in the inner vacuum vessel

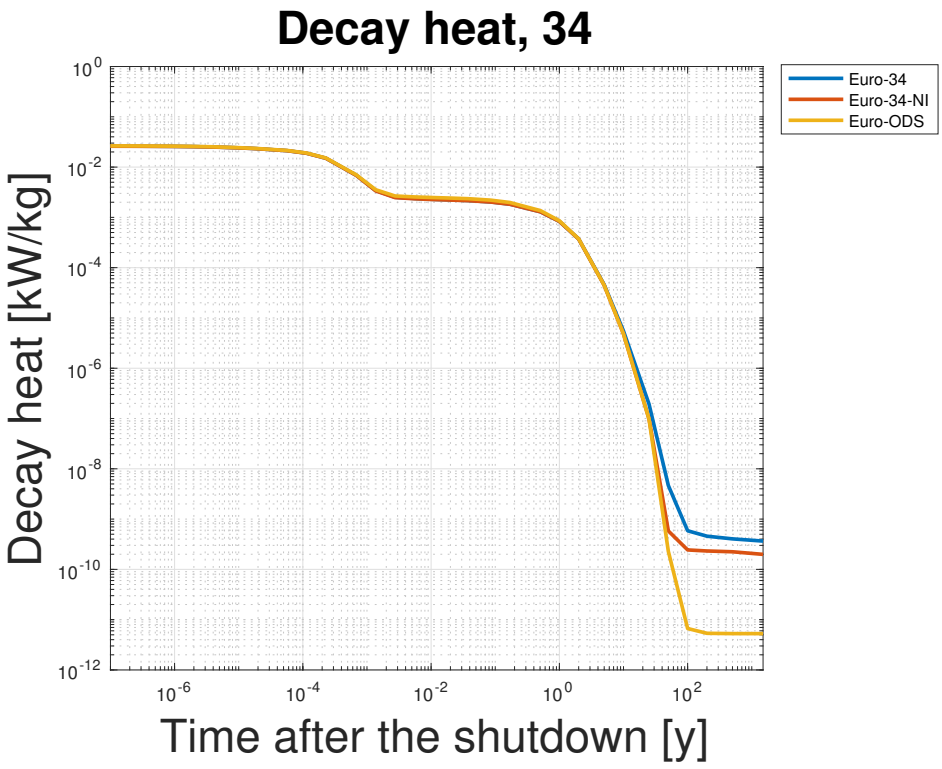

Figure 3.32: Decay heat of Eurofer97 and Eurofer-ODS in the outer vacuum vessel

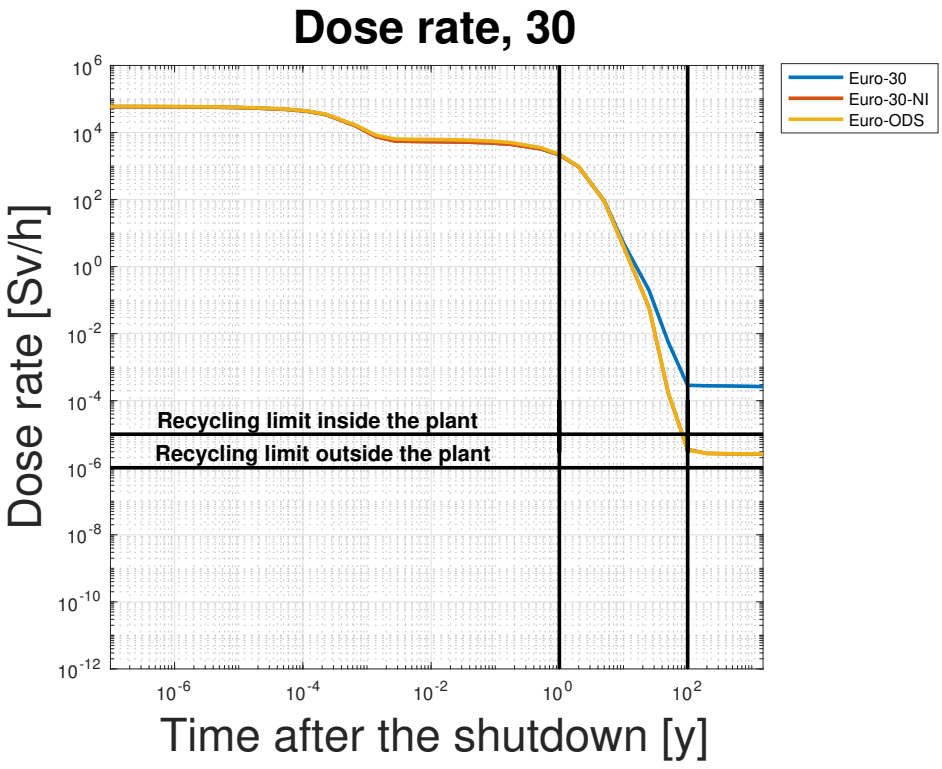

Figure 3.33: Dose rate of Eurofer97 and Eurofer-ODS in the inner vacuum vessel

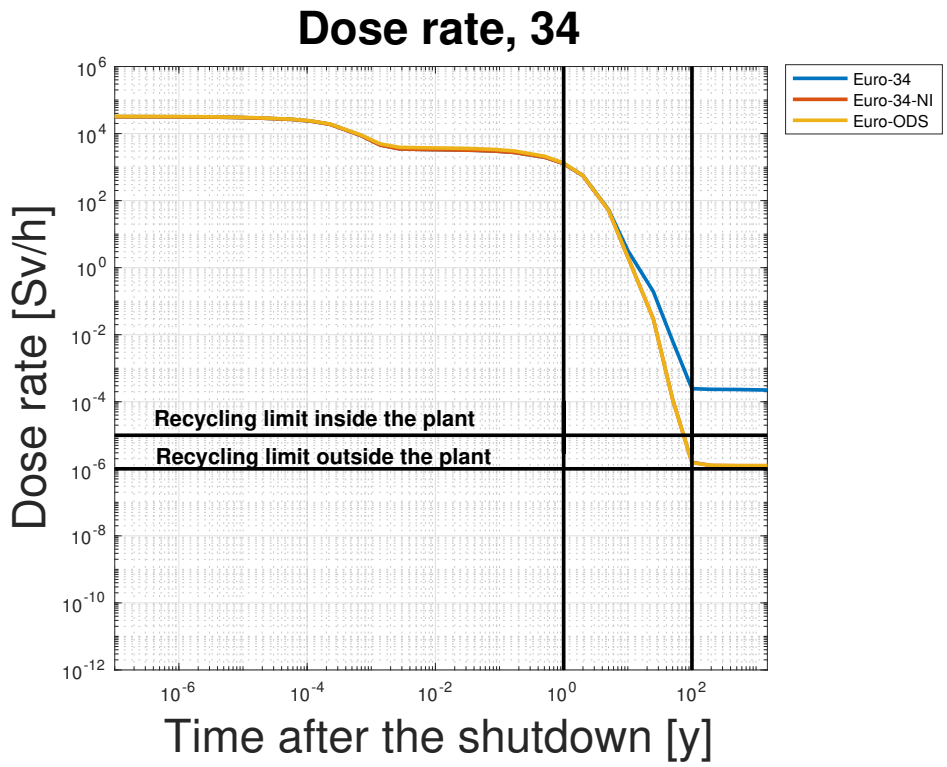

Figure 3.34: Dose rate of Eurofer97 and Eurofer-ODS in the outer vacuum vessel

The evolution of the specific activity, dose rate and decay in the first years after the shutdown is almost the same, while after almost 100 years it is possible to notice an improvement for Eurofer-ODS. That reduction is due to the non-presence of high activation impurities, like Nickel, Nitrogen and Molybdenum, which can be found in the standard Eurofer97.

Table 3.16: Clearance and SLB indexes for the analysed RAFM steels

	Clearance Index after 100 years	**SLB**
Eurofer97, with impurities, inner region	5.28E+004	8.75E-001
Eurofer97, with impurities, outer region	3.53E+004	7.17E-001
Eurofer97, without impurities, inner region	4.55E+004	1.25E-001
Eurofer97, without impurities, outer region	2.91E+004	7.86E-002
Eurofer-ODS, inner region	1.33E+002	4.84E-003
Eurofer-ODS outer region	6.41E+001	2.32E-003

SLB is respected for both Eurofer-ODS and standard Eurofer97, while they don't reach the limit for the clearance index. In the second alloy this is due to the presence of Nitrogen in the nominal composition of the steel, which is characterised by N-14 and N-15, two natural isotopes that can interact with neutrons can lead the formation of C-14 [22], a long-lived radioactive isotope considered in the calculation of the clearance criteria.

3.4.6 Stainless steels 316 and 304

Stainless steels 316 and 304 are used in ITER project; and even if they are not characterized by good mechanical properties at high temperature like Inconel-718, their very low price (316 SS price is $9.6\frac{\$}{kg}$ [26]) makes them a possible good choice as substitute for Inconel-718.

Table 3.17: Mass percentage compositions of stainless steel 316 with and without impurities and stainless steel 304 [20], which were used for the activation analysis

	SS316	**SS316 no impurities**	**SS304**
C	0.0225%	0.0225%	0.18%
Si	0.5%	-	0.98%
Mn	1.8%	1.8%	1.00%
P	0.025%	-	0.041%
S	0.0075%	-	0.026%
Cr	17.5%	17.5%	20.08%
Ni	12.25%	12.25%	8.66%
Mo	2.5%	2.5%	-
Ti	0.15%	-	-
N	0.07%	0.07%	-
Al	0.15%	-	-
Co	0.05%	-	-
Nb	0.01%	-	-
Fe	64.65%	65.86	69.04%
Cu	0.3%	-	-
B	0.002%	-	-
Ta	0.001%	-	-
O	0.002%	-	-
K	0.0005%	-	-
Bi	0.0008%	-	-
V	0.004%	-	-
Zr	0.002%	-	-
Ag	0.0002%	-	-
Cd	0.0002%	-	-
Sn	0.002%	-	-
Sb	0.0005%	-	-
Ba	0.0005%	-	-
Tb	0.0005%	-	-
W	0.001%	-	-
Ir	0.0005%	-	-
Pb	0.0008%	-	-
As	0.0005%	-	-

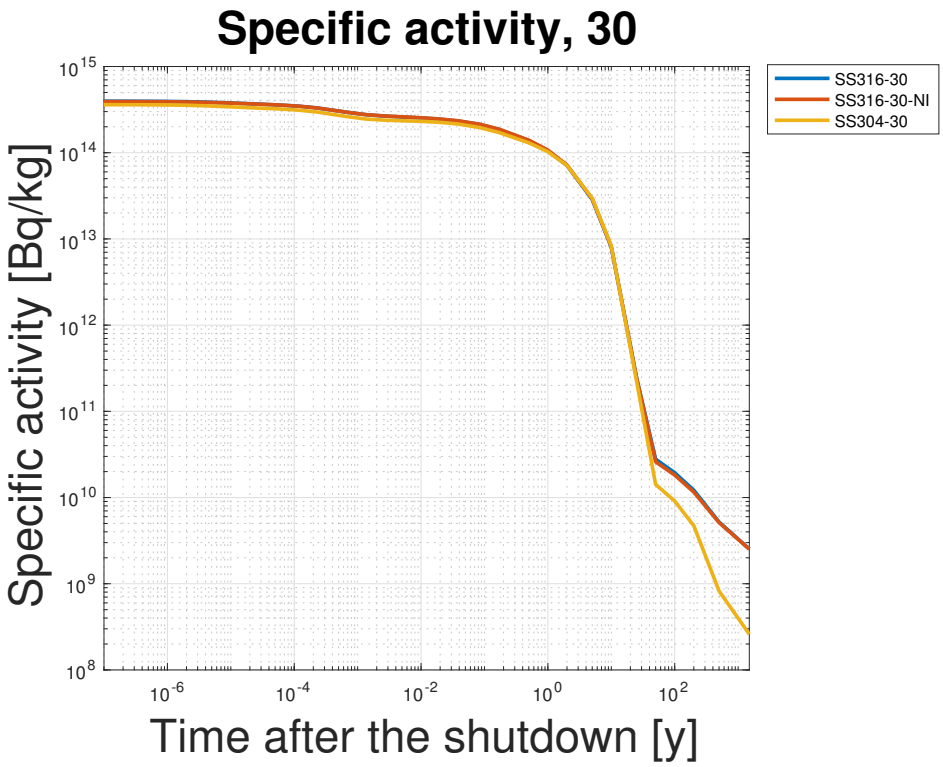

Figure 3.35: Specific activity of stainless steel 316 and 304 in the inner region of the vessel

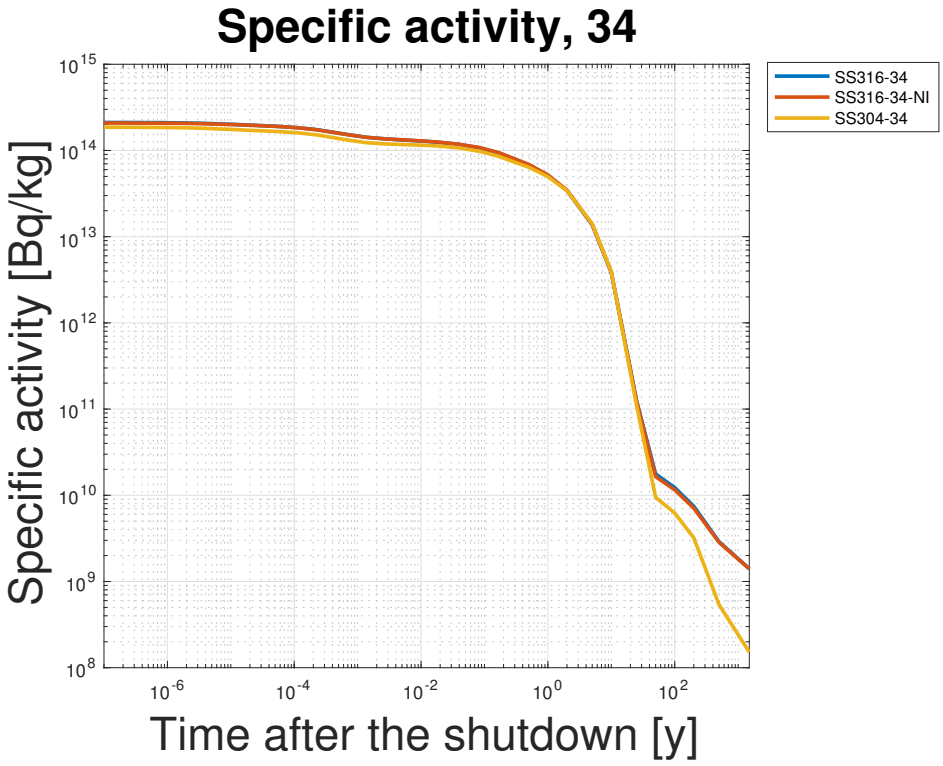

Figure 3.36: Specific activity of stainless steel 316 and 304 in the outer region of the vessel

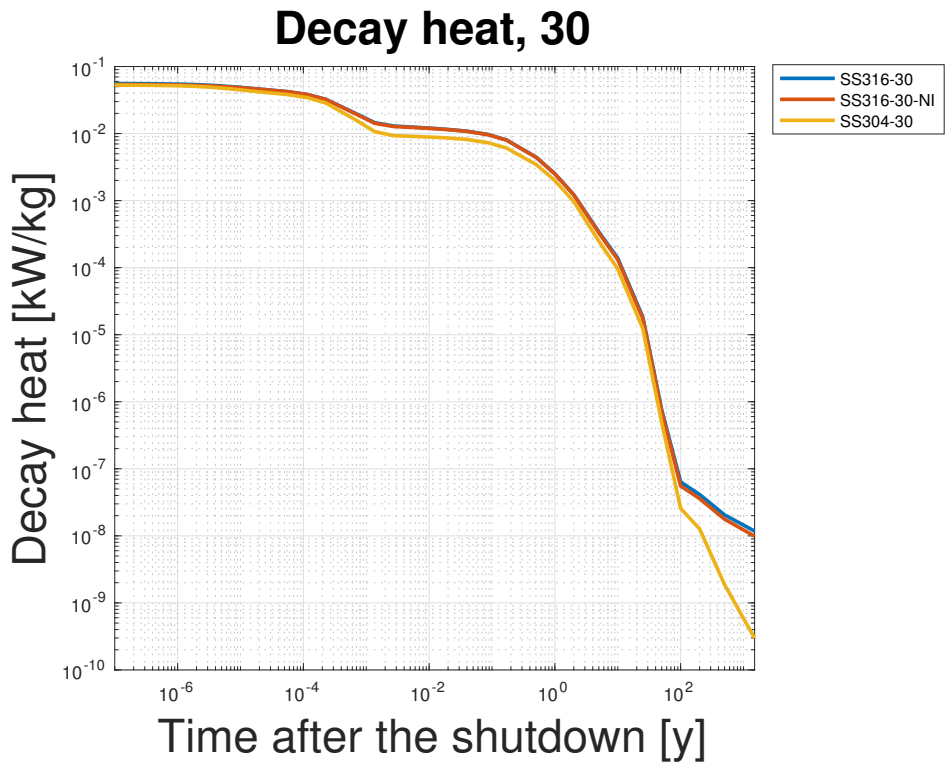

Figure 3.37: Decay heat of stainless steel 316 and 304 in the inner region of the vessel

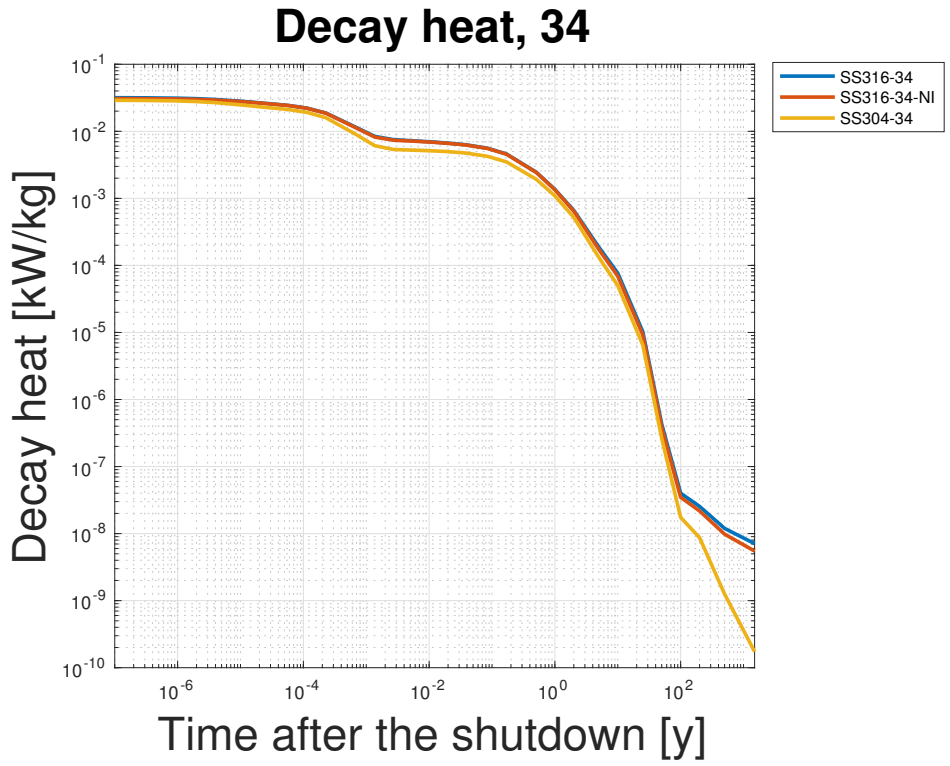

Figure 3.38: Decay heat of stainless steel 316 and 304 in the outer region of the vessel

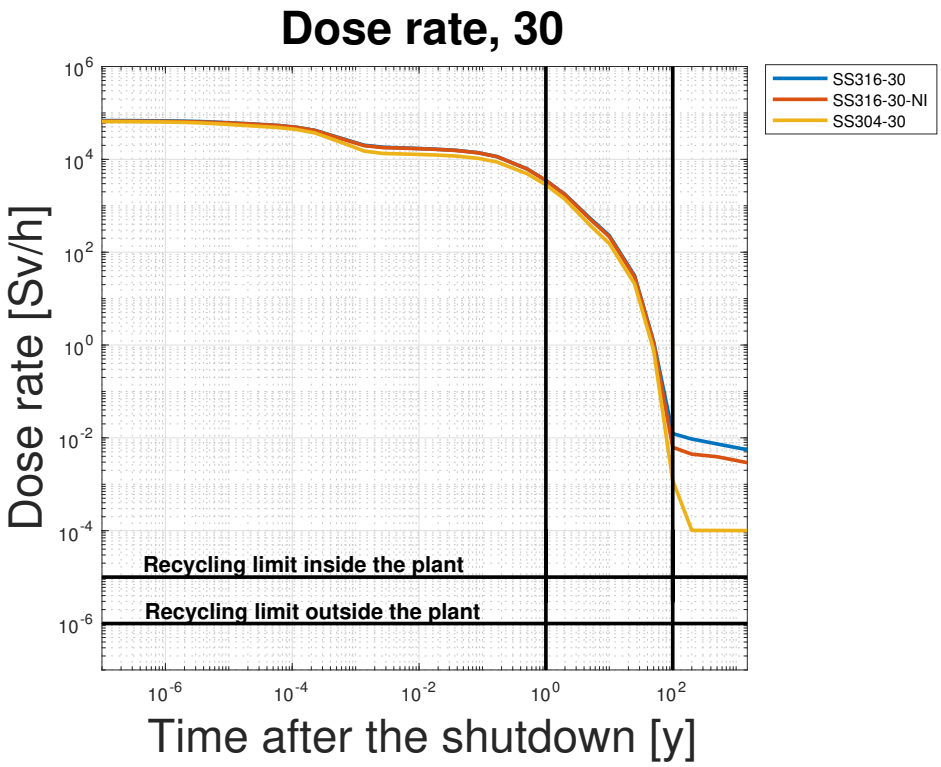

Figure 3.39: Dose rate of stainless steel 316 and 304 in the inner region of the vessel

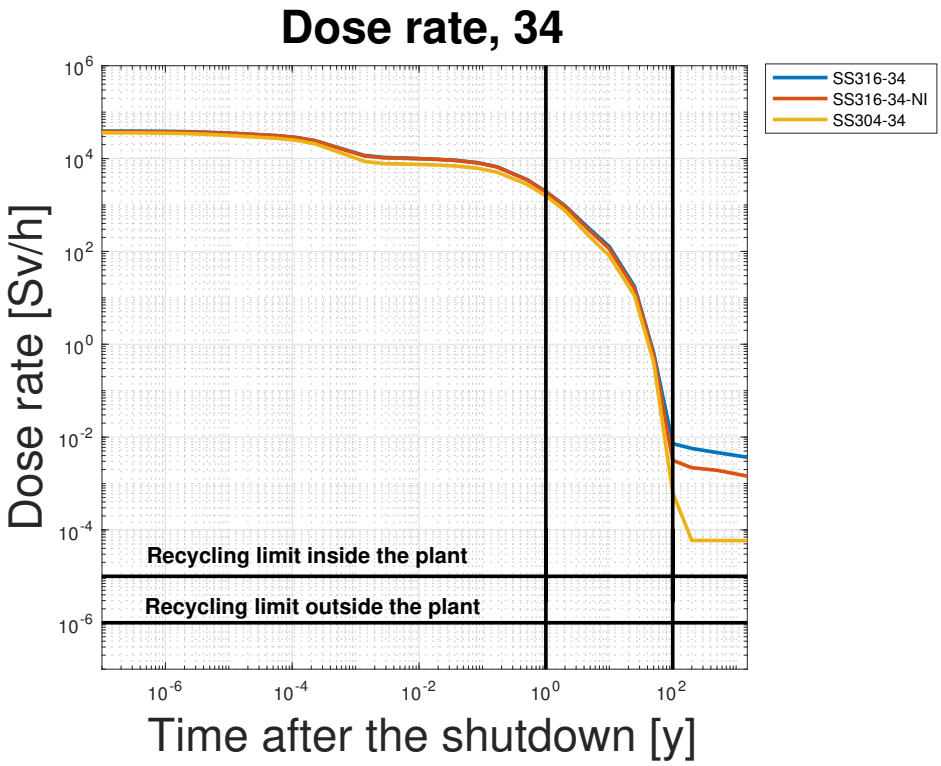

Figure 3.40: Dose rate of stainless steel 316 and 304 in the outer region of the vessel

The results of the activation analysis show that the three different compositions have got the same behaviour at the beginning of the storage period, while the evolution after many years highlights improvements for stainless steel 304, that is characterized by a faster decrease of the three parameters. The different evolution of the type 304 could be influenced by the lower percentage of Nickel and the absence of impurities that could lead the formation of long-lived isotopes. As it was explained for Inconel-718, Nickel is an element that should be avoided in the nominal composition of an alloy in order to avoid the high activation.
Even if SS 304 could seem a better choice for the activation analysis, Figure 3.39 and 3.40 show that none of the three materials reach the recycling limits after more than 100 years from the shutdown of the plant.
For what concern the clearance and decommissioning criteria the results are in the following table:

Table 3.18: Clearance index after 100 years from the shutdown and Shallow Land Burial criteria for SS 316, with and without impurities, and 304

	Clearance index after 100 years	**SLB**
SS316 impurities inner wall of VV	4.25E+005	2.36E+001
SS316 impurities outer wall of VV	2.84E+005	1.56E+001
SS316 no impurities inner wall of VV	3.45E+005	1.55E+001
SS316 no impurities outer wall of VV	2.17E+005	8.88E+000
SS304 inner wall of VV	1.06E+005	5.17E-001
SS304 outer wall of VV	7.02E+004	3.30E-001

The CI is not respected in each steel due to the high specific activity of H-3, Nb-94, C-14, Ni-63 and Ni-59, which are the main radioisotopes that influence the final high values for the clearance requirement and they come from interactions between neutrons and Molybdenum, Nitrogen and Nickel. SLB criteria is respected just in the case of stainless steel 304 .

3.5 Summary of the results

After having seen all the results for the different type of materials a brief summary is required, in order to compare them and understand which options are feasible for the design of ARC's vacuum vessel. The goal of the research is to find an alloy that behaves better than Inconel-718 when it is subjected to high values of neutron fluxes. A comparison between the different materials is done through the following plots, which show just the results for the inner wall of the vacuum vessel:

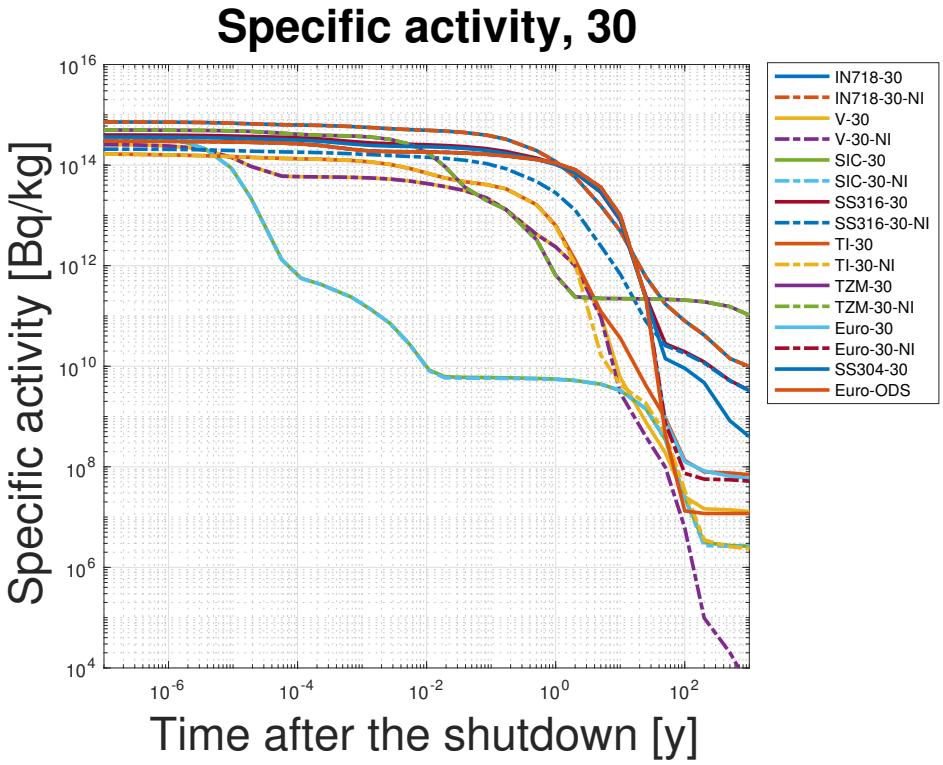

Figure 3.41: Specific activity: final comparison between all structural materials analysed

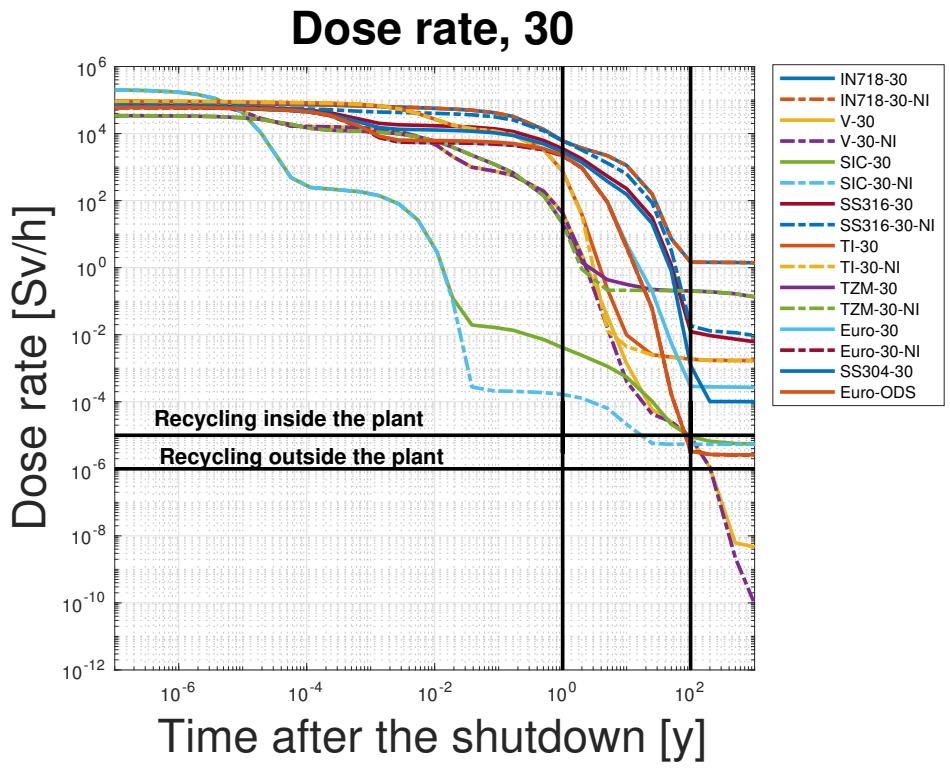

Figure 3.42: Contact dose rate: final comparison between all structural materials analysed

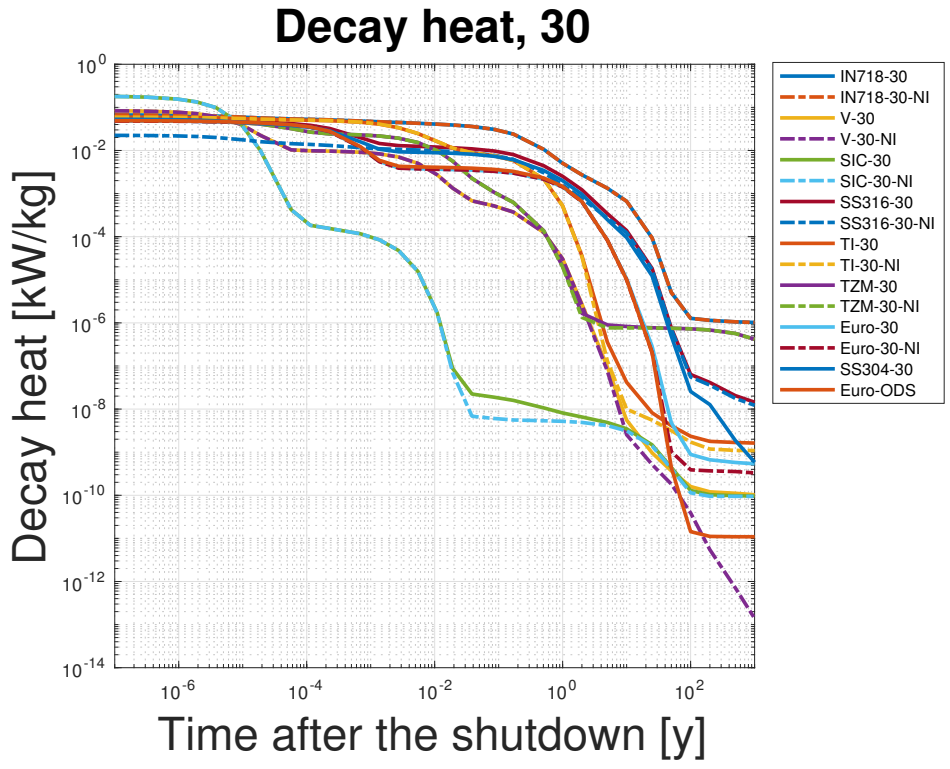

Figure 3.43: Decay heat: final comparison between all structural materials analysed

The first thing that is possible to notice is the very different behaviour of Silicon Carbide, of which specific activity, contact dose rate and decay heat decrease very fast after the shutdown of the reactor. Let's recalling what was said in section 3.4.4, SiC is supposed to be a low activation structural material, but due to the fact that it is not a metal alloy it has got very different physical and mechanical properties compared to Inconel-718. The vacuum vessel of ARC is designed as a single piece with an entire volume of 15.7 m3 [4], a ceramic material like SiC is not recommended for the entire construction of a component with those dimensions, so the final choice should be an alloy.
TZM didn't show good results from the activation analysis and it has got the same problem of Inconel: the main constituent is Molybdenum, which is a high activation element.
After having compared the specific activity, dose rate and decay heat between the remaining options, the Vanadium one seems to be the valid substitute (yellow continuous line for the composition with impurities, purple dashed line for the pure alloy). Both the composition with and without impurities show a rapid decrease of the specific activity and dose rate in time, in addition from Figure 3.42 it is possible to notice that it is the only material that reaches the recycling limits after 100 years of storage. For what concern the decay heat it must be analysed at the beginning, because in case of accident and shutdown of the system radioisotopes continue to decay and produce heat and it must be controlled and removed in order to avoid dangerous situations, such as melting of the piece or explosions. Immediately after the end of the operation the decay heat of V-15Cr-5Ti is equal to 1.04 MW in the inner wall and 2.40 MW in the outer one, then it decreases faster than Inconel-718 along the time and that is an advantage in case of possible accidental scenario (see chapter 6.2), because the temperature evolution can be controlled easier and it is possible to intervene in time for avoiding serious damages to the entire structure.
ARC's vacuum vessel is very close to the plasma's chamber in which the fusion reaction occurs and there is no shielding between them, then the goal of the tokamak is to reach a steady state operational mode, so the materials are supposed to be constantly exposed to the neutron flux that comes from the plasma. The long irradiation time caused the non-respect of the low-activation criteria for the majority of the alloys that were studied.
In the next chapter some of the studied materials will be analysed through the application of Elemental substitution and Isotopic tailoring processes, that act directly on the composition of the material, in order to substitute or eliminate the elements or isotopes that cause the long-term activation. The results will be compared with the ones showed in this chapter in order to see if there are significant improvements.

Table 3.19: Summary of the results for the low-activation criteria for the structural materials analyzed

Material	Recycling inside	Recycling outside	CI	SLB
Inconel-718, inner VV	NO	NO	NO	NO
Inconel-718, outer VV	NO	NO	NO	NO
TZM, inner VV	NO	NO	NO	NO
TZM, no imp., inner VV	NO	NO	NO	NO
TZM, outer VV	NO	NO	NO	NO
TZM, no imp., outer VV	NO	NO	NO	NO
V-15Cr-5Ti, inner VV	YES	YES	NO	YES
V-15Cr-5Ti, no imp., inner VV	YES	YES	NO	YES
V-15Cr-5Ti, outer VV	YES	YES	NO	YES
V-15Cr-5Ti, no imp., outer VV	YES	YES	NO	YES
Ti-6Al-4V, inner VV	NO	NO	NO	NO
Ti-6Al-4V, no imp., inner VV	NO	NO	NO	NO
Ti-6Al-4V, outer VV	NO	NO	NO	YES
Ti-6Al-4V, no imp., outer VV	NO	NO	NO	YES
SiC, inner VV	YES	NO	NO	YES
SIC, no imp., inner VV	YES	NO	NO	YES
SiC, outer VV	YES	NO	NO	YES
SIC, no imp., outer VV	YES	YES	NO	YES
Eurofer97, inner VV	NO	NO	NO	YES
Eurofer97, no imp., inner VV	YES	NO	NO	YES
Eurofer97, outer VV	NO	NO	NO	YES
Eurofer97, no imp., outer VV	YES	NO	NO	YES
Eurofer-ODS inner VV	YES	NO	NO	YES
Eurofer-ODS outer VV	YES	NO	NO	YES
316 SS, inner VV	NO	NO	NO	NO
316 SS, no imp., inner VV	NO	NO	NO	NO
304 SS, inner VV	NO	NO	NO	YES
316 SS, outer VV	NO	NO	NO	NO
316 SS, no imp., outer VV	NO	NO	NO	NO
304 SS, outer VV	NO	NO	NO	YES

Chapter 4

Optimization methods

In the following chapter the alloys that didn't respect the low-activation limits, even in the case without impurities, will be analysed after having applied the following procedures [22]:

- Elemental substitution, which is based on the modification of the mass composition of the material, so one or more alloying elements that cause the long-activation of the alloy are substituted with other ones with the same properties, but that don't lead the formation of long-lived radioactive isotopes.
- Isotopic tailoring acts on the isotopic composition, due to the fact that each element is characterised by the presence of one or more natural isotopes, each of them can react with the neutrons that come from the plasma and cause the formation of radioactive long-lived isotopes through the following reactions with a neutron [22]:
    1. (n,2n): one neutron is absorbed by the isotope and two of them are realised;
    2. (n,gamma ray): one neutron is absorbed by the isotope and a gamma ray is realised;
    3. (n,proton): one neutron is absorbed by the isotope and a proton is realised;
    4. (n,alpha): one neutron is absorbed by the isotope and an alpha particle is realised.

After having identified the isotopes of an element that lead the formation of radionuclides through the previous reactions, they can be eliminated or their percentages can be reduced. Before to see the results of the analysis, let's remind that the elemental substitution method permits to modify directly the composition of an alloy, but this change could cause the variation of the physical and mechanical properties of the material, and this is a disadvantage that must be considered during the analysis, while Isotopic Tailoring modify just the presence of some isotopes, but the nominal composition remains the same [22]. These processes can't be applied if an element is essential or if it is constituted just by one isotope, such as Manganese (Mn-55), Niobium (Nb-93) or Aluminium (Al-27) [22].
The last thing that must be considered is the cost of the two methods, that is not negligible, especially for Isotopic tailoring, while elemental substitution is less expensive [22].
As regards the new code that must be created with FISPACT-II for the application

Isotopic Tailoring, the mass percentage composition was substituted by the isotopic one (like in the case of FLiBe code in Appendix A), so it possible to consider the modified percentage of the undesired isotope.

4.1 Elemental substitution

As it was said in the introduction of the chapter, through elemental substitution it is possible to substitute one or more alloying elements of the initial composition that cause problem for the long-term activation. In particular this method will be applied to stainless steels 316 and 304, where Nickel is substituted with Manganese [22], which is characterised just by one natural isotopes, Mn-55, that doesn't cause the production of long-term isotopes when it reacts with neutrons. Inconel-718 will not be considered in this part of the analysis because Nickel is the main constituent and not an alloying one.

4.1.1 Stainless steels 316 and 304

Stainless steels 316 and 304 contain Nickel as an alloying element, which is one of the main responsible for their high activation. Through elemental substitution the percentage of Nickel is entirely substituted with Manganese.

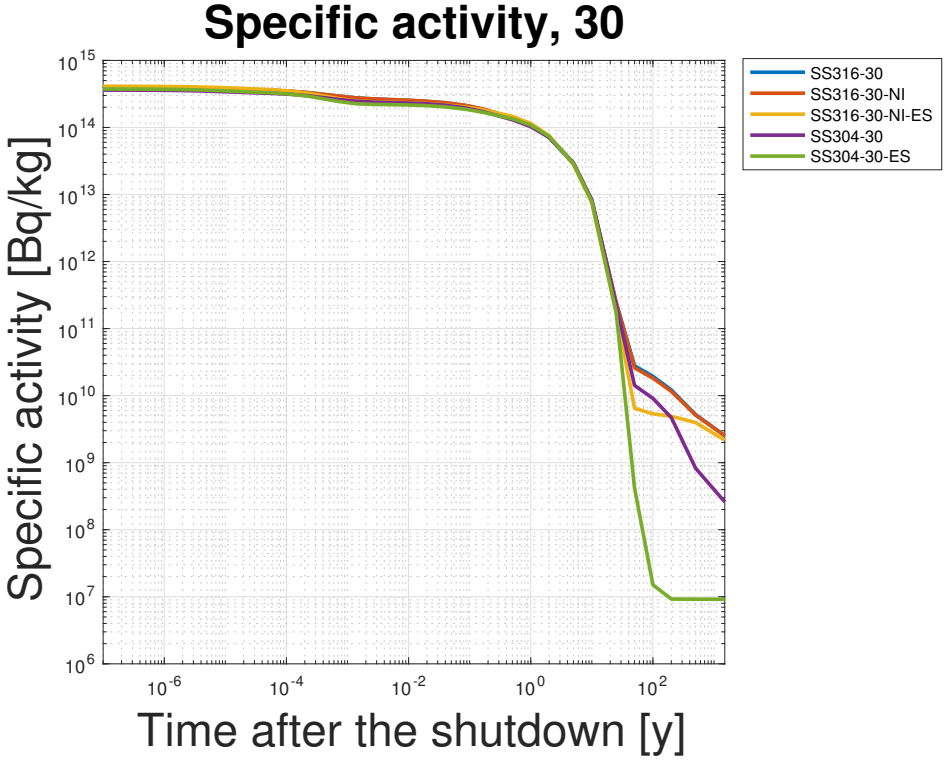

Figure 4.1: Comparison between specific activity of stainless steels 316 and 304 at the beginning of the analysis and after elemental substitution (ES) in the inner region of the vessel

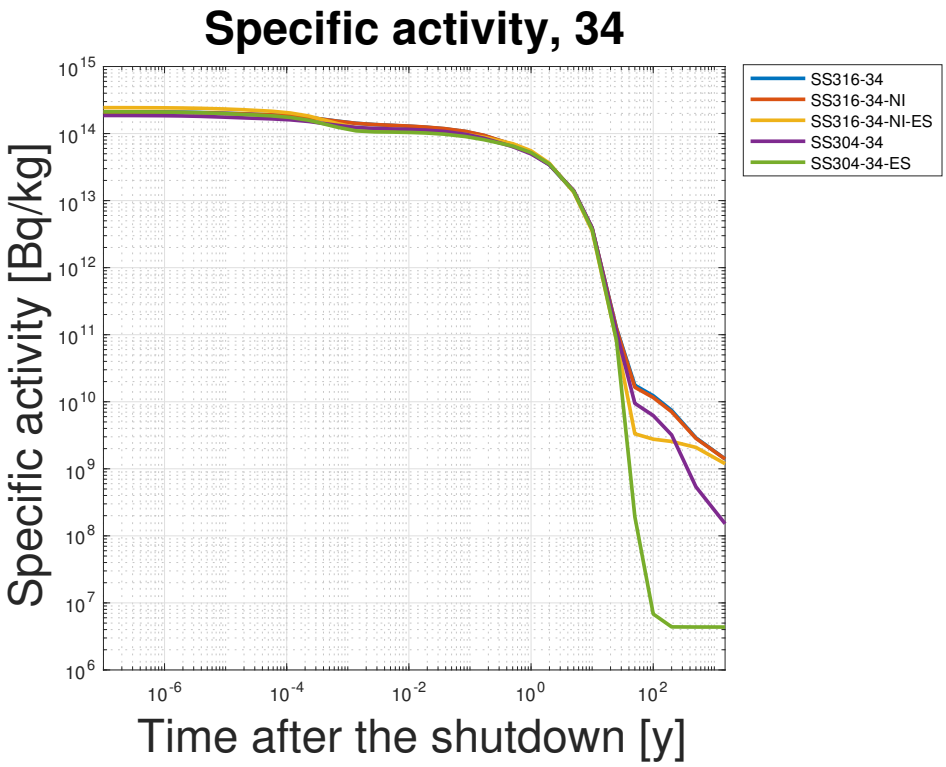

Figure 4.2: Comparison between specific activity of stainless steels 316 and 304 at the beginning of the analysis and after elemental substitution (ES) in the outer region of the vessel

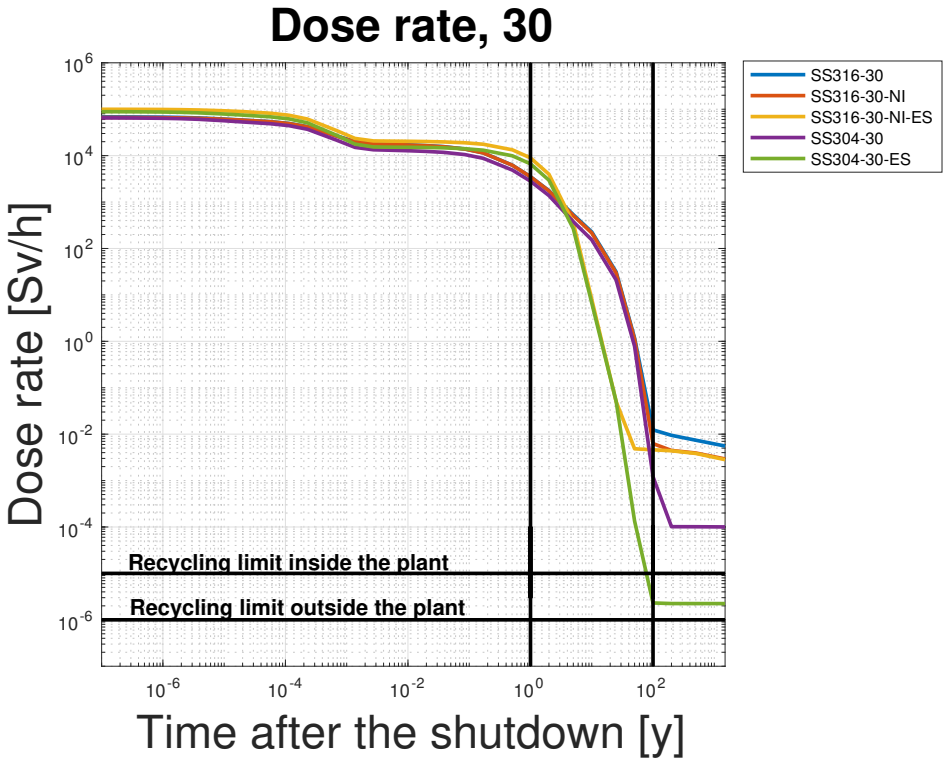

Figure 4.3: Comparison between dose rate of stainless steels 316 and 304 at the beginning of the analysis and after elemental substitution (ES) in the inner region of the vessel

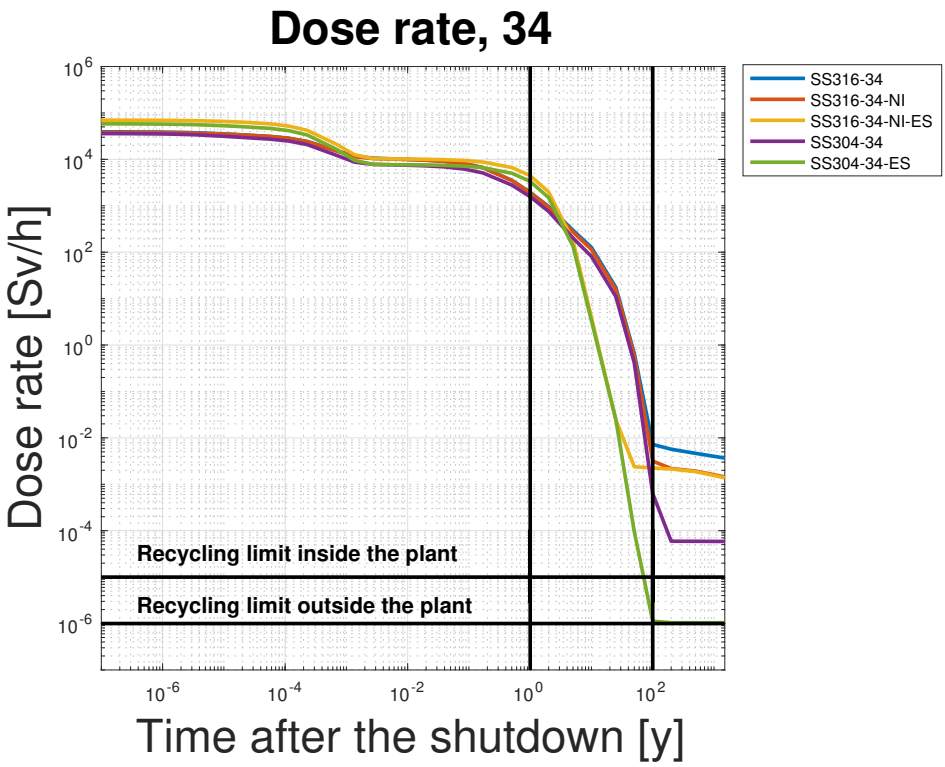

Figure 4.4: Comparison between dose rate of stainless steels 316 and 304 at the beginning of the analysis and after elemental substitution (ES) in the outer region of the vessel

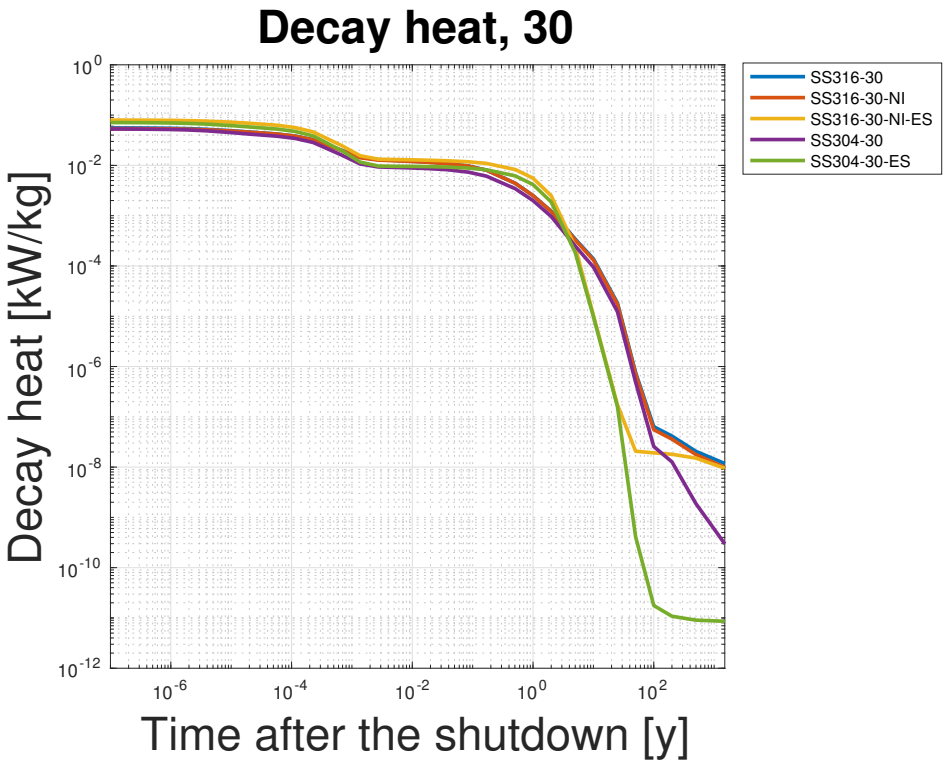

Figure 4.5: Comparison between decay heat of stainless steels 316 and 304 at the beginning of the analysis and after elemental substitution (ES) in the inner region of the vessel

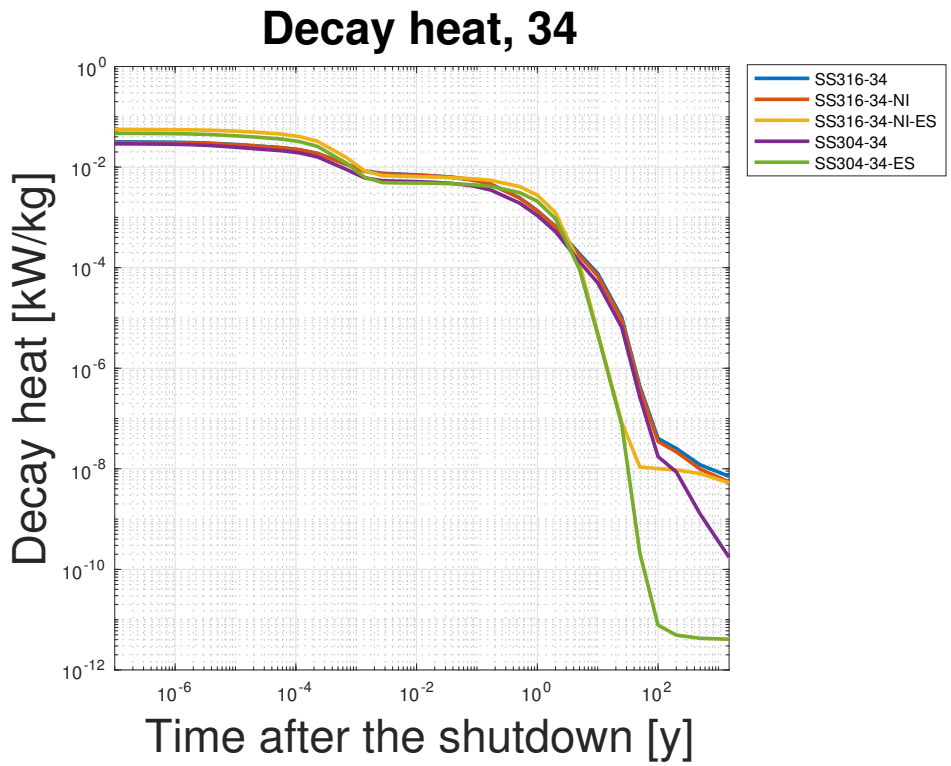

Figure 4.6: Comparison between decay heat of stainless steels 316 and 304 at the beginning of the analysis and after elemental substitution (ES) in the outer region of the vessel

After having seen the last plots it is possible to conclude that elemental substitution didn't affect too much the results at the beginning of the storage period, in fact the comparison can underline that the initial behaviour of the three parameters is almost the same. Figures 4.9 and 4.10 show a faster decrease of the contact dose rate of stainless steel 304, after elemental substitution, which permit to reach the recycling limit inside the plant in the inner wall of the vacuum vessel, while in the outer area it reaches both recycling limits by 100 years after the shutdown.
Stainless steel 316 shows a worse behaviour with respect to the type 304 and the reason can be related to the presence of Molybdenum, a high activation element, in its nominal composition.

In the following table there are the values obtained from the evaluation of the clearance index and waste disposal rating:

Table 4.1: Clearance index and SLB after the application of elemental substitution for stainless steels 316 and 304

	Clearance index after 100 years	**SLB**
SS 316, no impurities, elemental substitution, inner wall of VV	1.94E+005	1.48E+001
SS 316, no impurities, elemental substitution, outer wall of VV	1.17E+005	8.40E+000
SS 304, elemental substitution, inner wall of VV	1.53E+002	3.89E-003
SS 304, elemental substitution, outer wall of VV	7.07E+001	5.87E-003

SLB is reached just for stainless steel 304, while the clearance index is still higher than 1 after 100 years for both alloys. In the next section isotopic tailoring will be applied to these steels, then a final comparison between all the analysis will be done in order to understand how these methods can affect the final results.

4.2 Isotopic tailoring

This section is based on the analysis of the natural isotopes of each element that can lead to the creation of long-lived radioactive isotopes in the alloys analysed in Chapter 3. None of them respected the main criteria for the decommissioning and the goal of this chapter is the analysis of their compositions, in order to see if the reduction or elimination of certain isotopes can lead improvements for the activation analysis.

4.2.1 Inconel-718

The first alloy that was analysed is Inconel-718, of which composition (Table 3.3) permits to highlight the high presence of Nickel, the primary element, followed by Molybdenum and Niobium in lower percentages. In this section the reduction or elimination of specific isotopes will be studied, in order to see how much their presence is relevant for the analysis. The main natural isotopes that were observed for Inconel-718 are [22]:

- Nickel: Ni-58 (67.76%), Ni-60 (26.6%), Ni-61 (1.25%), Ni-62 (3.66%) and Ni-64 (1.16%) [28]. Ni-58 and Ni-60 produce Ni-59, with half-life of 76000 years, through (n,gamma) and (n,2n) reactions. Ni-62 and Ni-64 through the same previous reactions cause the formation of Ni-63 [22], which is another radioactive isotopes with a half-life of 100 years, that characterises the 74% of the total specific activity after 100 years.

- Molybdenum: Mo-92 (15.8%), Mo-94 (9.12%), Mo-95 (15.7%), Mo-96 (16.5%), Mo-97 (9.45%), Mo-98 (23.75%) and Mo-100 (9.72%) [28]. Except for Mo-97, which doesn't have significant reactions, the other isotopes can become radioactive when they interact with neutrons that come from the plasma, in particular Mo-94 through a (n,proton) reaction produces Nb-94 [22], with half-life of 20326 years [28].

- Niobium: Nb-93(100%) and it leads the formation of Nb-94 like in the case of Mo-94, but the main problem is that it is the only natural isotope that constitute Niobium and it is difficult to act on it, especially when this element is an alloying one of the original composition of Inconel-718 (5.5% mass percentage, Table 3.3) [22].

From the last considerations the two main isotopes that don't create particular dangers when they interact with neutrons are: Ni-61 and Mo-97. So through the Isotopic tailoring process we can enrich the alloy with the last two isotopes, in order to see how the results of the activation analysis can change.
The code that is used is FISPACT-II is shown in the Appendix and the results of Inconel-718 with 100% of Ni-61 and Mo-97 are shown in the plots below, in which there is a comparison with the analysis of the original composition.

Before to see the results let's remind that the total enrichment of those two isotopes is an ideal assumption; actually 100% isotopic selectivity can't be reached, normally the maximum level could be 99.95%[22], but as it was said at the beginning of the research ARC is still a design of a reactor, so it is possible to apply this kind of analysis, just for having a rough idea of the possible final results, for the final construction of the plant a more precise analysis will be required.

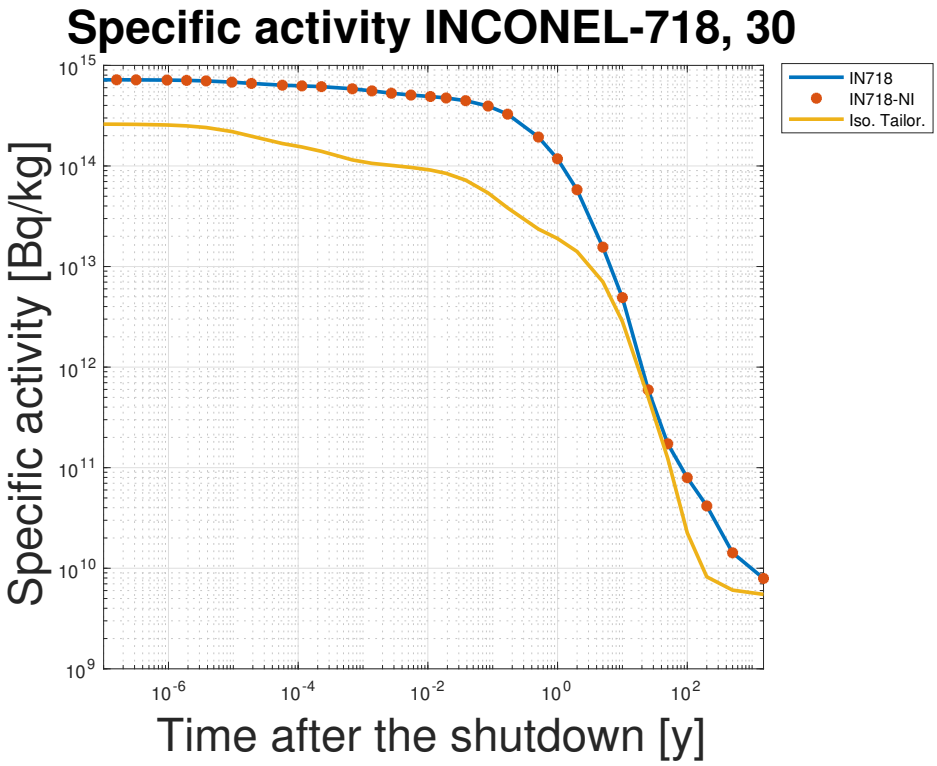

Figure 4.7: Specific activity of Inconel-718 in the inner region of the vessel

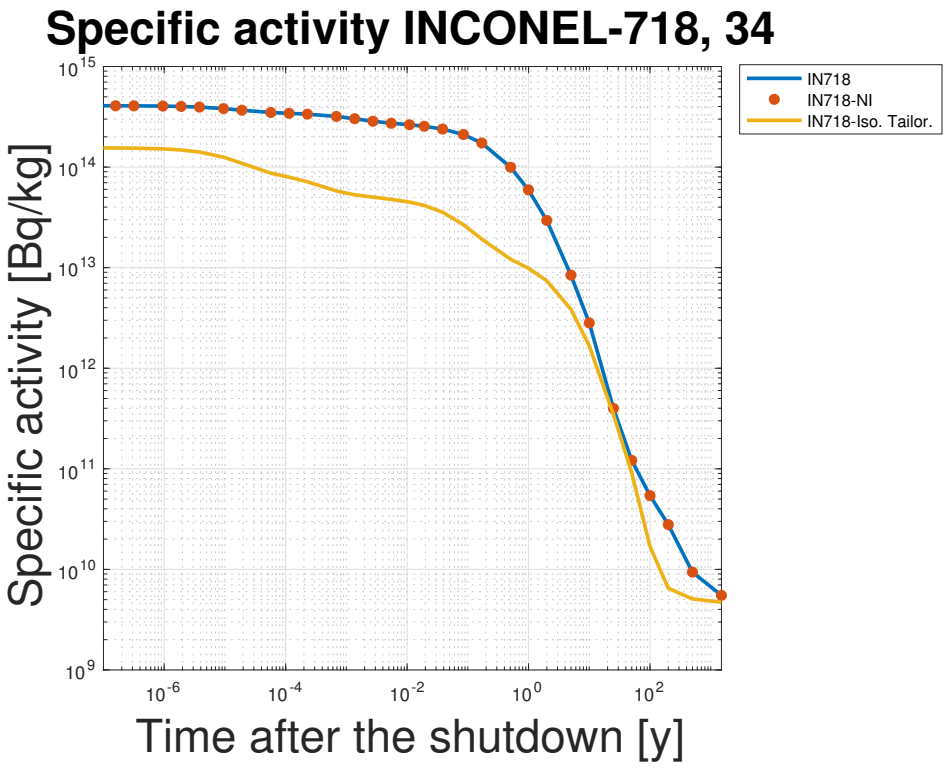

Figure 4.8: Specific activity of Inconel-718 in the outer region of the vessel

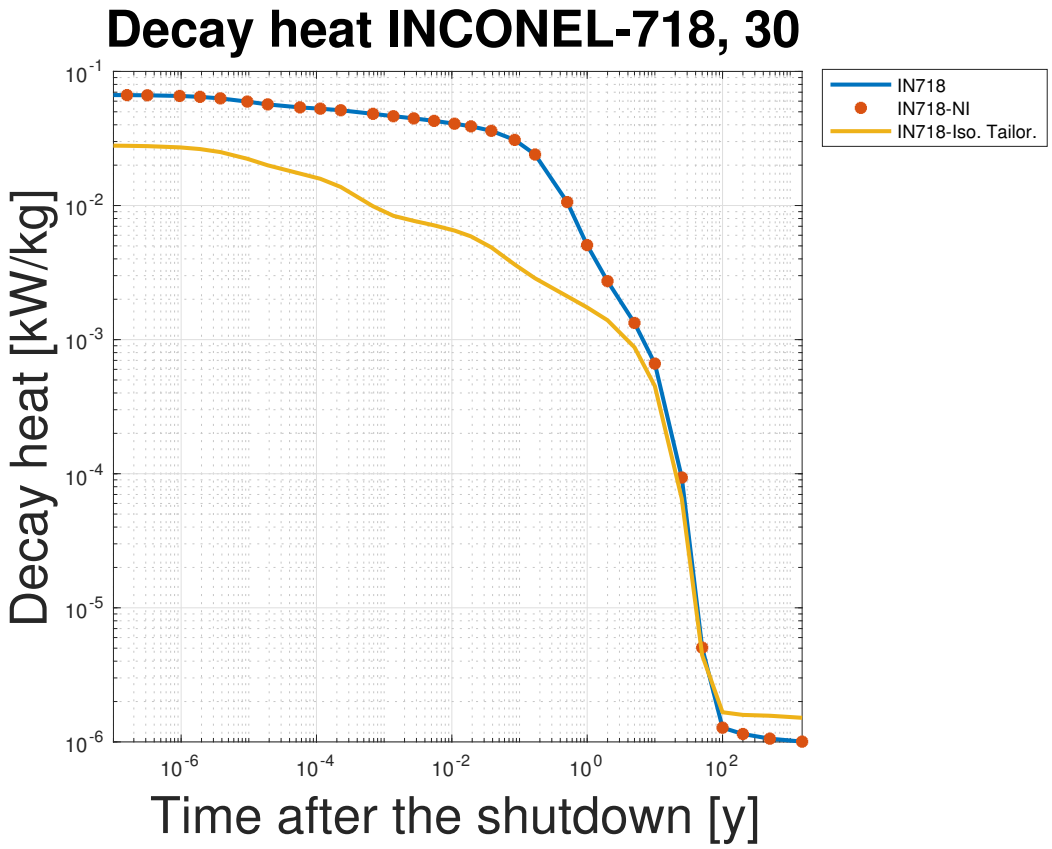

Figure 4.9: Decay heat of Inconel-718 in the inner region of the vessel

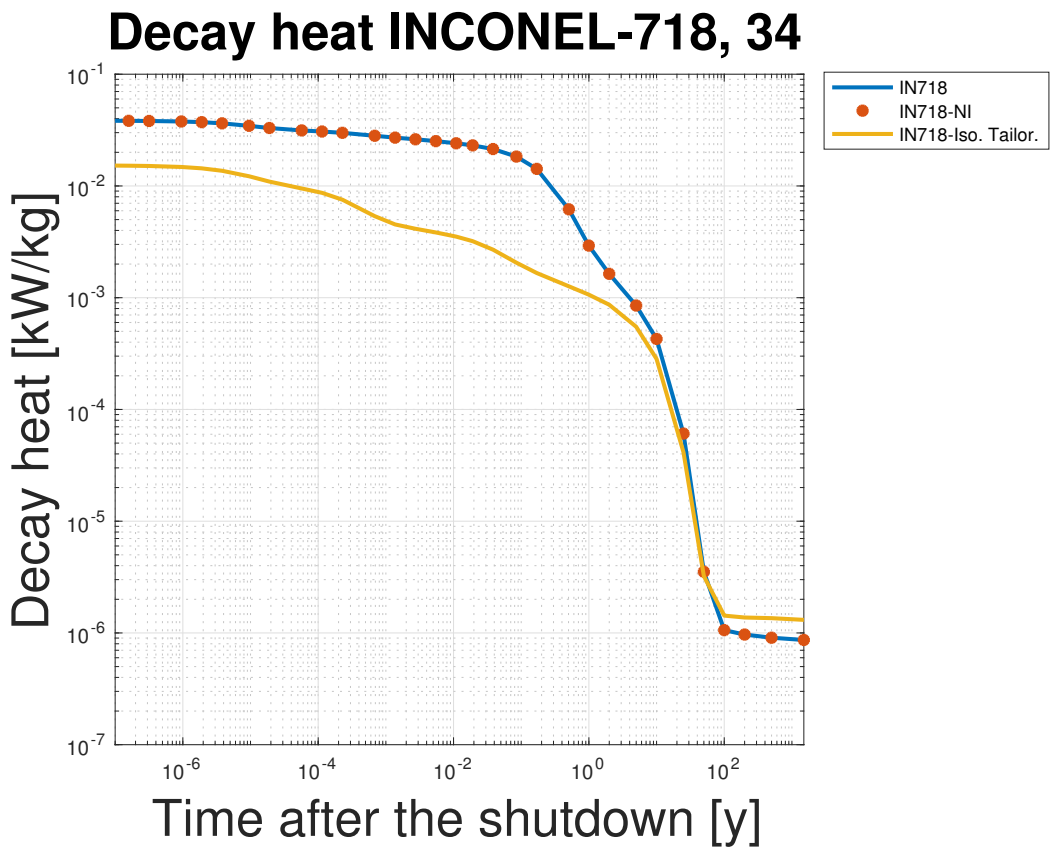

Figure 4.10: Decay heat of Inconel-718 in the outer region of the vessel

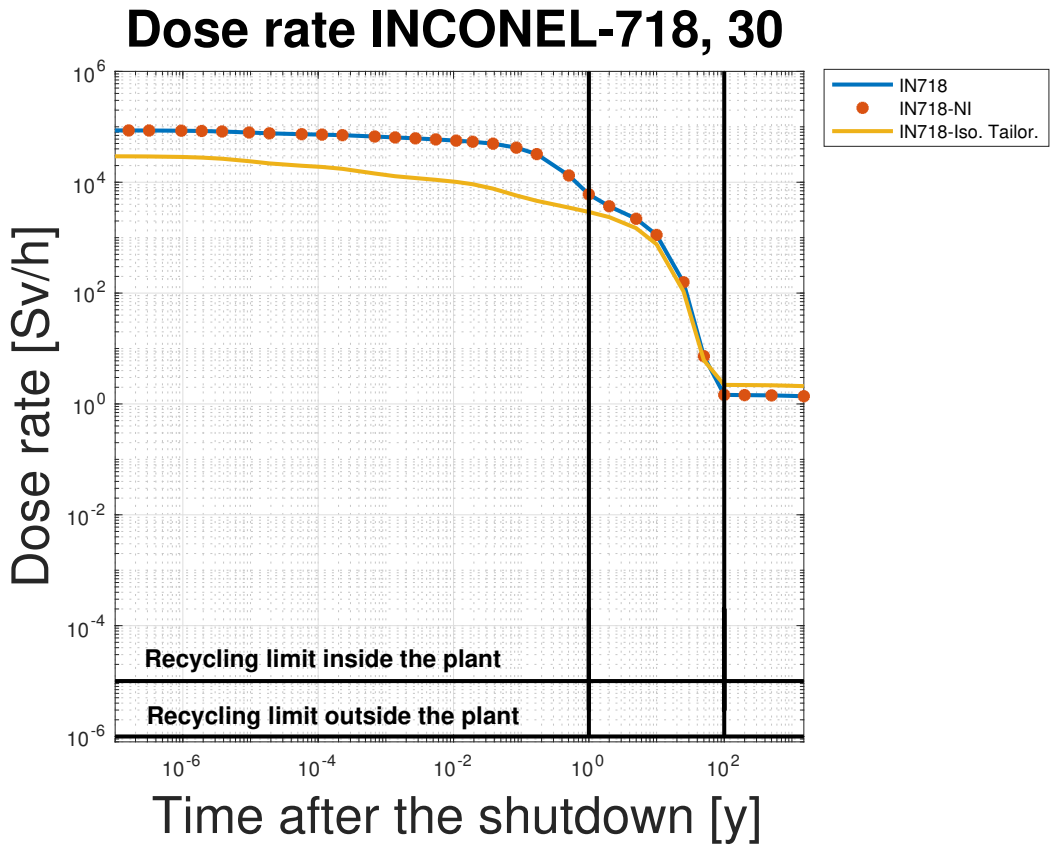

Figure 4.11: Dose rate of Inconel-718 in the inner region of the vessel

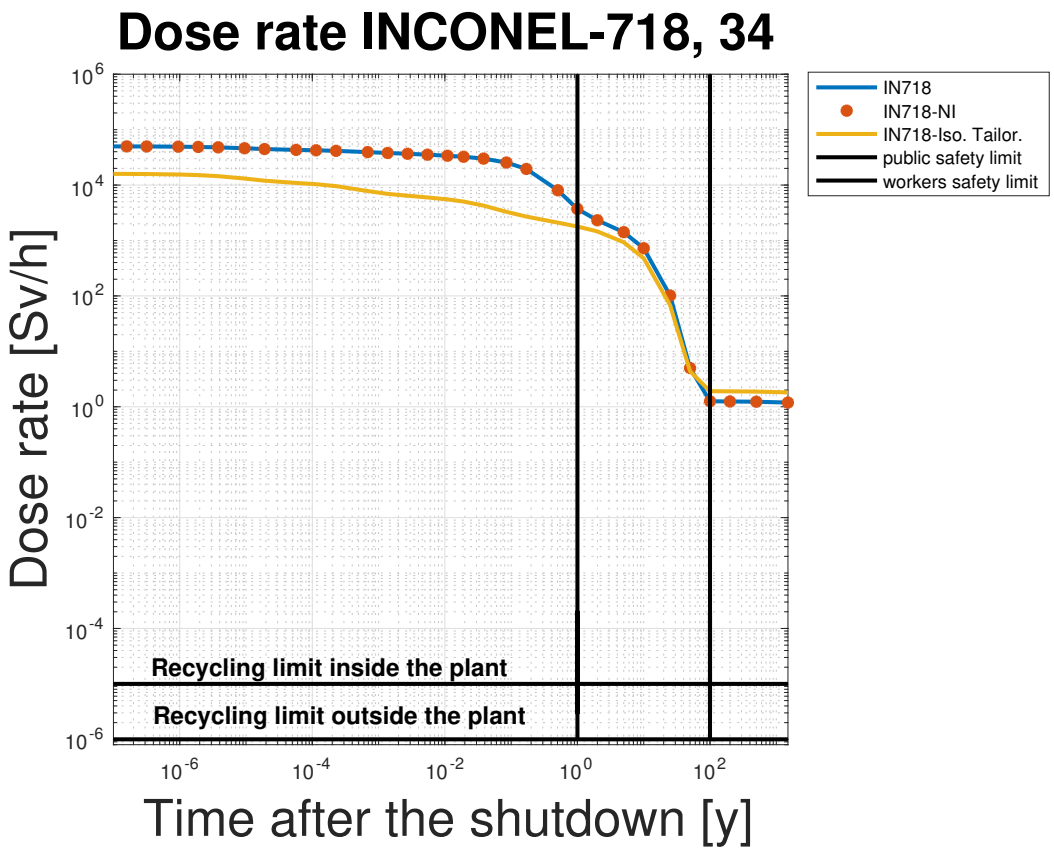

Figure 4.12: Dose rate of Inconel-718 in the outer region of the vessel

The final comparison between the results of all the activation analysis performed on Inconel-718 shows that despite of its excellent mechanical properties it is not good from the low-activation point of view. Even after the application of isotopic tailoring the recycling limits are not reached and even the decommissioning criteria proves that it can't be wasted without particular restrictions:

Table 4.2: Clearance index and SLB for Inconel-718 after isotopic tailoring

	Clearance index at 100 years	**SLB**
Inconel-718 inner wall VV	6.04E+007	6.67E+003
Inconel-718 outer wall VV	5.23E+007	5.78E+003

The only parameter that shows an improvement immediately after the end of the operation is the decay heat, which is decreased of one order of magnitude, but it is not enough in order to define Inconel-718 the best choice for ARC.

4.2.2 TZM

The main problem for the activation of TZM is related to its primary component, Molybdenum, like in the case of Inconel-718 with Nickel. As it was explained in the previous subsection, Molybdenum is characterized by natural isotopes that through reactions with neutrons can lead to the production of long-lived radioisotopes, which influence its long-term activation and the non-respect of the low-activation criteria. The idea for this alloy is the 100% enrichment of Mo-97, which is the only one that doesn't create dangerous isotopes when it interacts with neutrons [22]. The final results of the activation analysis are reported in the following plots, compared with the ones from the original composition.

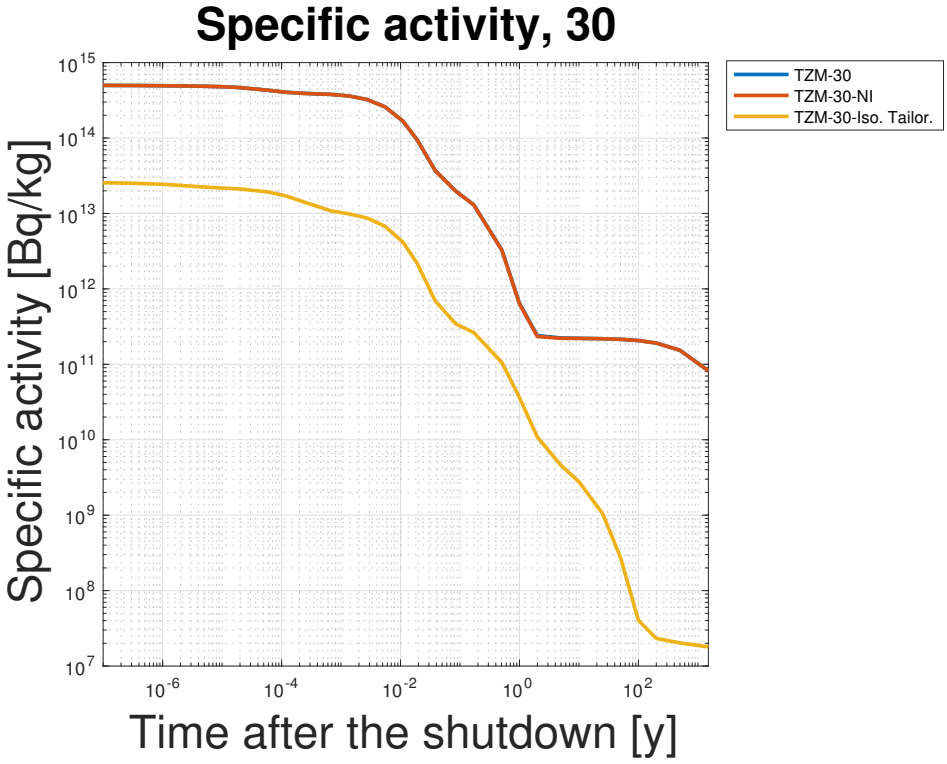

Figure 4.13: Specific activity of TZM after Isotopic tailoring process in the inner region of the vessel

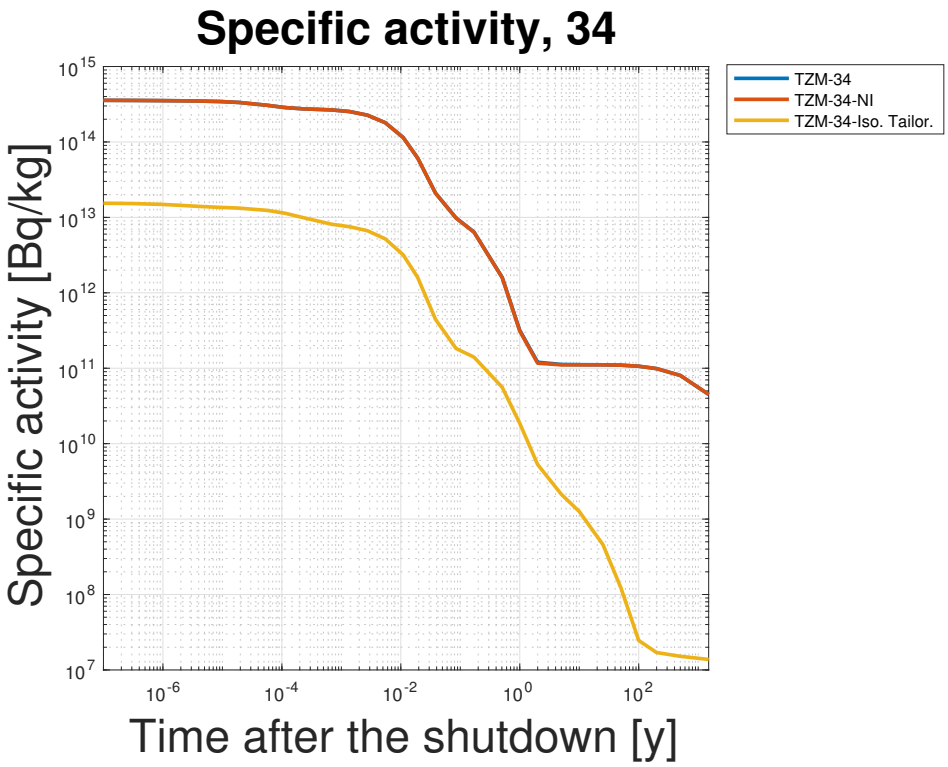

Figure 4.14: Specific activity of TZM after Isotopic tailoring process in the outer region of the vessel

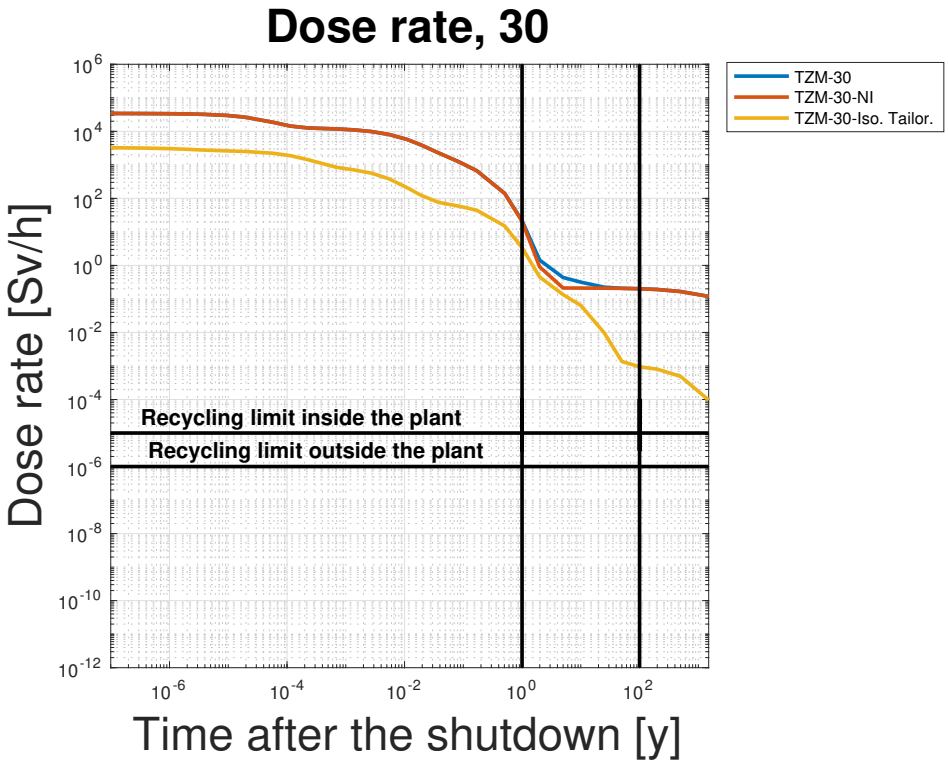

Figure 4.15: Dose rate of TZM after Isotopic tailoring process in the inner region of the vessel

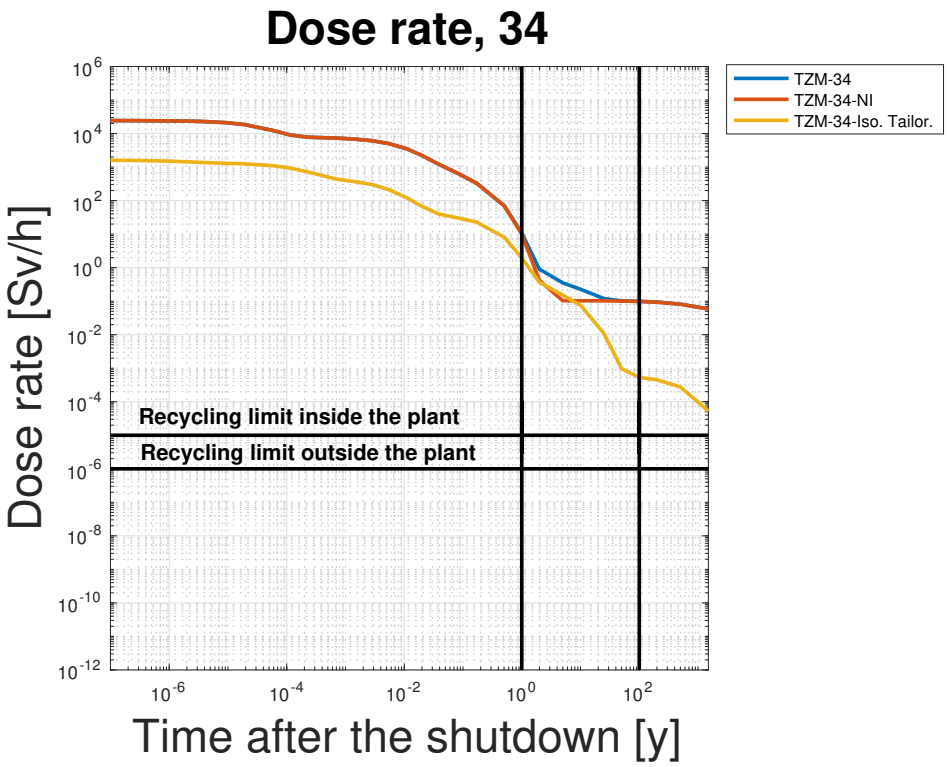

Figure 4.16: Dose rate of TZM after Isotopic tailoring process in the outer region of the vessel

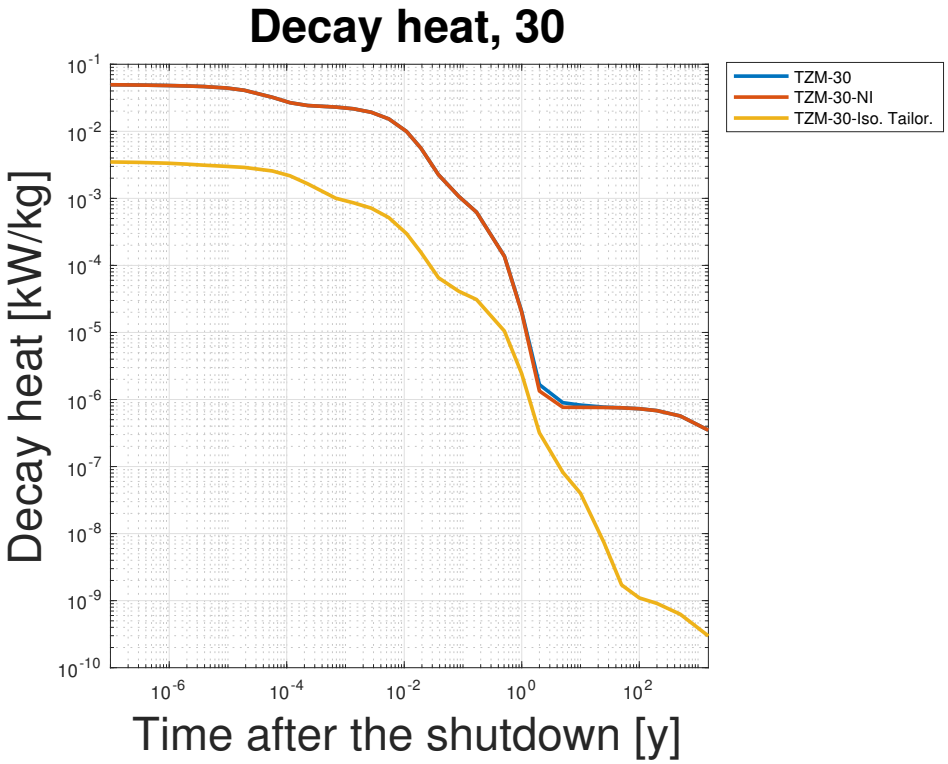

Figure 4.17: Decay heat of TZM after Isotopic tailoring process in the inner region of the vessel

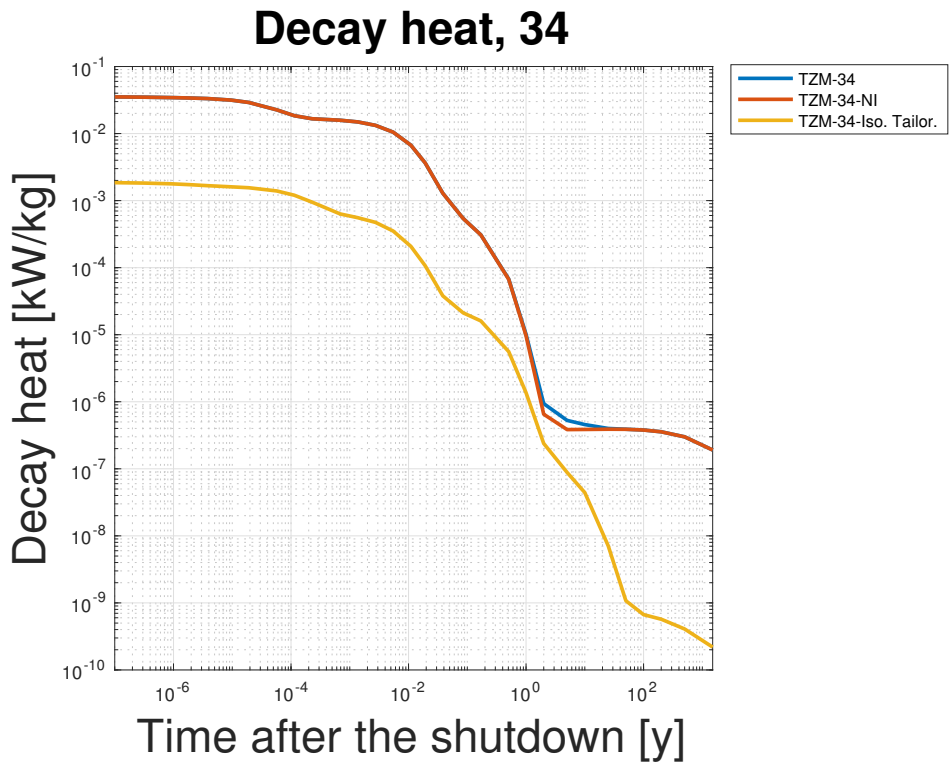

Figure 4.18: Decay heat of TZM after Isotopic tailoring process in the outer region of the vessel

As it is possible to notice isotopic tailoring permitted to obtain good improvements for TZM; the elimination of the main isotopes that caused the creation of long-lived radioisotopes shows good results for the activation analysis, in particular a reduction of two orders of magnitude of the decay heat and its faster decrease is an important goal, especially in case of accidents in which the decay heat is the main problem that must be taken under controlled and limited as much as possible. For what concern the contact dose rate Figure 4.15 and 4.16 underline a reduction and rapid decrease in time, but the requirements for a possible recycling inside or outside the plant are still not reached.
In the following table there are the new values for the clearance and Shallow Land Burial indexes of the modified alloy:

Table 4.3: Cleareance index and SLB of TZM alloy after isotopic tailoring

	Clearance index at 100 years	**SLB**
TZM inner wall VV	2.17E+004	1.99E+000
TZM outer wall VV	1.74E+004	1.60E+000

The improvements related to the application of isotopic tailoring can be seen in the final values of clearance and SLB indexes. The comparison between the results of Table 3.11 and the last one permits to notice a reduction of two orders of magnitude for both cases, especially SLB is almost close to the limit value 1 at 100 years after the shutdown.

4.2.3 Eurofer97

In chapter 3 Eurofer97 was analysed both in the case with and without impurities, but in each situation it didn't respect the low-activation criteria, so in the following section the isotopic tailoring will be applied in order to see if acting directly on the isotopic composition the results can be improved.
The main impurities that cause problems are Nitrogen, that is characterized by N-14 (99.365%) and N-15 (0.365%), in particular the first one leads the formation of the radioisotope C-14 [22], which is at fault for the non-respect of the clearance index of Eurofer97. The composition with the presence of impurities contains Nickel and Molybdenum, and even for this analysis all their isotopes are substituted with Ni-61 and Mo-97, as it was explained for Inconel-718; then N-14 is eliminated and there is the 100% of N-15, that still causes the production of C-14, but in lower quantity [22]. For the composition without impurities the main action is the elimination of N-14. After this step the activation analysis was performed and the results are shown in the next plots.

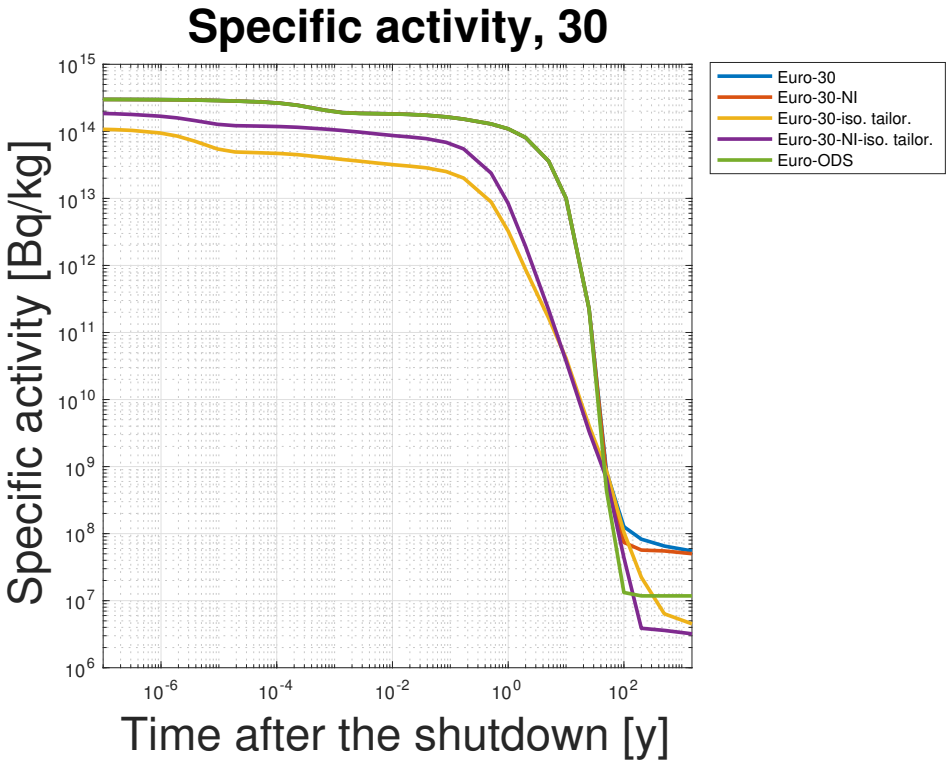

Figure 4.19: Specific activity of Eurofer97: comparison before and after isotopic tailoring in the inner region of the vessel

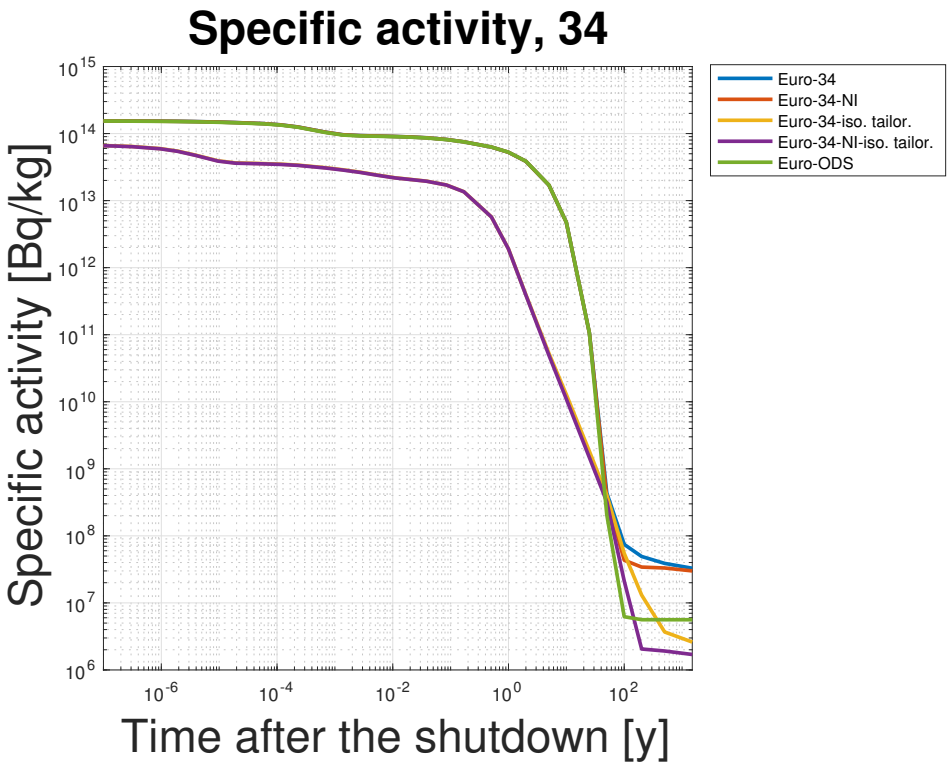

Figure 4.20: Specific activity of Eurofer97: comparison before and after isotopic tailoring in the outer region of the vessel

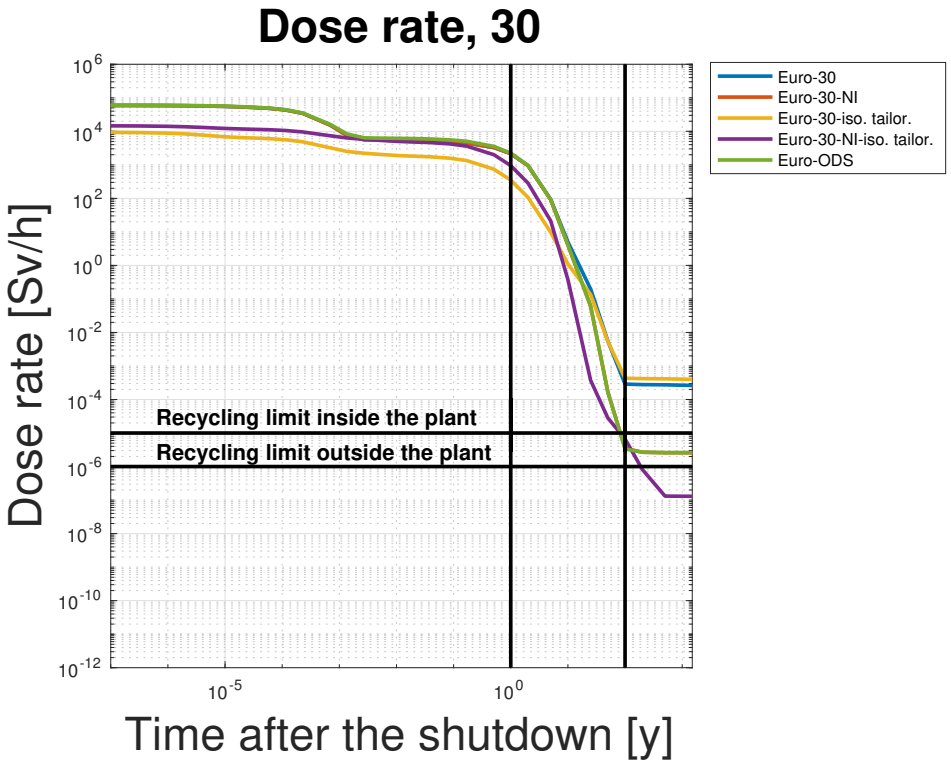

Figure 4.21: Dose rate of Eurofer97: comparison before and after isotopic tailoring in the inner region of the vessel

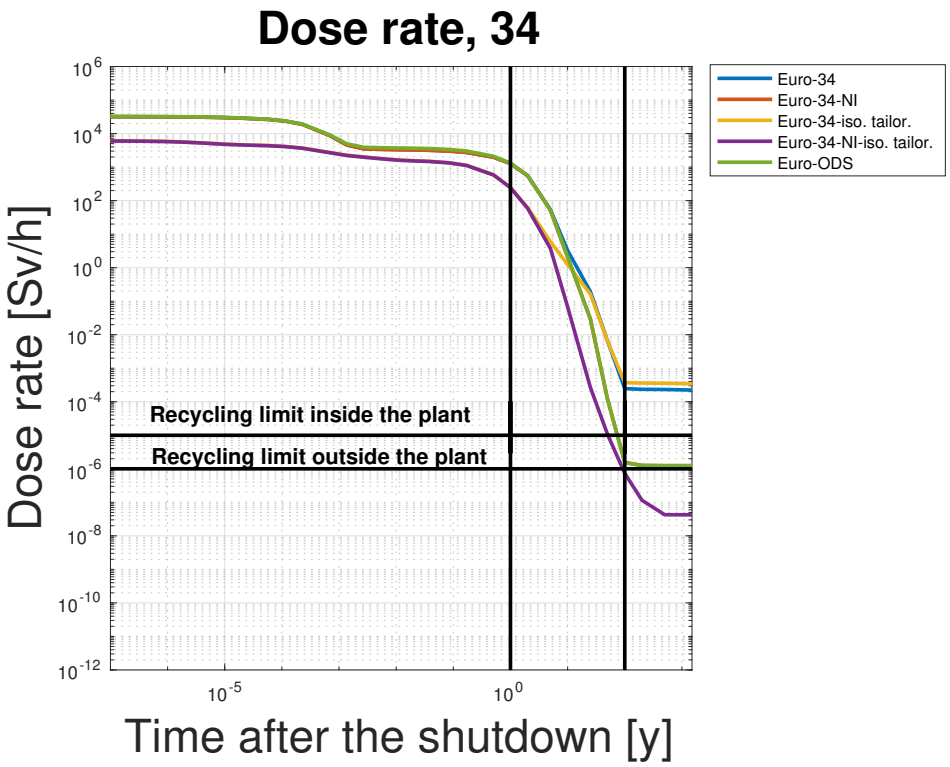

Figure 4.22: Dose rate of Eurofer97: comparison before and after isotopic tailoring outer region of the vessel

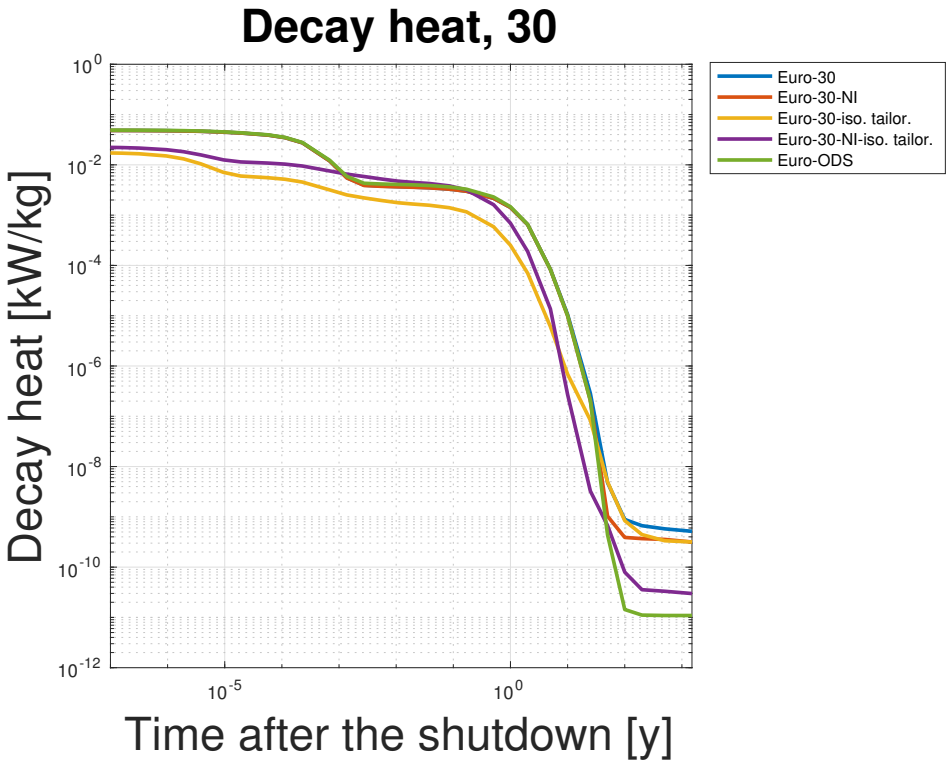

Figure 4.23: Decay heat of Eurofer97: comparison before and after isotopic tailoring in the inner region of the vessel

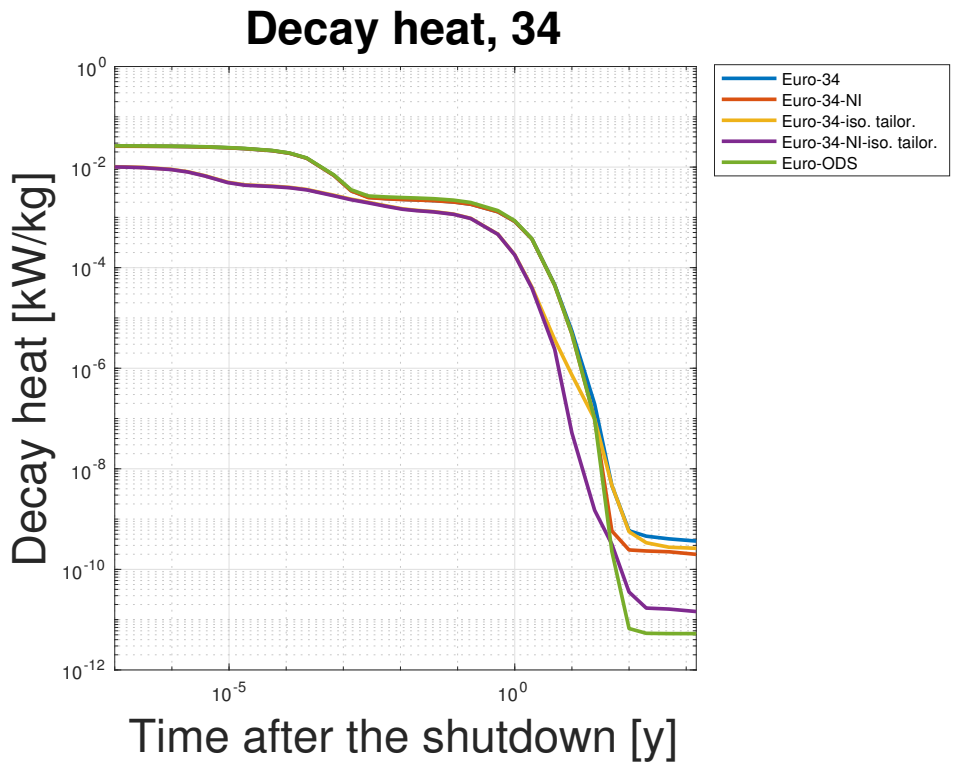

Figure 4.24: Decay heat of Eurofer97: comparison before and after isotopic tailoring in the outer region of the vessel

The final comparison for each parameter underline significant improvements for the steel without impurities with the application of isotopic tailoring.
Through the composition without impurities it is possible to avoid the presence of Niobium, which is the main at fault for the high activation of this alloy. The application of isotopic tailoring doesn't permit to act on the percentage of that impurities, due to the fact that it is characterized by just one natural isotope, so the only way for having improvements for the low-activation of the material is the total elimination of the undesired impurity. The contact dose rate of Eurofer97 without impurities and with the application of isotopic tailoring reaches the recycling limit both inside and outside the plant, while in the case of the original steel the last requirement wasn't satisfied (Figure 3.33 and Figure 3.34).

As regards the other two criteria for the low activation analysis the results for the composition without impurities are in the following table:

Table 4.4: Clearance index and SLB criteria for Eurofer97 without impurities, after isotopic tailoring

	Clearance index at 100 years	**SLB**
Eurofer97 no imp inner wall VV	1.65E+004	1.28E-002
Eurofer97 no imp outer wall VV	2.32E+003	5.86E-003

SLB criteria is respected, like at the beginning of the analysis (Table 3.15), while the problem was related to the clearance index, which is lower than the original composition but still higher than 1.

4.2.4 Stainless steels 316 and 304

The compositions of the two types of stainless steels analysed for this research are both characterized by the high percentage of Nickel, as it is shown in Table 3.16, and in particular the type 316 contains a relevant quantity of Molybdenum (2.5%). These elements, as it was explained for Inconel-718 and TZM, lead the formation of long-lived radioisotope and the results explained in section 3.4.6 demonstrated that these steels didn't respect the low-activation criteria. In this section their activation analysis was performed after the application of isotopic tailoring to their nominal composition (without impurities) and the main modification for both alloys was related to the enrichment of Ni-61. In addition for the type 316 the isotopic composition of Molybdenum was modified and just Mo-97 was considered [22]:

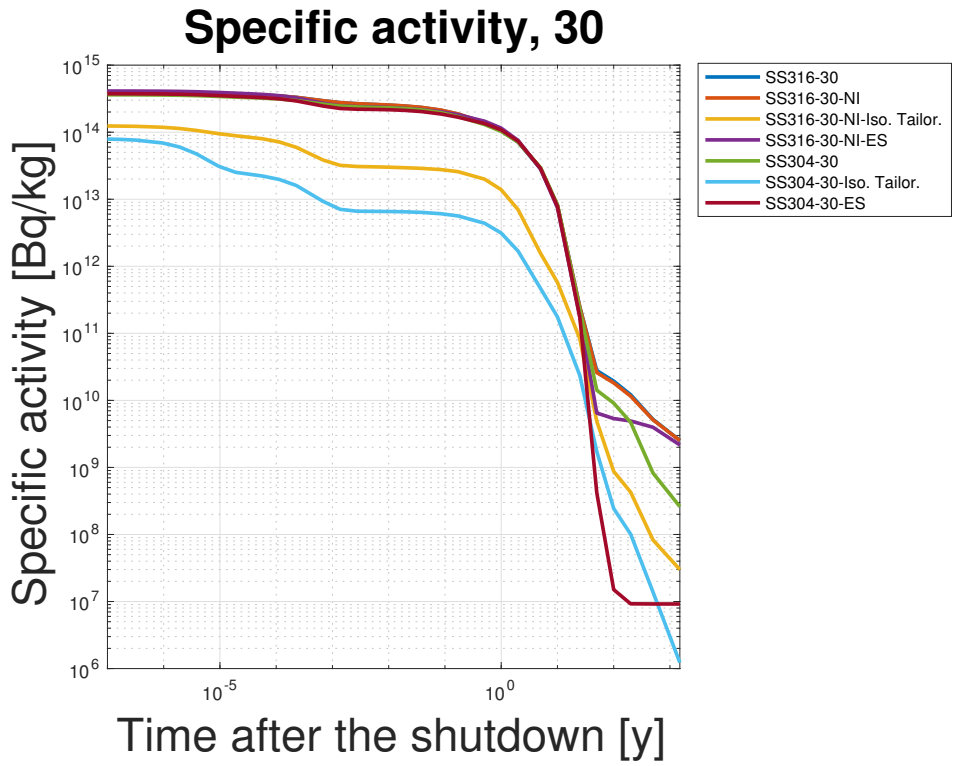

Figure 4.25: Specific activity of stainless steels 316 and 304 after Isotopic tailoring process in the inner region of the vessel

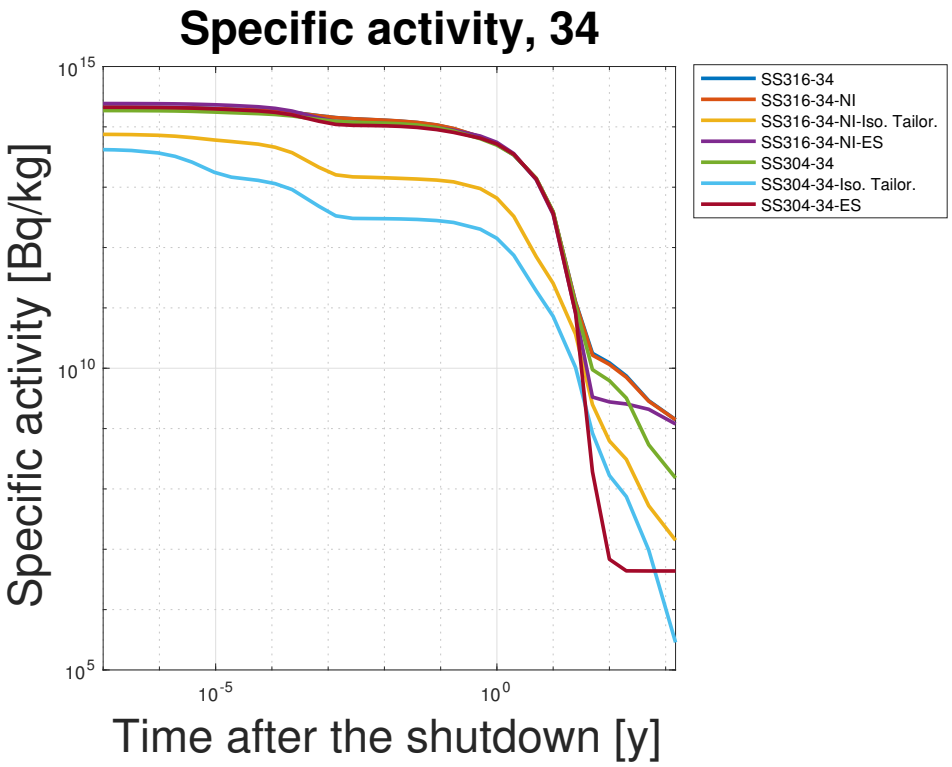

Figure 4.26: Specific activity of stainless steels 316 and 304 after Isotopic tailoring process in the outer region of the vessel

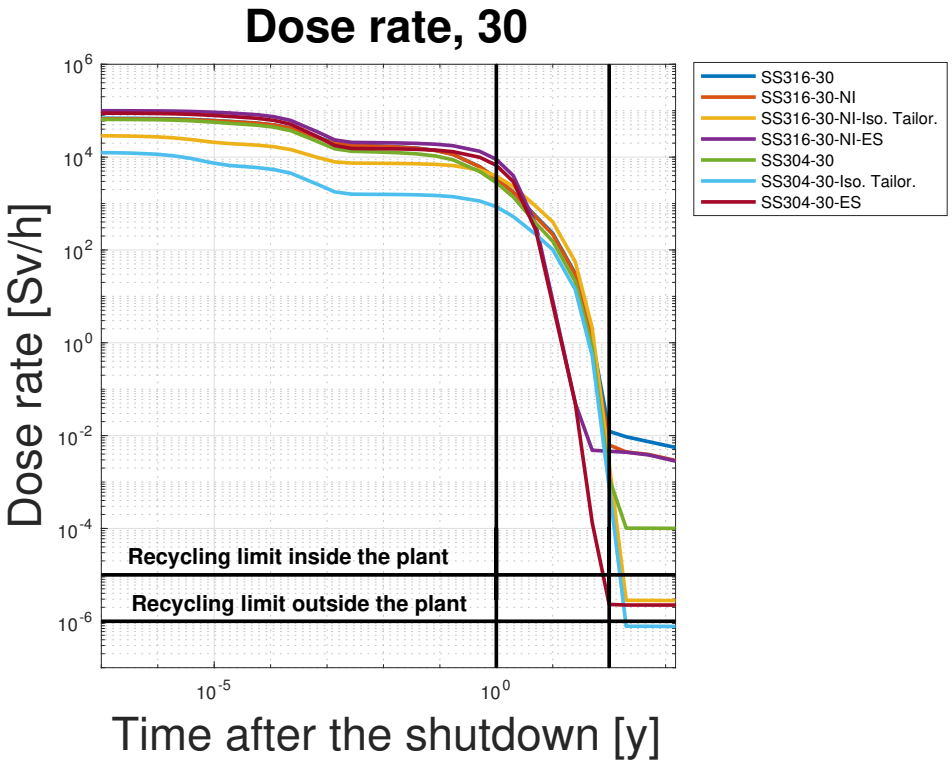

Figure 4.27: Dose rate of stainless steels 316 and 304 after Isotopic tailoring process in the inner region of the vessel

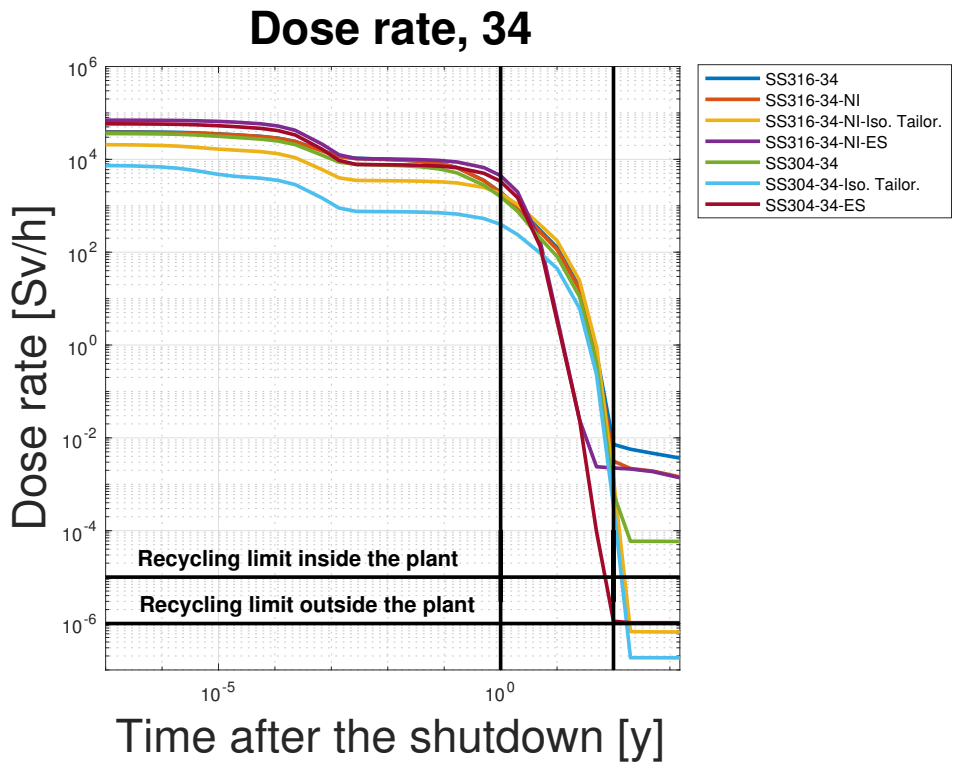

Figure 4.28: Dose rate of stainless steels 316 and 304 after Isotopic tailoring process in the outer region of the vessel

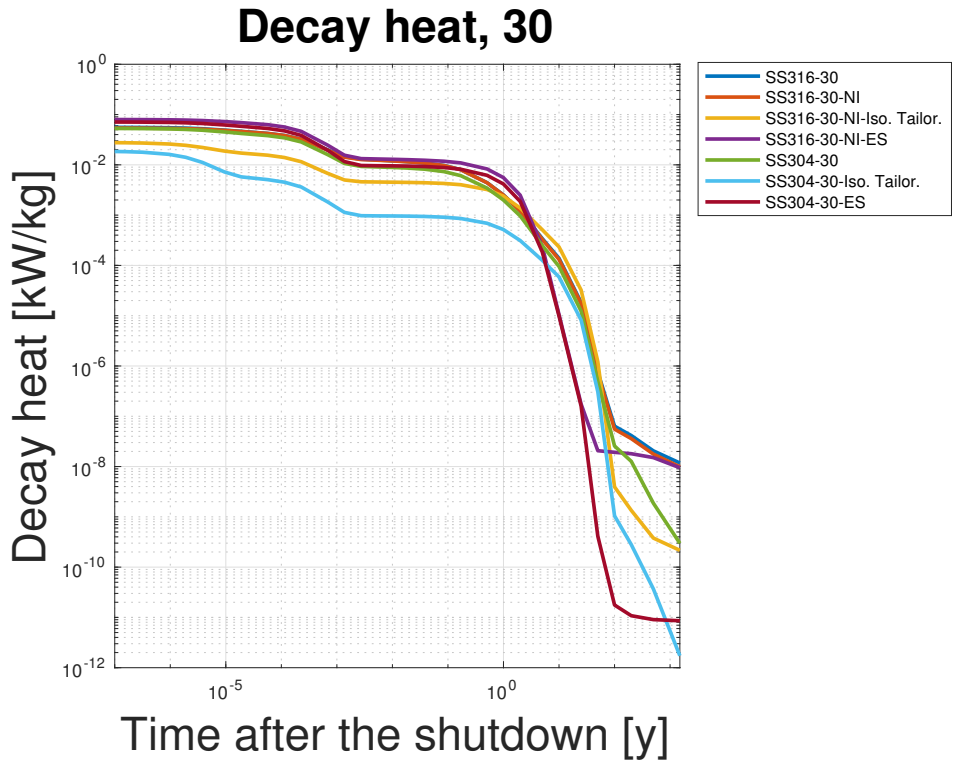

Figure 4.29: Decay heat of stainless steels 316 and 304 after Isotopic tailoring process in the inner region of the vessel

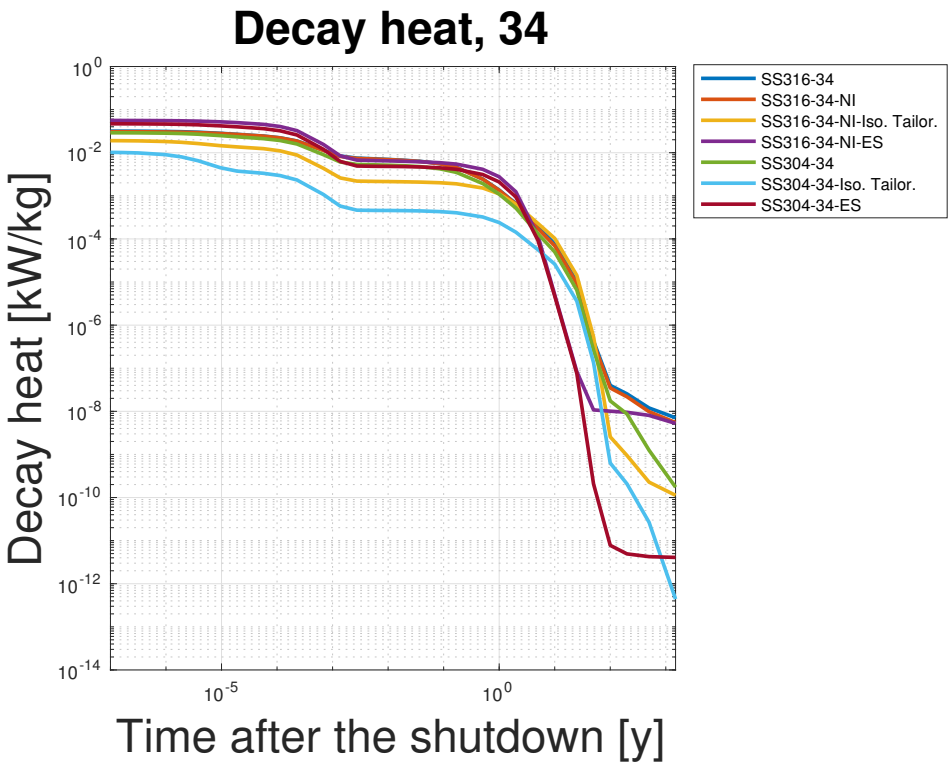

Figure 4.30: Decay heat of stainless steels 316 and 304 after Isotopic tailoring process in the outer region of the vessel

The final comparison between the original compositions and the ones after the application of elemental substitution and isotopic tailoring highlights the following differences:

- the contact dose rate shows big improvements for the stainless steel 316 after isotopic tailoring, and the recycling limit inside the plant is reached in the inner region of the vessel, while the limit outside the plant is achieved just in the outer wall of the vacuum vessel.
- Both alloys are characterised by lower values of decay heat after isotopic tailoring.

Table 4.5: Clearance and SLB indexes for SS316 without impurities and SS 304 after the application of isotopic tailoring

	Clearance index at 100 years	**SLB**
SS316 no imp. inner wall VV	2.62E+004	8.76E-002
SS316 no imp. outer wall VV	4.45E+003	1.94E-002
SS304 inner wall VV	1.35E+004	7.97E-003
SS304 outer wall VV	2.13E+003	5.03E-003

The application of isotopic tailoring to stainless steel 316 permits to reach a value of the waste disposal rating lower than 1 after 100 years, which is the requirement for Shallow Land Burial criteria, while with the original composition and even in the case after elemental substitution it wasn't obtained.
The clearance index is lower than the values at the beginning of the analysis but still higher than 1, so even after the isotopic modification these stainless steels can't be cleared after 100 years from the shutdown of the system.

The application of Isotopic Tailoring and Elemental substitution permitted to see that they could lead to some improvements in the final results, but they are not enough for justifying the high cost related to the application of the two methods. In particular Isotopic Tailoring applied to Inconel-718 didn't reach the hoped results, so this is the final proof that demonstrates that even through the modification of the nominal composition, it is not possible to transform the original alloy of ARC in a low-activation one.

Chapter 5

Liquid blanket activation analysis

The selected blanket for ARC is a molten salt: FLiBe. For its activation analysis both the coolant region (the channel, 31) and the tank (region 40) were considered (Figure 3.1). For the simulations with FISPACT-II the following considerations were taken into account:

1. Enrichment of Li-6 at least equal to 90% in order to obtain a Tritium breeding ratio greater than one (TBR>1). As it was explained in chapter 1.2 this is a very important requirement for the breeding function of the blanket, because Tritium can't be found in nature, so it must produce in situ and it is the fuel for the D-T fusion reaction.

2. For the irradiation time a pulsed mode was used and it took into account the residence time of FLiBe inside the reactor. FLiBe can flow inside the channel and in the tank, so considering a length of 6 meter from the inlet and outlet points and a velocity of 2 m/s in the coolant channel (inside the vacuum vessel) and 0.2 m/s in the tank [4], the residence times for the two regions are respectively 3 seconds for the channel and 30 seconds for the tank.

FLiBe will be considered both with and without the presence of impurities and in order to consider the enrichment of Lithium-6 the isotopic composition was considered for the creation of the code for FISPACT-II (see Appendix A).
After the activation analysis of FLiBe a comparison with another liquid blanket, Lithium Lead, was done in order to see if the molten salt can be replaced with a liquid metal or if it remains the best choice for ARC from the activation point of view. Even for Lithium Lead the analysis took into account the mixture with and without impurities and the same considerations explained for FLiBe.

5.1 FLiBe activation analysis

The procedure that was adopted for the activation analysis of the FLiBe is equal to the one explained for the structural materials of the vacuum vessel. From MCNP simulation the neutron flux was evaluated both in the cooling channel and in the tank and the final values are:

- 5.35E+014$\frac{neutrons}{cm^2 s}$ for FLiBe with impurities in the cooling channel;
- 2.11E+013$\frac{neutrons}{cm^2 s}$ for FLiBe with impurities in the breeding tank;
- 6.71E+014$\frac{neutrons}{cm^2 s}$ for FLiBe without impurities in the cooling channel;
- 3.51E+013$\frac{neutrons}{cm^2 s}$ for FLiBe without impurities in the breeding tank;

For what concern the case with impurities, the mass percentage composition that was used for the simulation with FISPACT-II is shown in Table 5.1 [23]:

Table 5.1: Mass percentage composition of FLiBe with the presence of impurities

Elements	**Mass % composition**
Lithium	28.57
Fluorine	57.14
Beryllium	14.29
Chromium	0.0005
Iron	0.007
Nickel	0.0016
Copper	0.000099
Molybdenum	0.000099
Tungsten	0.000099

The final results obtained from FISPACT-II for FLiBe are in the next plots (for the final explanation just the results of the cooling channel are shown, while tables with the values both for the cooling channel and the tank are in Appendix B):

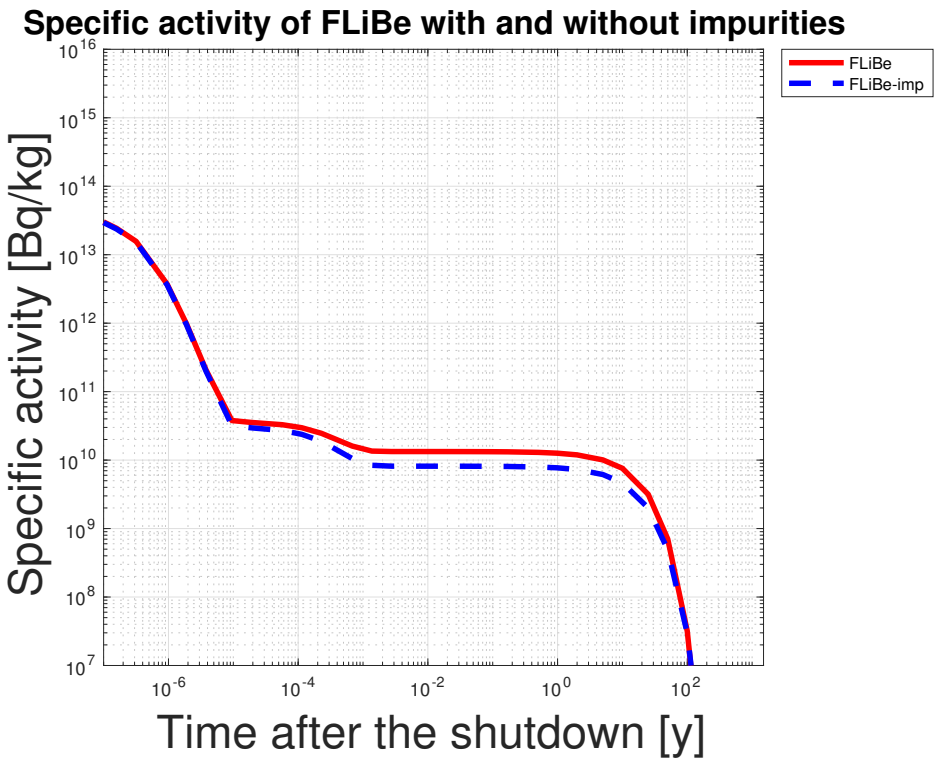

Figure 5.1: Specific activity of FLiBe in the cooling channel

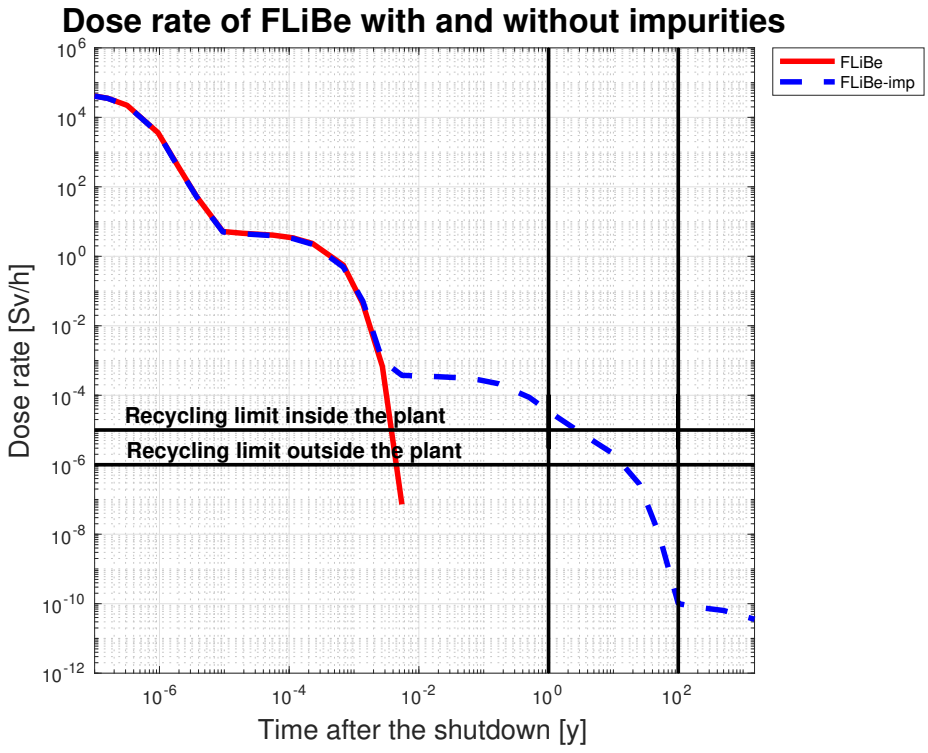

Figure 5.2: Contact dose rate of FLiBe in the cooling channel

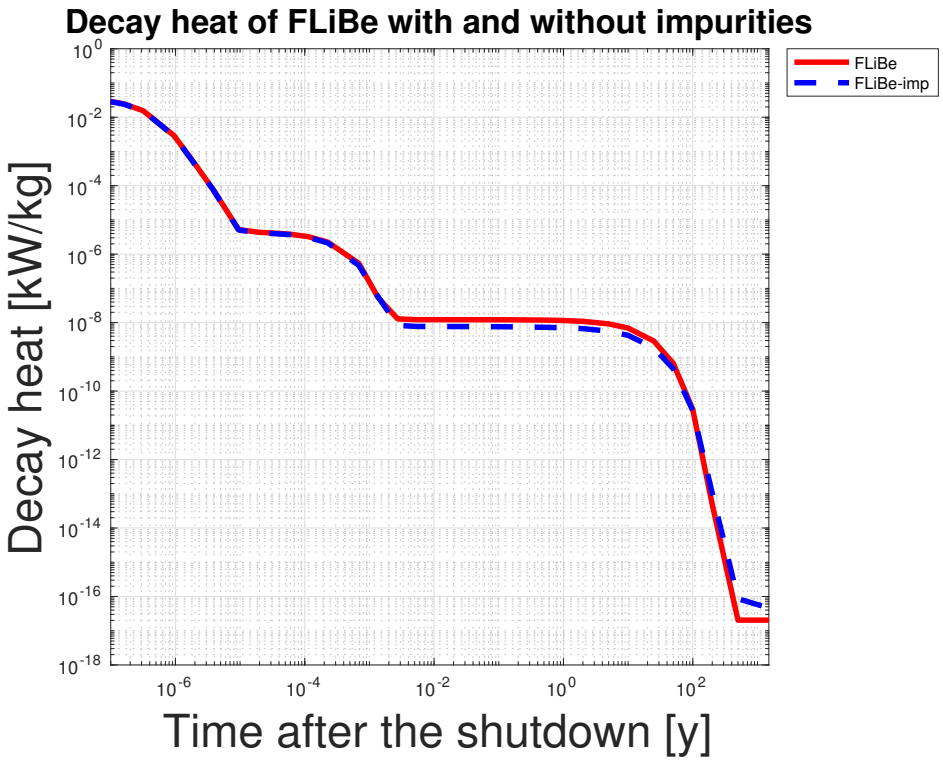

Figure 5.3: Decay heat of FLiBe in the cooling channel

5.2 FLiBe vs PbLi

In this section the comparison between the molten salt FLiBe and the liquid metal Lithium-Lead is explained.

Table 5.2: Comparison of the property of liquid FLiBe and Lithium-Lead. The temperature-dependent properties are given for liquid FLiBe at 950 K and for Lithium-Lead at 900 K [4,30,31]

Property	**FLiBe**	**Pb83-17Li**
Density [kg/m3]	1940	9200
Thermal conductivity [W/m/K]	1.0	22.0
Specific heat [kJ/kg/K]	2.40	0.85
Melting point [K]	732	508

Liquid metal is the option of liquid blanket that is under investigation for DEMO [2]. The main disadvantage for the application of liquid metal is related to the MHD (Magneto Hydro-Dynamics) effects, when it is subjected to a magnetic field, that causes the perturbation of the flow of the blanket itself [2]. In order to bypass this problem specific isolating pipes should be designed, but this option could be more expansive for the final project of a fusion reactor.
The procedure adopted for the analysis of PbLi was the same explained for FLiBe and the neutron fluxes that were used for the analysis are:

- 1.18E+015$\frac{neutrons}{cm^2 s}$ for PbLi with impurities in the cooling channel;
- 1.66E+014$\frac{neutrons}{cm^2 s}$ for PbLi with impurities in the breeding tank;
- 1.18E+015$\frac{neutrons}{cm^2 s}$ for PbLi without impurities in the cooling channel;
- 1.66E+014$\frac{neutrons}{cm^2 s}$ for PbLi without impurities in the breeding tank;

Table 5.2 shows the composition for PbLi with the presence of impurities [17]:

Table 5.3: Mass percentage composition of liquid Lithium-Lead with the presence of impurities

Elements	**Mass percentage composition [%]**
Pb	99.2925
Li	0.7
Bi	0.0043
Cd	0.0005
Ag	0.0005
Ni	0.0002
Sn	0.0005
Fe	0.001
Zn	0.001

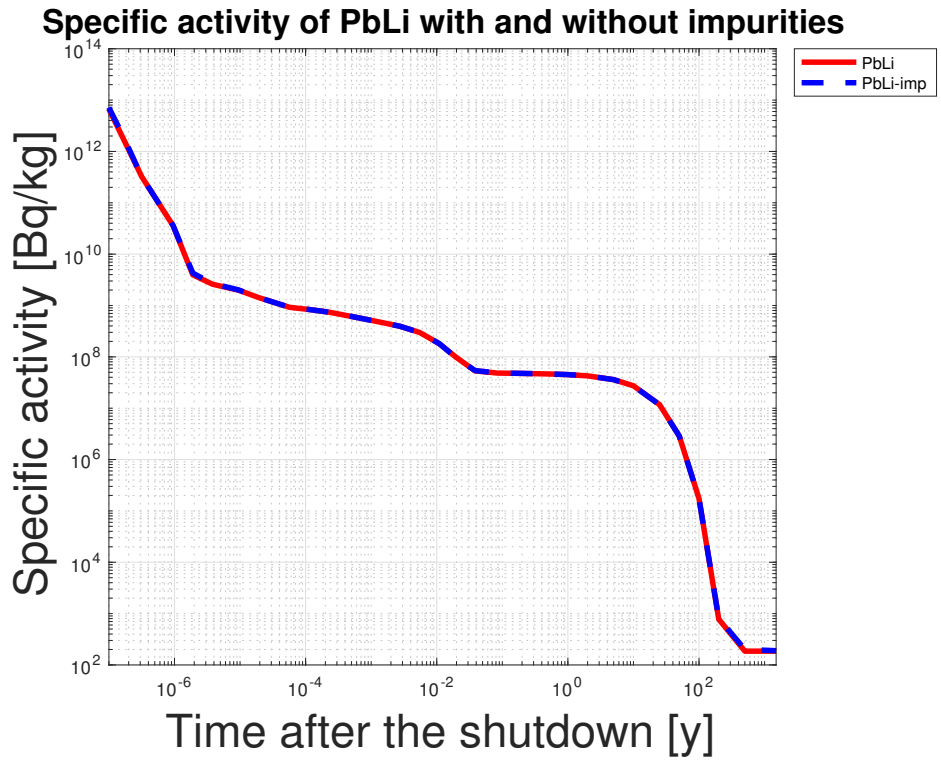

Figure 5.4: Specific activity of PbLi in the cooling channel

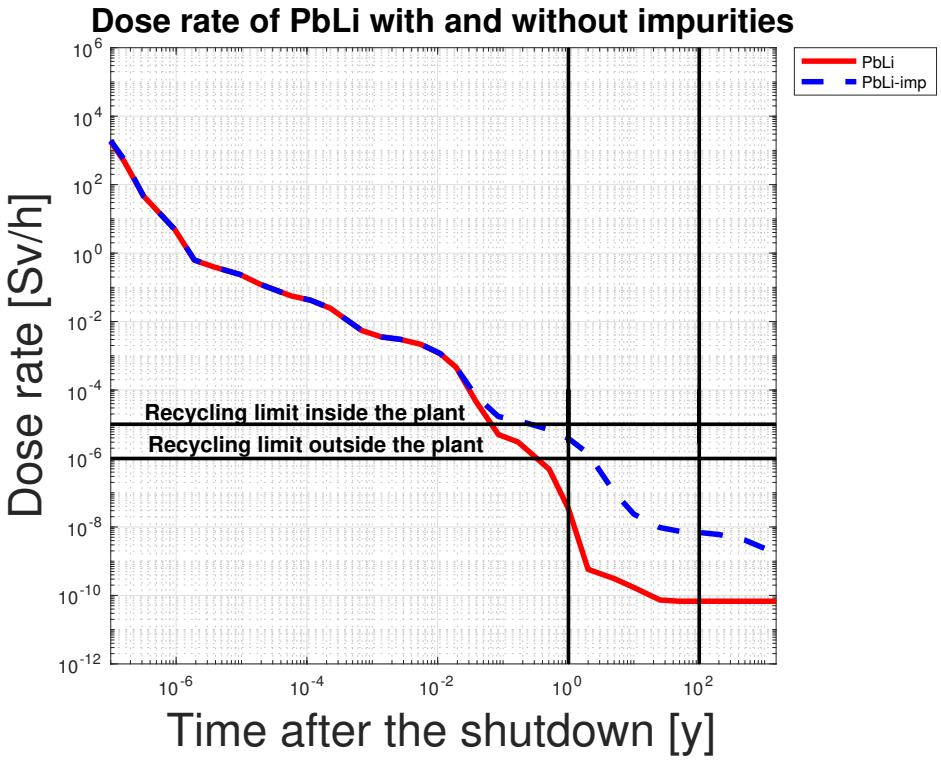

Figure 5.5: Dose rate of PbLi in the cooling channel

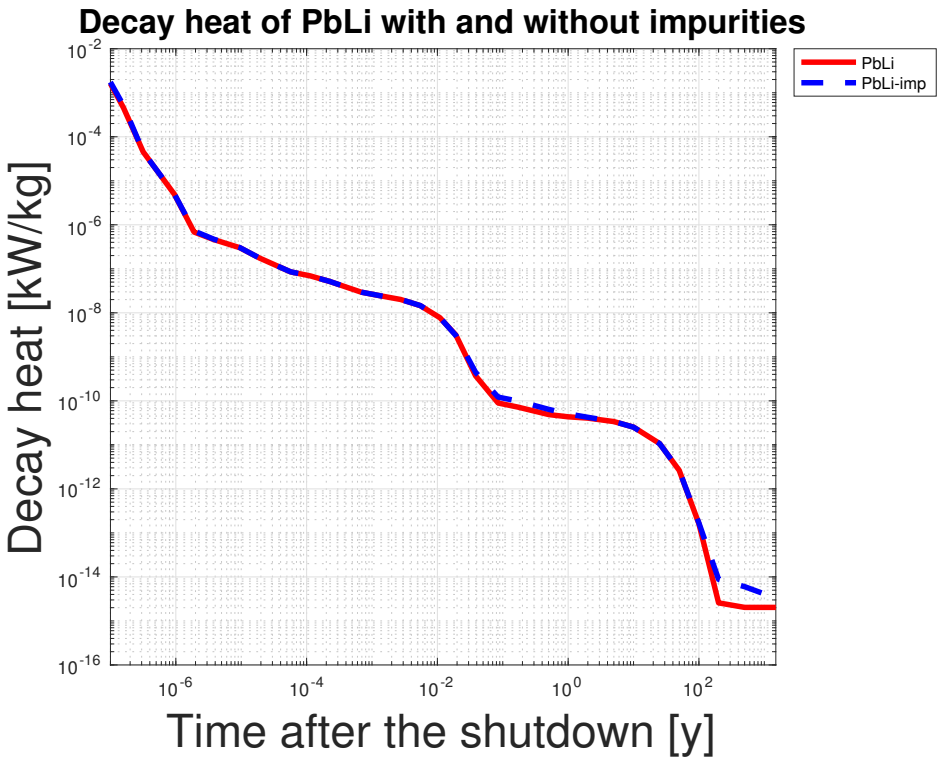

Figure 5.6: Decay heat of PbLi in the cooling channel

After having analysed separately the two liquid blankets a final comparison was done in order to better understand which one is the best choice from the activation analysis.

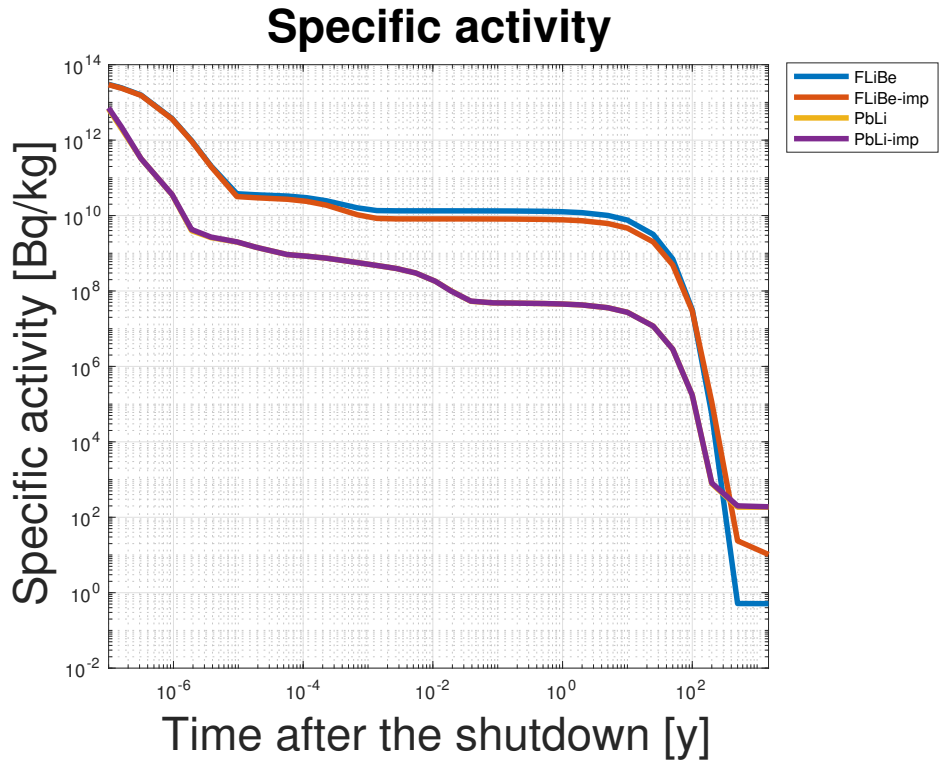

Figure 5.7: Specific activity: comparison between FLiBe and PbLi in the cooling channel

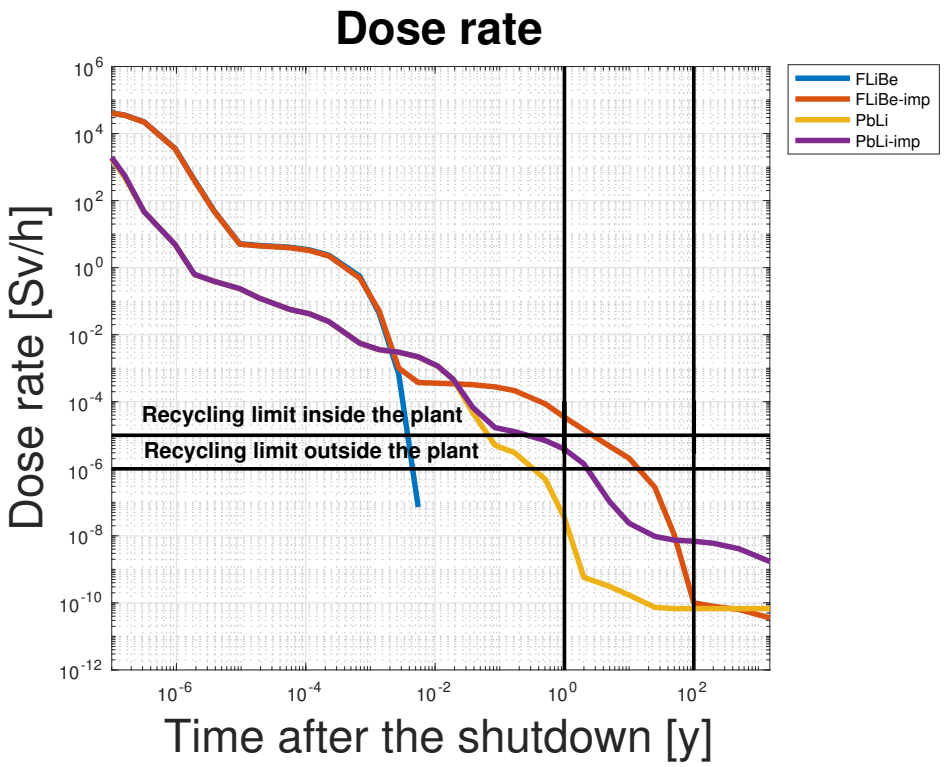

Figure 5.8: Dose rate: comparison between FLiBe and PbLi in the cooling channel

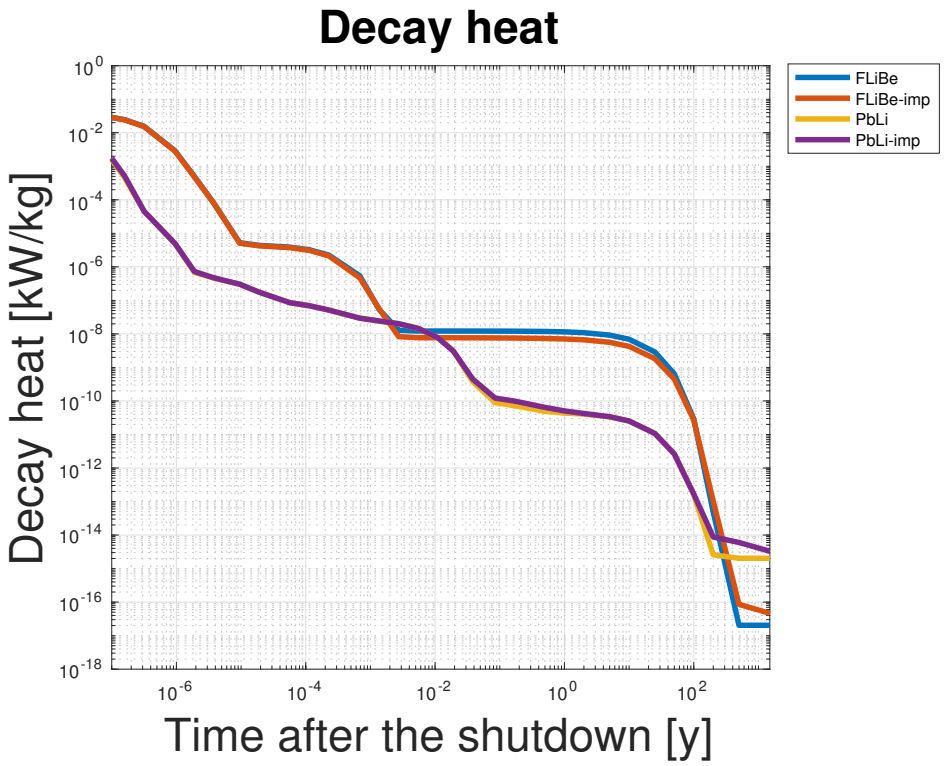

Figure 5.9: Decay heat: comparison between FLiBe and PbLi in the cooling channel

For what concern the contact dose rate in both cases the recycling limits are reached by 100 years, but from Figure 5.8 it is possible to notice that pure FLiBe is the one with the best behaviour, because it decreases quickly in few days. For the specific activity and decay heat the highest values at the beginning are reached from the FLiBe, but in both cases they decrease fast along the time. As regards the clearance index and SLB criteria, they could be considered quite useless for the analysis of the liquid blanket, because as it was explained in chapter 3 it is not thrown away after its use due to its high price, especially FLiBe [4]. It is recycled and for this reason the evaluation on the contact dose rate is enough. Before to reuse the liquid blanket the Tritium must be extracted, so in order to do this it is reheated and purified by the presence of Tritium.
After having compared and discussed the previous results it is possible to confirm that FLiBe remains the best choice as liquid blanket for ARC, especially the one without the presence of impurities. Furthermore, thanks to the fact that it doesn't suffer of the presence of magnetic fields, it is possible to reduce the presence of solid materials, their consequent activation and costs, in the final design of ARC with the liquid immersion blanket.

Chapter 6

Conclusion

The main goal of this research was the activation analysis of possible structural materials for the vacuum vessel and of the liquid blanket, FLiBe. ARC reactor is still a design of a fusion reactor, the single piece vacuum vessel is supposed to be substituted after a qualitative lifetime of 2 years, so it needs a material that can support high thermal loads and at the same time it must be constituted by the presence of elements that for long exposure to high neutron fluxes don't produce long-lived radioactive isotopes, which could cause problems for the safety of workers and for the final disposal.

6.1 Summary of the results for the vacuum vessel

Inconel-718 could be the best choice as a structural material for its good thermal-mechanical properties at high temperature (Table 3.4), which is the main reason of its choice as original structural material for ARC, but through the activation analysis it is possible to conclude that it doesn't respect the low-activation criteria explained in section 3.1 due to the high presence Nickel, Molybdenum and Niobium. In order to see if the modification of its composition could change the results isotopic tailoring was applied. Through that method it is possible to eliminate or reduce the presence of undesired isotopes. The results of this process, compared with the initial analysis, show that in each case it is not possible to obtain a low-activation alloy, so after having had this confirmation, the next step of the thesis was based on the research of new possible structural materials, with good mechanical properties and low-activation characteristics.

The Molybdenum-based alloy, TZM, didn't respect the low-activation requirements both with and without undesired impurities. The main problem is related to the primary element of the alloy: Molybdenum (99.369% of the total composition). Its natural isotopes tend to interact with neutrons and lead the formation of long-lived radioisotopes like Nb-94 (half-life 20'326 years [28]) and Tc-99 (half life 211'100 years [28]), so for this reason it was analysed after the modification of its composition through isotopic tailoring process. In this case just Mo-97 was considered as natural isotope, while the other ones that cause the production of undesired radioisotopes were eliminated. The activation analysis with the modified alloy showed good improvements, the main one is related to the reduction of the initial values of decay heat and its faster decrease in time, which can be noticed both for the specific activity and dose rate (section 4.2.2). The low-activation requirements weren't achieved, but the comparison of the results with the initial ones shows a relevant

reduction of the decommissioning indexes, in fact the waste disposal rating is very close to the limit at 100 years.

As regards the RAFM steel Eurofer97 the presence of Nitrogen in its nominal composition leads the non-respect of the clearance requirement. N-14, which is the most abundant natural isotope of Nitrogen, through the (n, protons) reaction leads the formation of C-14 [22], a long-lived radioisotope that is the main at fault for the high value of CI even after 100 years of cooling (Table 3.16). The waste disposal rating (SLB criteria) reached the limit in both cases, while the evolution of the contact dose rate reaches only the recycling limit inside the plant both in the inner and outer wall of the vacuum vessel.
After the first analysis Eurofer97 was analysed the application of isotopic tailoring, which was based on the reduction of the presence of N-14. Relevant improvements were shown just in the case of the composition without impurities, which reached both recycling limits, while for the waste treatment it didn't reach the limit for the clearance index. Another interesting composition that is under study is Eurofer-ODS (Oxide Dispersion Strenghtened), where there is the addiction of Yttrium Oxide (Y2O3) in order to increase the mechanical properties of the steel at high temperature [19]. This last material compared with the standard Eurofer97 shows better behaviours of the specific activity, contact dose rate and decay heat after the shutdown of the reactor.

Stainless steels 316 and 304 are characterised by high percentages of Nickel in their compositions, which affect the results at the beginning of the activation analysis, so in order to try to obtain an alloy that respects the low-activation requirements both elemental substitution and isotopic tailoring were applied. In the first one Nickel was substituted with Manganese and some improvements were achieved just with stainless steel 304, while the type 316 contains a low percentage of Molybdenum, which affects the final results. The next step was the application of isotopic tailoring, with the enrichment of Mo-97 for the type 316 (like in the case of TZM) and Ni-61 for both steels. In section 4.2.4 from Table 4.6 it is possible to notice the achievement of SLB criteria for each case, while at the beginning and even after elemental substitution just the type 304 reached this requirement, but CI was still higher than 1. Another comparison can be done through the contact dose rate in Figure 4.33 and 4.34, where it is possible to see that after the isotopic modification just stainless steel 304 reached both recycling limits, while the type 316 was able to reach both of them just in the outer region of the vacuum vessel, which is exposed to a lower value of neutron flux than the inner wall.

V-15Cr-5Ti, Ti-6Al-4V and SiC are supposed to be low-activation alloys thanks to the presence of elements like Vanadium, Chromium, Titanium and Silicon, which are considered low-activation elements, so when their natural isotopes interact with neutrons they don't cause the production of long-lived radioisotopes.
SiC is a ceramic with physical and mechanical properties very different from Inconel-718; as it was explained in chapter 3 its application for the construction of huge components is very complicated, especially for the vacuum vessel of ARC, that must be exposed for very long time to high mechanical loads and neutron fluxes, because the presence of a small crack can be propagated quickly and without obstacles through the entire stressed area [13] and this would cause the damage of the entire piece of the reactor, so this is the main reason for which Silicon Carbide can't be considered

a feasible choice.
The activation analysis of Titanium alloy didn't show good results and the main problem is the formation of Al-26, that comes from Al-27, which is the only natural isotope of Aluminium, that is a constitutive element of the material and it can't be eliminated. V-Cr-Ti alloy is the material that showed the best results from its analysis, even if the clearance criteria wasn't respected the Shallow Land Burial requirement was reached both with and without the presence of impurities.
The contact dose was characterized by a rapid decrease, like the specific activity, and both recycling limits are reached after 100 years of storage.
In the following plot there is the final comparison between Inconel-718 and Vanadium-alloy, in order to highlight the improvements of the second choice and why it could be a good option for ARC's design.

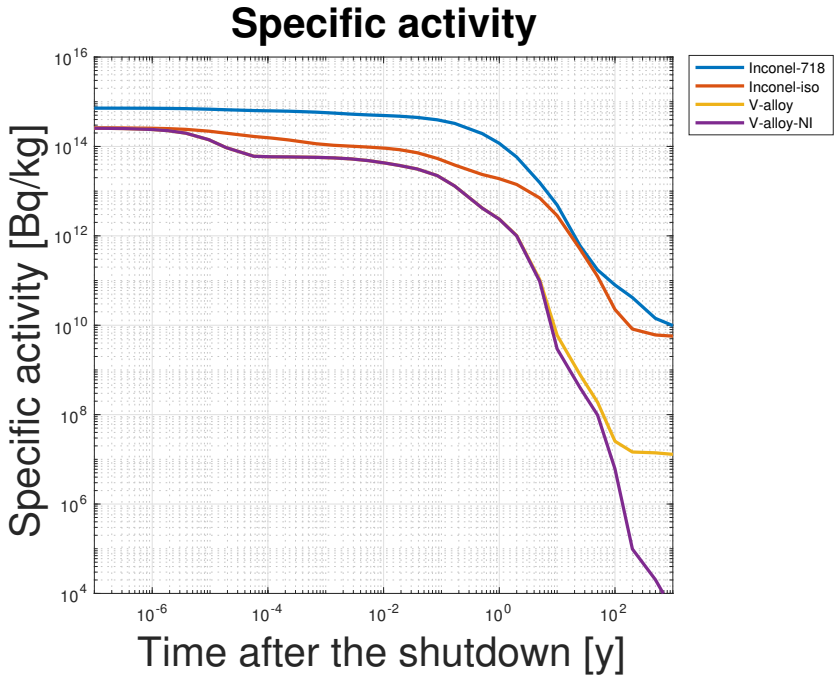

Figure 6.1: Specific activity: comparison between Inconel-718 and V-15Cr-5Ti

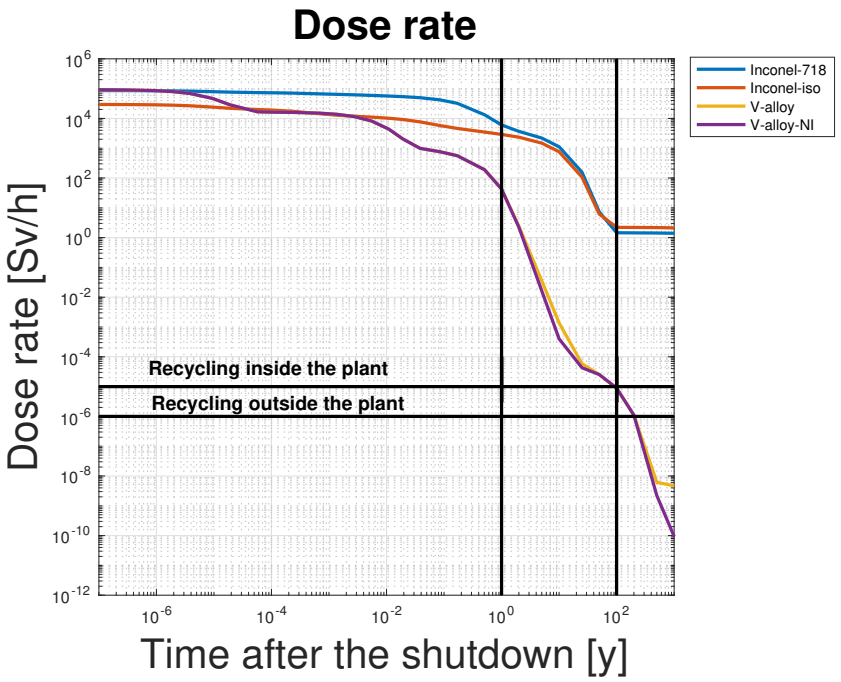

Figure 6.2: Dose rate: comparison between Inconel-718 and V-15Cr-5Ti

The final comparison of the decay heat was done just for the first two days after the shutdown, because in case of accident the initial evolution is taken into account:

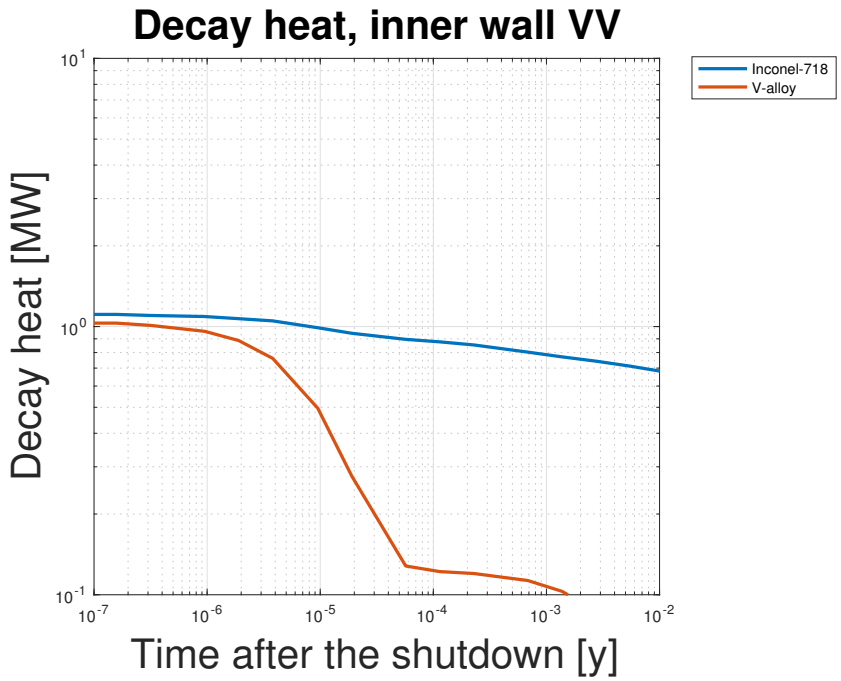

Figure 6.3: Decay heat: comparison between Inconel-718 and V-15Cr-5Ti in the inner wall of the vacuum vessel after two days from the shutdown of the reactor

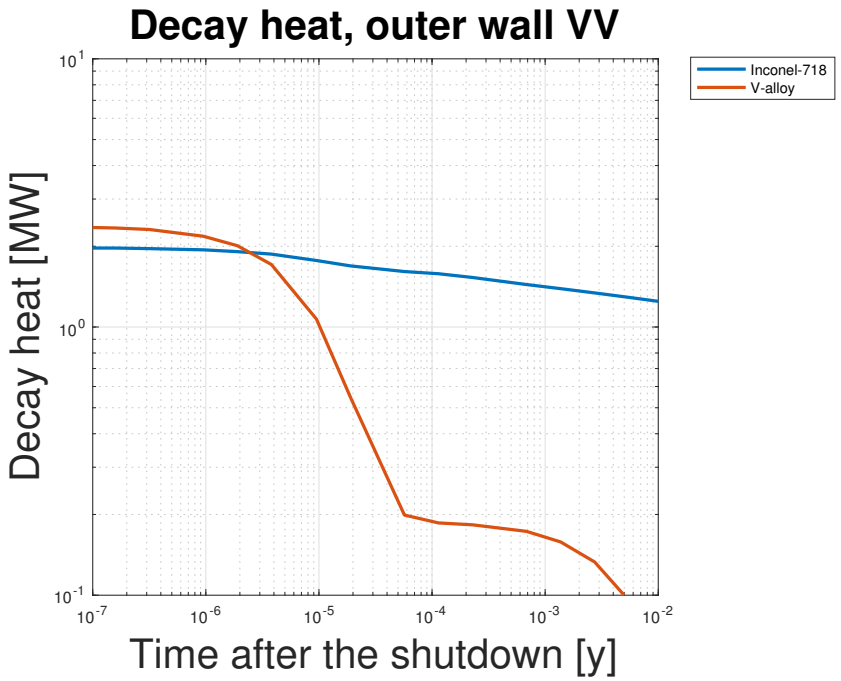

Figure 6.4: Decay heat: comparison between Inconel-718 and V-15Cr-5Ti in the outer wall of the vacuum vessel after two days from the shutdown of the reactor

Table 6.1: Decay heat [MW] of Inconel-718 and V-15Cr-5Ti in the inner and outer region of the vacuum vessel immediately after the shutdown

	Decay Heat Inner wall [MW]	**Decay Heat Outer wall [MW]**
Inconel	1.11	1.97
V-15Cr-5Ti	1.04	2.4

Even if in the outer wall the decay heat of V-15Cr-5Ti is a little bit higher than Inconel, the previous plots show that its reduction is quicker and that is the important point. The benefits of those results will be shown in the next section, where the temperature evolution will be analyzed for two different accidents.

6.2 Temperature evolution in case of LOFA and LOCA accidents

The evolution of the decay heat after the shutdown of the reactor allowed to do a qualitative analysis of the temperature evolution of the system composed by the vacuum vessel and liquid blanket in case of two accidental situations: Loss of Flow Accident (LOFA), that could be characterised by the break of a pump which stops the flow of the FLiBe, and Loss of Coolant Accident (LOCA). The main problem in both cases is the decay heat produced after the stop of the operation and the consequent temperature evolution, that could cause damages to the reactor and lead to the melt of the vacuum vessel.

Loss of Flow Accident

Considering the break of a pump and assuming the achievement of a thermal equilibrium between the liquid blanket and the vacuum vessel after the shutdown of the reactor, the final evolution of the temperature is influenced by the behaviour of the decay heat over the time, that is related to the type of material. The variation of the temperature was calculated with a certain time step taking into account: the decay heat, the mass and the specific heat of the cooling channel, blanket tank, both with FliBe, and inner and outer walls of the vacuum vessel. The formula is the following one:

$$\Delta T = \frac{\int P_{decayinnerVV}\,\mathrm{d}t + \int P_{decaycoolchannel}\,\mathrm{d}t + \int P_{decayouterVV}\,\mathrm{d}t + \int P_{decaytank}\,\mathrm{d}t}{m_{innerVV}\cdot cp_{innerVV} + m_{coolchannel}\cdot cp_{coolchannel} + m_{outerVV}\cdot cp_{outerVV} + m_{tank}\cdot cp_{tank}} \tag{6.1}$$

Assuming 1000 K as the initial temperature of the vacuum vessel immediately after the shutdown, the system with Inconel-718 showed a rapid increase of the temperature, that reached the melting point of the alloy after four days from the shutdown of the reactor (Figure 6.5). The main problem is that the decay heat of the Nickel based alloy doesn't decrease fast along the time and that is related to the long-lived radioactive isotopes, which cause the high activation of the material. Considering the selected low-activation Vanadium alloy, where the reduction of the decay heat is faster (Figure 6.3 and 6.4), the evaluation of the temperature evolution shows the achievement of an asymptotic value ($\simeq$1240 K, Figure 6.6), that is lower than the melting point of the material (2153 K for V-15Cr-5Ti [13]), which won't be reached even after one year from the shutdown.

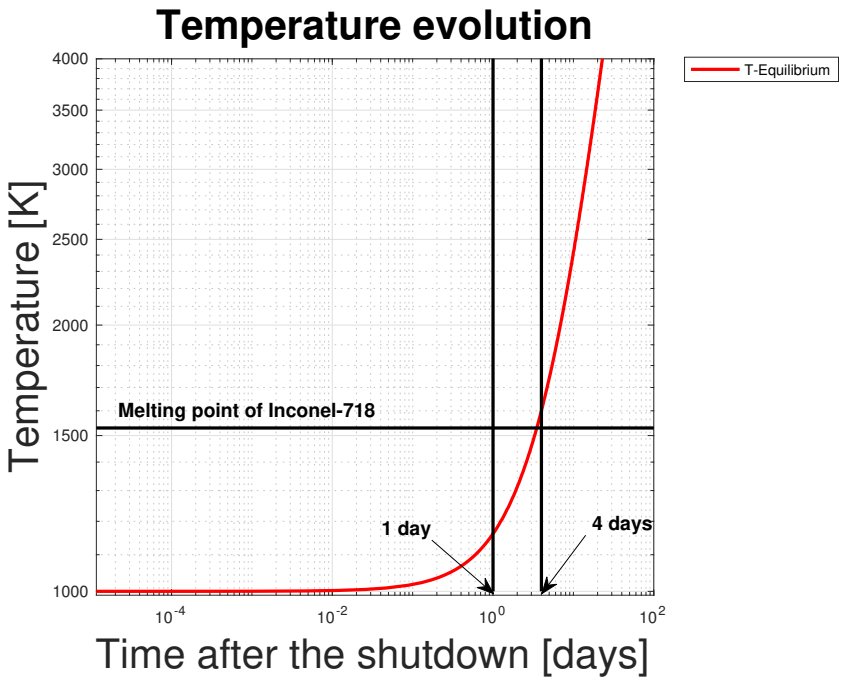

Figure 6.5: Temperature evolution of Inconel-718 in case of Loss of Flow Accident after the shutdown of the system

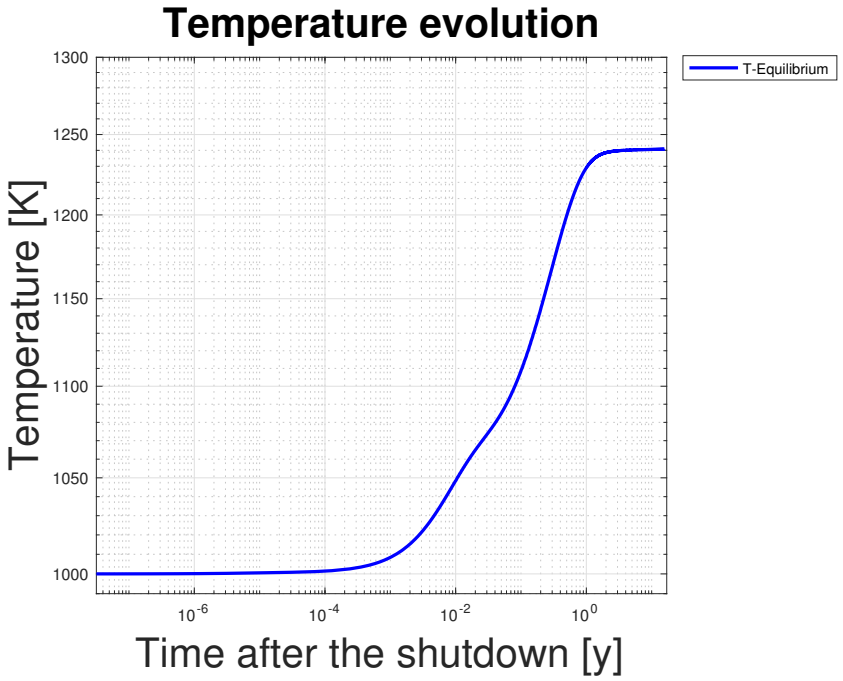

Figure 6.6: Temperature evolution of V-15Cr-5Ti in case of Loss of Flow Accident after the shutdown of the system

Loss of Coolant Accident

Considering the complete loss of liquid blanket from the reactor it is possible to evaluate the temperature evolution of the vacuum vessel, after the shutdown of the reactor, from black body radiative cooling:

$$m_{VV} \cdot c_p \cdot \frac{\partial T}{\partial t} = P_{decay}(t) - \sigma \cdot T^4 \cdot A_p \tag{6.2}$$

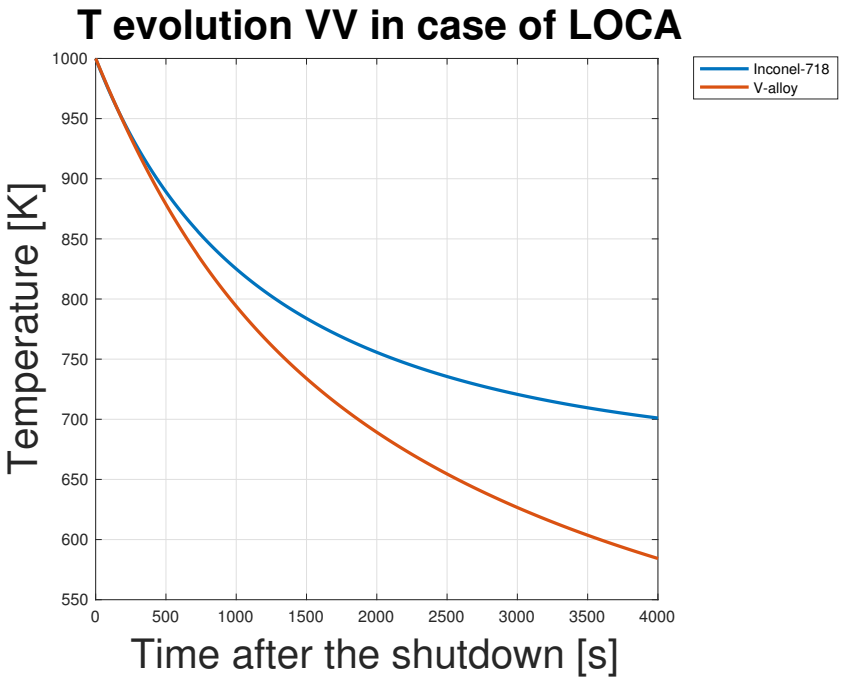

Figure 6.7: Temperature evolutions of Inconel-718 and V-15Cr-5Ti in case of Loss of Coolant Accident after two days from the shutdown of the system

The analysis considered a maximum period of intervention of two days and even in this accidental scenario the best behaviour is shown by the Vanadium alloy.
This analysis permitted to have an extra confirmation on the advantages related to the using of low-activation materials. The presence of short-lived isotopes leads to a faster decrease of the decay heat, which permits to have more time for the resolution of the problem in order to avoid serious damages to the entire structure.

6.3 Waste decommissioning: cost analysis

At the end of the lifetime of the vacuum vessel, the component can be recycled or permanently disposed and the choice is based on the low-activation criteria explained at the beginning of Chapter 3: Clearance Index, recycling and Shallow Land Burial. As it was possible to notice during the explanation of the activation analysis, each material didn't respect the clearance requirement, so the only possible option is the decommissioning of the piece. The Nuclear Regulatory Commission divided the waste in three different classes on the base of the concentration of some specific isotopes inside the material [24]. The three classes are "A" (Low Level Waste), "B" and "C". If an alloy doesn't respect the different limits it is defined as a High Level Waste (HLW).
The cost of the decommissioning process is different between the different type of waste classes, in particular [25]:

- Class A: 20 $\frac{\$}{ft^3}$
- Class C: 2000 $\frac{\$}{ft^3}$
- HLW: greater than 20000 $\frac{\$}{ft^3}$

The analysis was performed for Inconel-718 and Vanadium alloy, which is the best option analysed as possible substitute.
The final results are shown in the following table:

Table 6.2: Material and decommissioning costs: Inconel-718 and V-15Cr-5Ti

	Material cost [$]	**Waste Class**	**Decommissioning cost [$]**	**Total Cost [$]**
Inconel-718	2.38E+006	HLW	5.86E+006	8.24E+006
V-15Cr-5Ti	6.33E+006	A	5.86E+003	6.33E+006

The last table permits to have a comparison of the total cost for the two different structural materials. Vanadium has got a higher material cost ($\sim 125\frac{\$}{kg}$ [26]) than Inconel-718 ($\sim 35\frac{\$}{kg}$ [26]), but thanks to the fact that it is a low-activation alloy, it is possible to reduce the decommissioning cost at the end of the lifetime of the Vacuum vessel of three order of magnitude. Through the evaluation of the Waste Disposal Rating and considering the different limits imposed by the NRC it is possible to classify V-15Cr-5Ti as a low level waste (Class A), so the entire cost for its permanent disposal is much lower than in the case of a High Level Waste, such as the analysed Nickel-based alloy.
An interesting comparison that helps to underline the advantage of using a low-activation material for ARC reactor is related to the decommissioning cost of a solar panel systems.
Considering a solar system that produces 2 MW of electric power, after 20 years of operation the disposal cost is 98'000$[27]. ARC should produce 283MW [4] of electric power and its vacuum vessel is replaced after 2 years of operation and the using of a low-activation material permits to spend almost 6'000$ for its decommissioning (without considering first wall and layer of neutron multiplier), so if we want to produce the same electric power through the solar system the final decommissioning cost after 20 years becomes almost 100 times higher, equal to 10 million dollars. If

we consider to replace the vacuum vessel, the final disposal cost of the Vanadium alloy is almost equal to 1.5 million dollars, so 10 times lower than the cost of the solar panel, and in both cases there is the production of Carbon-free energy.

6.4 Conclusions

ARC has got a very innovative design, and the position of its vacuum vessel so close to the chamber where plasma is generated makes it subjected constantly to a very high neutron flux, without any type of shielding, which is very different from the design of ITER and DEMO.
The activation analysis of different alloys showed that for a long and constant exposure to high neutron fluxes it is very difficult to reach acceptable levels of radioactivity, even after many years from the shutdown.
The results obtained through Elemental substitution and Isotopic tailoring showed good improvements, but they are not enough and their costs are quite high compared to the benefits that they lead.
The final comparison in chapter 3 underlines that the best alternative for the vacuum vessel is the using of a Vanadium-based alloy. It showed very interesting results and, even if its mechanical properties are not as good as the ones of Inconel-718, ARC is still a design and its parameters can be modified and it is possible to consider the option of using a combination of alloys.
Another important aspect is related to the waste decommissioning of the piece, because the using of a low-activation material permits to reduce drastically the final cost for the final disposal. Table 6.2 shows the big difference between the using of Inconel-718 and Vanadium alloy and that is an important goal, which must be taken into account for the economical analysis of ARC.
For what concern the liquid blanket analysis it permitted to have the confirmation that the initial choice of FLiBe for ARC was good, and even if the cost of the molten salt is higher than Lithium-Lead, at the end it permits to reduce the presence of solid materials in the breeding tank, which reduce the final cost for the design.
The activation analysis performed in this thesis permitted to find in the selected Vanadium alloy a new possible option of structural material for the final fulfillment of ARC reactor; furthermore it showed the importance related to the choice of a low-activation alloy, in order to create a tokamak cheaper, safer and more efficient under each point of view.

Bibliography

[1] http://en.wikipedia.org/wiki/File:Deuterium-tritium-fusion

[2] L.V. Boccaccini, "Blanket Technology for the Fusion Reactor", Karlsruhe Institute of Technology (KIT), 2016.

[3] https://en.wikipedia.org/wiki/Torus

[4] B.N. Sorbom, J. Ball, T.R. Palmer, F.J. Mangiarotti, J.M. Sierchio, P. Bonoli,C. Kasten, D.A. Sutherland, H.S. Barnard, C.B. Haakonsen, J. Goh, C. Sung, D.G.Whyte, "ARC: A compact, high-field, fusion nuclear science facility and demonstration power plant with demountable magnets", Plasma Science and Fusion Center,Massachusetts Institute of Technology, Cambridge, MA 02139, USA

[5] B.N. Sorbom, "Liquid immersion blankets for fusion power plants", Plasma Science Fusion Center, October 2015

[6] R. A. Pitts, "The ITER project", ITER Organization, Plasma Operations Directorate, Cadarache, France.

[7] S.Segantin, "Load following concept feasibility of ARC reactor power plant based on the thermo-mechanical analysis of the vacuum vessel", Master thesis at Politecnico di Torino, Luglio 2017

[8] Jean-Christophe C. Sublet, James W. Eastwood, J. Guy Morgan, Michael Fleming and Mark R. Gilbert, "The FISPACT-II user manual", UKAEA-R(11)11 Issue7, September 2015.

[9] Luigi Di Pace, Laila El-Guebaly, Boris Kolbasov, Vincent Massaut, Massimo Zucchetti, "Radioactive Waste Management of Fusion Power Plants", in: Rehab Abdel Rahman (ed.), Radioactive Waste, InTech Publisher Rijeka, Croatia, April, 2012, pp. 303-328, ISBN 978-953-51-0551-0. DOI: 10.5772/35045

[10] "Report on the improvement of the Management of Radiation Protection Aspects in the Recycling of Metal Scrap", United Nations, New York and Geneva, 2002, pp.52.

[11] C. Ponti, "Recycling and Shallow Land Burial as Goals for Fusion Reactor Materials Development", April 1987.
Available at: http://dx.doi.org/10.13182/FST88-A25093

[12] "Product handbook of high-performance Nickel alloys", Special metals,pp.12.

[13] Panayiotis J Karditsas and Marc-Jean Baptiste, "Thermal and Structural Properties of Fusion related Materials".
Available at: http://aries.ucsd.edu/LIB/PROPS/PANOS/matintro.html

[14] B. A. Loomis, H. M. Chung, L. J. Nowicki and D. L. Smith, "Effects of neutron irradiation and hydrogen on ductile-brittle transition temperatures of V-Cr-Ti alloys", Energy Technology Division, Argonne National Laboratory, Argonne, Illinois, USA, August 1993.

[15] M. Zucchetti, D. Boerman, G. Piatti, "Characterization of a Titanium alloy for nuclear fusion applications", Proc. 6-th International Meet on Titanium, Torino, November 1990, pp. 18.1.

[16] D.G. Cepraga, E. Menapace, G. Cambi, S. Ciattaglia, L. Petrizzi, G. Cavallone,M. Costa, U. Broccoli, "Activation of TZM and stainless steel divertor materials in the NET fusion machine", Journal of nuclear materials 212-215 (1994), pp. 644-648.

[17] Laila El-Guebaly and the ARIES Team, "ARIES-CS Radial Builds and Compositions", Fusion Technology Institute University of Wisconsin - Madison, November 2004.
Available at: http://fti.neep.wisc.edu/aries-cs/builds/build.html

[18] M. Rieth, M. Schirra, A. Falkenstein, P. Graf, S. Heger, H. Kempe, R. Lindau,H. Zimmermann, "Eurofer97: tensile, charpy, creep and structural tests", Karlsruhe, October 2003.

[19] I.Kubena, T.Krumla, P.Spatigb, N. Balucb, Z. Oksiutab, M. Petreneca, K. Obrt-lika, J.Polak,"Fatigue behaviour of ODS ferritic-martensitic Eurofer steel",Czech Republic and Switzerland, March 2010, pp. 717-724, doi:10.1016/j.proeng.2010.03.077

[20] R.J. McConn Jr, C.J. Gesh, R.T. Pagh, R.A.Rucker, R.G. Williams III, "Compendium of Material Composition Data for Radiation Transport Modeling", Pacific Northwest National Laboratory, March 2011.

[21] "High temperature characteristic of stainless steels", distributed by Nickel development institute and produced by American Iron and Steel Institute.

[22] Robert W. Conn, Kevin Okula, A. Wayne Johnson, "Minimizing Radioactivity and Other Features of Elemental and Isotopic Tailoring of Materials for Fusion Re-actors", July 1978.

[23] T.Nagasaka, M. Kondo, T. Muroga, N. Noda, A. Sagara, O. Motojima, A.Suzuki, T. Terai, "Progress in Flibe Corrosion Study toward Material Research Loop and Advanced Liquid Breeder Blanket", IAEA, October 2008

[24] US-NRC. (1982). 10CFR61, Licensing requirements for land disposal of radioactive waste, U.S. Nuclear Regulatory Commission Federal Register 47 FR 57463,Dec. 27, 1982 and subsequent amendments.
http://www.nrc.gov/reading-rm/doc-collections/cfr/part061/

[25] L.El-Guebaly, L. Cadwallader, "Lifecycle Waste Disposal and Decommisioning costs for ARIES Systems Code", University of Wisconsin, Madison, May 2008.

[26] Alibaba site available at: https://www.alibaba.com/

[27] "Decommissioning Solar Panel Systems", NY-sun.

[28] http://www.periodictable.com/

[29] L. El-Guebaly, M. Zucchetti, "Progress and challenges of handling fusion radioactive materials", University of Wisconsin and Politecnico of Torino, October2015, pp.484-491.
Available at: http://dx.doi.org/10.13182/FST14-952

[30] N. J . Hoffman, A. Darnell, J. A. Blink, "Properties of lead-lithium solutions", Energy Technology Engineering Center and Lawrence Livermore National Laboratory, California, October 1980

[31] P.J. Gierszewski, B. Mikic, N.E. Todreas, "Natural circulation of electrically conducting liquids in fusion reactor blankets", Plasma Fusion Center (MIT), Nuclear Engineering and Design, Volume 68-3, April 1982, pp. 255-264

List of Figures

List of Tables

Appendix A

Appendix

Example of inventory input file for FISPACT-II for Inconel-718 in the region close to plasma's chamber (inner wall of VV, region 30):

```
CLOBBER
MONITOR 1
GETXS 0
GETDECAY 0
FISPACT
* INCONEL-718 VV1-30: activation analysis
DENSITY 8.192
MASS 1.65956E+04 12
NI 55.00
CR 21.00
FE 11.1
CO 1.0
NB 5.5
MO 3.3
AL 1.15
TI 0.3
MN 0.35
CU 0.8
C 0.08
P 0.015
MIND 1.E5
GRAPH 3 2 1 1 2 3
FLUX 7.54E+014
ATOMS

PULSE 4
FLUX 0.0
TIME 24 HOURS ATOMS
FLUX 7.54E+014
TIME 180 DAYS ATOMS
ENDPULSE

TAB2 45

FLUX 0.
```

```
ZERO
TIME 1 SECS ATOMS
TIME 1 SECS ATOMS
TIME 3 SECS ATOMS
TIME 5 SECS ATOMS
TIME 20 SECS ATOMS
TIME 30 SECS ATOMS
TIME 1 MINS ATOMS
TIME 3 MINS ATOMS
TIME 5 MINS ATOMS
TIME 20 MINS ATOMS
TIME 30 MINS ATOMS
TIME 1 HOURS ATOMS
TIME 4 HOURS ATOMS
TIME 6 HOURS ATOMS
TIME 12 HOURS ATOMS
TIME 1 DAYS ATOMS
TIME 2 DAYS ATOMS
TIME 3 DAYS ATOMS
TIME 7 DAYS ATOMS
TIME 17 DAYS ATOMS
TIME 31 DAYS ATOMS
TIME 123 DAYS ATOMS
TIME 179 DAYS ATOMS
TIME 1 YEARS ATOMS
TIME 3 YEARS ATOMS
TIME 5 YEARS ATOMS
TIME 15 YEARS ATOMS
TIME 25 YEARS ATOMS
TIME 50 YEARS ATOMS
TIME 100 YEARS ATOMS
TIME 300 YEARS ATOMS
TIME 1000 YEARS ATOMS
END
*END
```

Example of inventory input file for FLiBe without impurities in the cooling channel, with 90% of enrichment for Li-6:

```
CLOBBER
MONITOR 1
GETXS 0
GETDECAY 0
FISPACT
* FLiBe in the channel: activation analysis
DENSITY 1.94
FUEL 4
LI6 8.85E+028
LI7 9.83E+027
F19 1.97E+029
BE9 4.91E+028
```

```
MIND 1.E5
GRAPH 3 2 1 1 2 3
FLUX 6.71E+014
ATOMS

PULSE 730
FLUX 0.0
TIME 24 HOURS ATOMS
FLUX 6.71E+014
TIME 3 SECS ATOMS
ENDPULSE

TAB2 45

FLUX 0.
ZERO
TIME 1 SECS ATOMS
TIME 1 SECS ATOMS
TIME 3 SECS ATOMS
TIME 5 SECS ATOMS
TIME 20 SECS ATOMS
TIME 30 SECS ATOMS
TIME 1 MINS ATOMS
TIME 3 MINS ATOMS
TIME 5 MINS ATOMS
TIME 20 MINS ATOMS
TIME 30 MINS ATOMS
TIME 1 HOURS ATOMS
TIME 4 HOURS ATOMS
TIME 6 HOURS ATOMS
TIME 12 HOURS ATOMS
TIME 1 DAYS ATOMS
TIME 2 DAYS ATOMS
TIME 3 DAYS ATOMS
TIME 7 DAYS ATOMS
TIME 17 DAYS ATOMS
TIME 31 DAYS ATOMS
TIME 123 DAYS ATOMS
TIME 179 DAYS ATOMS
TIME 1 YEARS ATOMS
TIME 3 YEARS ATOMS
TIME 5 YEARS ATOMS
TIME 15 YEARS ATOMS
TIME 25 YEARS ATOMS
TIME 50 YEARS ATOMS
TIME 100 YEARS ATOMS
TIME 300 YEARS ATOMS
TIME 1000 YEARS ATOMS
END
* END
```

Appendix B

Tables

- **Inconel-718**

Table B.1: Specific activity Inconel-718 in the inner wall of the vacuum vessel

Time [years]	**Inconel-718 Specific act.** [Bq/kg]	**Inconel-718, no imp. Specific act.** [Bq/kg]	**Inconel-718, isotopic tail. Specific act.** [Bq/kg]
0.00E+000	7.20E+014	7.20E+014	2.61E+014
3.17E-008	7.20E+014	7.20E+014	2.61E+014
9.51E-007	7.14E+014	7.14E+014	2.56E+014
1.90E-006	7.10E+014	7.10E+014	2.50E+014
9.51E-006	6.81E+014	6.82E+014	2.20E+014
5.70E-005	6.35E+014	6.35E+014	1.67E+014
6.84E-004	5.85E+014	5.85E+014	1.15E+014
2.74E-003	5.29E+014	5.29E+014	1.01E+014
1.92E-002	4.74E+014	4.74E+014	8.44E+013
5.07E-001	1.94E+014	1.94E+014	2.36E+013
9.97E-001	1.18E+014	1.18E+014	1.90E+013
5.00E+000	1.55E+013	1.56E+013	7.04E+012
5.00E+001	1.73E+011	1.73E+011	1.24E+011
1.00E+002	7.95E+010	7.95E+010	2.25E+010
2.00E+002	4.16E+010	4.16E+010	8.22E+009
5.00E+002	1.42E+010	1.42E+010	6.06E+009
1.50E+003	7.92E+009	7.92E+009	5.50E+009

Table B.2: Specific activity of Inconel-718 in the outer wall of the vacuum vessel

Time [years]	**Inconel-718 Specific act. [Bq/kg]**	**Inconel-718, no imp. Specific act. [Bq/kg]**	**Inconel-718, isotopic tail. Specific act. [Bq/kg]**
0.00E+000	4.08E+014	4.08E+014	1.56E+014
3.17E-008	4.08E+014	4.08E+014	1.56E+014
9.51E-007	4.04E+014	4.04E+014	1.52E+014
1.90E-006	4.01E+014	4.01E+014	1.48E+014
9.51E-006	3.82E+014	3.82E+014	1.26E+014
5.70E-005	3.49E+014	3.49E+014	8.70E+013
6.84E-004	3.19E+014	3.19E+014	5.79E+013
2.74E-003	2.86E+014	2.86E+014	5.03E+013
1.92E-002	2.54E+014	2.55E+014	4.16E+013
5.07E-001	9.96E+013	9.97E+013	1.21E+013
9.97E-001	5.93E+013	5.94E+013	9.86E+012
5.00E+000	8.40E+012	8.42E+012	3.85E+012
5.00E+001	1.21E+011	1.21E+011	9.11E+010
1.00E+002	5.41E+010	5.41E+010	1.69E+010
2.00E+002	2.79E+010	2.79E+010	6.49E+009
5.00E+002	9.38E+009	9.39E+009	5.08E+009
1.50E+003	5.52E+009	5.52E+009	4.72E+009

Table B.3: Contact dose rate of Inconel-718 in the inner wall of the vacuum vessel

Time [years]	**Inconel-718, dose rate [Sv/h]**	**Inconel-718, no imp., dose rate [Sv/h]**	**Inconel-718, isotopic tail., dose rate [Sv/h]**
0.00E+000	8.62E+004	8.62E+004	2.95E+004
3.17E-008	8.61E+004	8.62E+004	2.94E+004
9.51E-007	8.50E+004	8.51E+004	2.86E+004
1.90E-006	8.40E+004	8.41E+004	2.78E+004
9.51E-006	7.90E+004	7.90E+004	2.40E+004
5.70E-005	7.35E+004	7.36E+004	1.98E+004
6.84E-004	6.68E+004	6.68E+004	1.44E+004
2.74E-003	6.19E+004	6.19E+004	1.19E+004
1.92E-002	5.38E+004	5.38E+004	9.21E+003
5.07E-001	1.32E+004	1.32E+004	3.49E+003
9.97E-001	6.05E+003	6.06E+003	2.91E+003
5.00E+000	2.19E+003	2.19E+003	1.48E+003
5.00E+001	7.26E+000	7.26E+000	6.14E+000
1.00E+002	1.46E+000	1.46E+000	2.21E+000
2.00E+002	1.44E+000	1.44E+000	2.19E+000
5.00E+002	1.43E+000	1.43E+000	2.17E+000
1.50E+003	1.38E+000	1.38E+000	2.10E+000

Table B.4: Contact dose rate of Inconel-718 in the outer wall of the vacuum vessel

Time [years]	**Inconel-718 dose rate [Sv/h]**	**Inconel-718, no imp., dose rate [Sv/h]**	**Inconel-718, isotopic tail., dose rate [Sv/h]**
0.00E+000	4.99E+004	4.99E+004	1.60E+004
3.17E-008	4.99E+004	4.99E+004	1.60E+004
9.51E-007	4.93E+004	4.93E+004	1.55E+004
1.90E-006	4.88E+004	4.88E+004	1.51E+004
9.51E-006	4.61E+004	4.61E+004	1.31E+004
5.70E-005	4.31E+004	4.31E+004	1.09E+004
6.84E-004	3.93E+004	3.93E+004	7.80E+003
2.74E-003	3.67E+004	3.67E+004	6.42E+003
1.92E-002	3.24E+004	3.24E+004	5.04E+003
5.07E-001	8.05E+003	8.05E+003	2.10E+003
9.97E-001	3.71E+003	3.71E+003	1.79E+003
5.00E+000	1.41E+003	1.41E+003	9.29E+002
5.00E+001	5.01E+000	5.01E+000	4.39E+000
1.00E+002	1.26E+000	1.26E+000	1.91E+000
2.00E+002	1.25E+000	1.25E+000	1.90E+000
5.00E+002	1.23E+000	1.23E+000	1.88E+000
1.50E+003	1.19E+000	1.19E+000	1.81E+000

Table B.5: Decay heat of Inconel-718 in the inner wall of the vacuum vessel

Time [years]	**Inconel-718 decay heat [kW/kg]**	**Inconel-718, no imp., decay heat [kW/kg]**	**Inconel-718, isotopic tail., decay heat [kW/kg]**
0.00E+000	6.68E-002	6.68E-002	2.83E-002
3.17E-008	6.67E-002	6.68E-002	2.81E-002
9.51E-007	6.56E-002	6.56E-002	2.71E-002
1.90E-006	6.46E-002	6.46E-002	2.64E-002
9.51E-006	5.96E-002	5.96E-002	2.23E-002
5.70E-005	5.39E-002	5.39E-002	1.73E-002
6.84E-004	4.83E-002	4.83E-002	9.87E-003
2.74E-003	4.47E-002	4.46E-002	7.68E-003
1.92E-002	3.90E-002	3.89E-002	5.89E-003
5.07E-001	1.06E-002	1.06E-002	2.11E-003
9.97E-001	5.07E-003	5.07E-003	1.74E-003
5.00E+000	1.33E-003	1.33E-003	8.77E-004
5.00E+001	5.05E-006	5.05E-006	4.43E-006
1.00E+002	1.28E-006	1.28E-006	1.66E-006
2.00E+002	1.15E-006	1.15E-006	1.59E-006
5.00E+002	1.06E-006	1.06E-006	1.57E-006
1.50E+003	1.00E-006	1.00E-006	1.51E-006

Table B.6: Decay heat of Inconel-718 in the outer wall of the vacuum vessel

Time [years]	**Inconel-718 decay heat [kW/kg]**	**Inconel-718, no imp., decay heat [kW/kg]**	**Inconel-718, isotopic tail., decay heat [kW/kg]**
0.00E+000	3.84E-002	3.84E-002	1.54E-002
3.17E-008	3.84E-002	3.84E-002	1.53E-002
9.51E-007	3.78E-002	3.78E-002	1.48E-002
1.90E-006	3.72E-002	3.72E-002	1.44E-002
9.51E-006	3.45E-002	3.45E-002	1.22E-002
5.70E-005	3.14E-002	3.14E-002	9.50E-003
6.84E-004	2.81E-002	2.81E-002	5.37E-003
2.74E-003	2.62E-002	2.62E-002	4.14E-003
1.92E-002	2.31E-002	2.31E-002	3.21E-003
5.07E-001	6.17E-003	6.18E-003	1.26E-003
9.97E-001	2.92E-003	2.93E-003	1.07E-003
5.00E+000	8.51E-004	8.51E-004	5.50E-004
5.00E+001	3.53E-006	3.53E-006	3.22E-006
1.00E+002	1.06E-006	1.06E-006	1.43E-006
2.00E+002	9.67E-007	9.67E-007	1.37E-006
5.00E+002	9.06E-007	9.06E-007	1.36E-006
1.50E+003	8.65E-007	8.65E-007	1.31E-006

- **V-15Cr-5Ti**

Table B.7: Specific activity of Vanadium alloy, with and without impurities, in the inner and outer region of the vacuum vessel

Time [years]	**V-15Cr-5Ti 30 specific act. [Bq/kg]**	**V-15Cr-5Ti 30 no imp., specific act. [Bq/kg]**	**V-15Cr-5Ti 34 specific act. [Bq/kg]**	**V-15Cr-5Ti 34 no imp., specific act. [Bq/kg]**
0.00E+000	2.58E+014	2.58E+014	1.77E+014	1.78E+014
3.17E-008	2.57E+014	2.57E+014	1.77E+014	1.77E+014
9.51E-007	2.40E+014	2.40E+014	1.64E+014	1.64E+014
1.90E-006	2.25E+014	2.25E+014	1.53E+014	1.53E+014
9.51E-006	1.42E+014	1.42E+014	8.91E+013	8.92E+013
5.70E-005	6.03E+013	6.03E+013	2.87E+013	2.87E+013
6.84E-004	5.71E+013	5.71E+013	2.69E+013	2.69E+013
2.74E-003	5.27E+013	5.26E+013	2.47E+013	2.47E+013
1.92E-002	3.73E+013	3.73E+013	1.73E+013	1.73E+013
5.07E-001	4.20E+012	4.17E+012	1.87E+012	1.86E+012
9.97E-001	2.38E+012	2.36E+012	1.04E+012	1.03E+012
5.00E+000	1.05E+011	9.58E+010	4.50E+010	4.07E+010
5.00E+001	1.89E+008	9.78E+007	9.10E+007	4.02E+007
1.00E+002	2.54E+007	6.10E+006	1.43E+007	2.47E+006
2.00E+002	1.46E+007	9.84E+004	9.22E+006	2.05E+004
5.00E+002	1.40E+007	2.03E+004	8.86E+006	4.61E+003
1.50E+003	1.24E+007	1.68E+003	7.84E+006	3.77E+002

Table B.8: Contact dose rate of Vanadium alloy, with and without impurities, in the inner and outer region of the vacuum vessel

Time [years]	**V-15Cr-5Ti 30 dose rate [Sv/h]**	**V-15Cr-5Ti 30 no imp. dose rate [Sv/h]**	**V-15Cr-5Ti 34 dose rate [Sv/h]**	**V-15Cr-5Ti 34 no imp., dose rate [Sv/h]**
0.00E+000	9.24E+004	9.24E+004	6.79E+004	6.79E+004
3.17E-008	9.22E+004	9.21E+004	6.77E+004	6.77E+004
9.51E-007	8.57E+004	8.57E+004	6.26E+004	6.26E+004
1.90E-006	7.95E+004	7.96E+004	5.78E+004	5.78E+004
9.51E-006	4.67E+004	4.67E+004	3.19E+004	3.19E+004
5.70E-005	1.67E+004	1.67E+004	8.34E+003	8.34E+003
6.84E-004	1.50E+004	1.50E+004	7.44E+003	7.45E+003
2.74E-003	1.15E+004	1.15E+004	5.73E+003	5.73E+003
1.92E-002	2.06E+003	2.06E+003	1.05E+003	1.05E+003
5.07E-001	1.90E+002	1.90E+002	1.02E+002	1.02E+002
9.97E-001	4.34E+001	4.30E+001	2.34E+001	2.31E+001
5.00E+000	3.57E-002	1.63E-002	1.81E-002	6.88E-003
5.00E+001	2.54E-005	2.54E-005	5.99E-006	5.96E-006
1.00E+002	8.89E-006	8.89E-006	2.09E-006	2.09E-006
2.00E+002	1.09E-006	1.10E-006	2.61E-007	2.51E-007
5.00E+002	6.13E-009	2.20E-009	1.40E-009	4.80E-010
1.50E+003	4.00E-009	1.48E-011	9.07E-010	4.83E-012

Table B.9: Decay heat of Vanadium alloy, with and without impurities, in the inner and outer region of the vacuum vessel

Time [years]	**V-15Cr-5Ti 30 decay heat [kW/kg]**	**V-15Cr-5Ti 30 no imp., decay heat [kW/kg]**	**V-15Cr-5Ti 34 decay heat [kW/kg]**	**V-15Cr-5Ti 34 no imp., decay heat [kW/kg]**
0.00E+000	8.39E-002	8.38E-002	6.20E-002	6.20E-002
3.17E-008	8.36E-002	8.36E-002	6.18E-002	6.18E-002
9.51E-007	7.74E-002	7.74E-002	5.70E-002	5.70E-002
1.90E-006	7.15E-002	7.15E-002	5.24E-002	5.25E-002
9.51E-006	4.00E-002	4.00E-002	2.79E-002	2.79E-002
5.70E-005	1.03E-002	1.03E-002	5.19E-003	5.19E-003
6.84E-004	9.10E-003	9.11E-003	4.51E-003	4.51E-003
2.74E-003	7.02E-003	7.03E-003	3.48E-003	3.49E-003
1.92E-002	1.33E-003	1.33E-003	6.75E-004	6.75E-004
5.07E-001	1.25E-004	1.25E-004	6.68E-005	6.66E-005
9.97E-001	3.09E-005	3.06E-005	1.63E-005	1.62E-005
5.00E+000	9.50E-008	7.66E-008	4.28E-008	3.28E-008
5.00E+001	3.69E-010	1.82E-010	1.70E-010	5.84E-011
1.00E+002	1.59E-010	3.90E-011	8.61E-011	1.01E-011
2.00E+002	1.20E-010	5.45E-012	7.41E-011	1.25E-012
5.00E+002	1.11E-010	7.11E-013	7.04E-011	1.62E-013
1.50E+003	9.81E-011	5.35E-014	6.22E-011	1.21E-014

- **Ti-6Al-4V**

Table B.10: Specific activity of Titanium alloy, with and without impurities, in the inner and outer regions of the vacuum vessel

Time [years]	**Ti-6Al-4V 30 specific act. [Bq/kg]**	**Ti-6Al-4V 30 no imp. specific act. [Bq/kg]**	**Ti-6Al-4V 34 specific act. [Bq/kg]**	**Ti-6Al-4V 34 no imp. specific act. [Bq/kg]**
0.00E+000	1.73E+014	1.73E+014	9.22E+013	9.21E+013
3.17E-008	1.67E+014	1.67E+014	8.94E+013	8.93E+013
9.51E-007	1.60E+014	1.60E+014	8.53E+013	8.53E+013
1.90E-006	1.57E+014	1.57E+014	8.34E+013	8.34E+013
9.51E-006	1.48E+014	1.48E+014	7.74E+013	7.74E+013
5.70E-005	1.36E+014	1.36E+014	6.97E+013	6.98E+013
6.84E-004	1.24E+014	1.24E+014	6.36E+013	6.37E+013
2.74E-003	1.03E+014	1.03E+014	5.29E+013	5.30E+013
1.92E-002	5.54E+013	5.53E+013	2.86E+013	2.86E+013
5.07E-001	1.63E+013	1.60E+013	8.24E+012	8.12E+012
9.97E-001	6.32E+012	6.05E+012	3.15E+012	3.02E+012
5.00E+000	1.23E+011	1.68E+010	5.83E+010	7.72E+009
5.00E+001	9.32E+008	4.55E+008	4.62E+008	1.97E+008
1.00E+002	1.34E+008	3.34E+007	7.51E+007	1.36E+007
2.00E+002	7.91E+007	3.49E+006	4.91E+007	1.22E+006
5.00E+002	7.54E+007	2.57E+006	4.71E+007	9.62E+005
1.50E+003	6.67E+007	2.24E+006	4.18E+007	8.85E+005

Table B.11: Contact dose rate of Titanium alloy, with and without impurities, in the inner and outer regions of the vacuum vessel

Time [years]	**Ti-6Al-4V 30 dose rate [Sv/h]**	**Ti-6Al-4V 30 no imp., dose rate [Sv/h]**	**Ti-6Al-4V 34 dose rate [Sv/h]**	**Ti-6Al-4V 34 no imp., dose rate [Sv/h]**
0.00E+000	9.22E+004	9.20E+004	4.90E+004	4.89E+004
3.17E-008	9.21E+004	9.20E+004	4.89E+004	4.89E+004
9.51E-007	9.10E+004	9.13E+004	4.83E+004	4.84E+004
1.90E-006	9.04E+004	9.07E+004	4.78E+004	4.80E+004
9.51E-006	8.73E+004	8.76E+004	4.56E+004	4.58E+004
5.70E-005	8.34E+004	8.37E+004	4.31E+004	4.32E+004
6.84E-004	7.43E+004	7.47E+004	3.84E+004	3.86E+004
2.74E-003	5.45E+004	5.48E+004	2.82E+004	2.84E+004
1.92E-002	1.78E+004	1.79E+004	9.48E+003	9.54E+003
5.07E-001	3.31E+003	3.32E+003	1.79E+003	1.79E+003
9.97E-001	7.56E+002	7.55E+002	4.07E+002	4.08E+002
5.00E+000	2.29E-001	1.31E-002	1.31E-001	4.31E-003
5.00E+001	2.15E-003	2.15E-003	7.83E-004	7.84E-004
1.00E+002	1.86E-003	1.86E-003	7.14E-004	7.15E-004
2.00E+002	1.72E-003	1.72E-003	6.82E-004	6.82E-004
5.00E+002	1.70E-003	1.70E-003	6.77E-004	6.77E-004
1.50E+003	1.70E-003	1.70E-003	6.77E-004	6.77E-004

Table B.12: Decay heat of Titanium alloy, with and without impurities, in the inner and outer regions of the vacuum vessel

Time [years]	**Ti-6Al-4V 30 decay heat [kW/kg]**	**Ti-6Al-4V 30 no imp. decay heat [kW/kg]**	**Ti-6Al-4V 34 decay heat [kW/kg]**	**Ti-6Al-4V 34 no imp. decay heat [kW/kg]**
0.00E+000	5.96E-002	5.94E-002	3.20E-002	3.19E-002
3.17E-008	5.95E-002	5.93E-002	3.20E-002	3.19E-002
9.51E-007	5.85E-002	5.86E-002	3.14E-002	3.14E-002
1.90E-006	5.79E-002	5.80E-002	3.09E-002	3.10E-002
9.51E-006	5.49E-002	5.51E-002	2.89E-002	2.89E-002
5.70E-005	5.11E-002	5.13E-002	2.64E-002	2.65E-002
6.84E-004	4.54E-002	4.56E-002	2.35E-002	2.36E-002
2.74E-003	3.36E-002	3.38E-002	1.74E-002	1.75E-002
1.92E-002	1.13E-002	1.14E-002	6.04E-003	6.08E-003
5.07E-001	2.16E-003	2.17E-003	1.16E-003	1.17E-003
9.97E-001	5.24E-004	5.23E-004	2.79E-004	2.80E-004
5.00E+000	3.57E-007	1.31E-007	1.83E-007	6.18E-008
5.00E+001	4.13E-009	3.16E-009	1.58E-009	1.00E-009
1.00E+002	2.34E-009	1.72E-009	9.81E-010	5.86E-010
2.00E+002	1.78E-009	1.18E-009	8.35E-010	4.56E-010
5.00E+002	1.68E-009	1.10E-009	8.02E-010	4.36E-010
1.50E+003	1.60E-009	1.09E-009	7.57E-010	4.33E-010

- **SiC**

Table B.13: Specific activity of Silicon Carbide, with and without impurities, in the inner and outer regions of the vacuum vessel

Time [years]	**SiC 30 specific act. [Bq/kg]**	**SiC 30 no imp., specific act. [Bq/kg]**	**SiC 34 specific act. [Bq/kg]**	**SiC 34 no imp., specific act. [Bq/kg]**
0.00E+000	3.80E+014	3.80E+014	2.04E+014	2.04E+014
3.17E-008	3.78E+014	3.78E+014	2.03E+014	2.03E+014
9.51E-007	3.26E+014	3.26E+014	1.75E+014	1.75E+014
1.90E-006	2.80E+014	2.80E+014	1.50E+014	1.50E+014
9.51E-006	8.61E+013	8.60E+013	4.61E+013	4.61E+013
5.70E-005	1.31E+012	1.31E+012	7.00E+011	7.01E+011
6.84E-004	2.37E+011	2.36E+011	9.93E+010	9.89E+010
2.74E-003	7.03E+010	7.01E+010	1.79E+010	1.76E+010
1.92E-002	6.16E+009	5.87E+009	2.38E+009	2.21E+009
5.07E-001	5.74E+009	5.62E+009	2.19E+009	2.13E+009
9.97E-001	5.55E+009	5.47E+009	2.11E+009	2.07E+009
5.00E+000	4.39E+009	4.38E+009	1.67E+009	1.66E+009
5.00E+001	3.52E+008	3.52E+008	1.34E+008	1.34E+008
1.00E+002	2.46E+007	2.37E+007	9.86E+006	9.33E+006
2.00E+002	3.11E+006	2.71E+006	1.62E+006	1.38E+006
5.00E+002	2.72E+006	2.63E+006	1.41E+006	1.35E+006
1.50E+003	2.58E+006	2.57E+006	1.33E+006	1.32E+006

Table B.14: Contact dose rate of Silicon Carbide, with and without impurities, in the inner and outer regions of the vacuum vessel

Time [years]	**SiC 30 dose rate [Sv/h]**	**SiC 30 no imp., dose rate [Sv/h]**	**SiC 34 dose rate [Sv/h]**	**SiC 34 no imp., dose rate [Sv/h]**
0.00E+000	2.04E+005	2.03E+005	1.09E+005	1.09E+005
3.17E-008	2.02E+005	2.02E+005	1.08E+005	1.08E+005
9.51E-007	1.73E+005	1.73E+005	9.30E+004	9.30E+004
1.90E-006	1.49E+005	1.49E+005	7.99E+004	7.99E+004
9.51E-006	4.49E+004	4.49E+004	2.40E+004	2.40E+004
5.70E-005	4.83E+002	4.83E+002	1.82E+002	1.83E+002
6.84E-004	1.84E+002	1.84E+002	4.33E+001	4.33E+001
2.74E-003	8.00E+001	8.02E+001	1.88E+001	1.88E+001
1.92E-002	1.24E-001	1.03E-001	3.81E-002	2.30E-002
5.07E-001	7.15E-003	1.88E-004	4.86E-003	1.60E-005
9.97E-001	4.12E-003	1.65E-004	2.93E-003	1.41E-005
5.00E+000	1.14E-003	6.39E-005	9.54E-004	6.03E-006
5.00E+001	2.12E-005	5.37E-006	1.31E-005	9.45E-007
1.00E+002	9.16E-006	5.37E-006	3.10E-006	9.44E-007
2.00E+002	6.64E-006	5.37E-006	1.61E-006	9.44E-007
5.00E+002	5.70E-006	5.37E-006	1.12E-006	9.44E-007
1.50E+003	5.42E-006	5.36E-006	9.71E-007	9.43E-007

Table B.15: Decay heat of Silicon Carbide, with and without impurities, in the inner and outer regions of the vacuum vessel

Time [years]	**SiC 30 decay heat [kW/kg]**	**SiC 30 no imp., decay heat [kW/kg]**	**SiC 34 decay heat [kW/kg]**	**SiC 34 no imp., decay heat [kW/kg]**
0.00E+000	1.83E-001	1.83E-001	9.81E-002	9.81E-002
3.17E-008	1.82E-001	1.82E-001	9.74E-002	9.74E-002
9.51E-007	1.56E-001	1.56E-001	8.36E-002	8.36E-002
1.90E-006	1.34E-001	1.34E-001	7.18E-002	7.18E-002
9.51E-006	4.05E-002	4.05E-002	2.17E-002	2.17E-002
5.70E-005	4.25E-004	4.25E-004	1.87E-004	1.87E-004
6.84E-004	1.17E-004	1.17E-004	3.17E-005	3.16E-005
2.74E-003	4.75E-005	4.76E-005	1.12E-005	1.12E-005
1.92E-002	8.69E-008	6.84E-008	2.92E-008	1.66E-008
5.07E-001	1.07E-008	5.36E-009	5.59E-009	2.00E-009
9.97E-001	8.14E-009	5.21E-009	4.04E-009	1.95E-009
5.00E+000	4.89E-009	4.14E-009	2.21E-009	1.57E-009
5.00E+001	4.42E-010	4.14E-010	1.87E-010	1.68E-010
1.00E+002	1.29E-010	1.14E-010	6.36E-011	5.43E-011
2.00E+002	1.03E-010	9.49E-011	5.24E-011	4.71E-011
5.00E+002	9.79E-011	9.47E-011	4.91E-011	4.70E-011
1.50E+003	9.46E-011	9.42E-011	4.70E-011	4.67E-011

- **TZM**

Table B.16: Specific activity of TZM in the inner wall of the vacuum vessel

Time [years]	**TZM specific act. [Bq/kg]**	**TZM no imp. specific act. [Bq/kg]**	**TZM isotopic tail. specific act. [Bq/kg]**
0.00E+000	5.01E+014	5.00E+014	2.58E+013
3.17E-008	5.00E+014	5.00E+014	2.57E+013
9.51E-007	4.94E+014	4.94E+014	2.44E+013
1.90E-006	4.91E+014	4.91E+014	2.36E+013
9.51E-006	4.80E+014	4.80E+014	2.18E+013
5.70E-005	4.32E+014	4.31E+014	1.94E+013
6.84E-004	3.79E+014	3.79E+014	1.08E+013
2.74E-003	3.24E+014	3.24E+014	8.71E+012
1.92E-002	9.39E+013	9.38E+013	2.16E+012
5.07E-001	3.27E+012	3.25E+012	1.06E+011
9.97E-001	6.49E+011	6.36E+011	3.63E+010
5.00E+000	2.24E+011	2.21E+011	4.57E+009
5.00E+001	2.15E+011	2.15E+011	2.74E+008
1.00E+002	2.07E+011	2.07E+011	4.04E+007
2.00E+002	1.91E+011	1.91E+011	2.32E+007
5.00E+002	1.53E+011	1.53E+011	2.02E+007
1.50E+003	8.22E+010	8.22E+010	1.80E+007

Table B.17: Specific activity of TZM in the outer wall of the vacuum vessel

Time [years]	**TZM specific act. [Bq/kg]**	**TZM no imp., specific act. [Bq/kg]**	**TZM isotopic tail., specific act. [Bq/kg]**
0.00E+000	3.57E+014	3.57E+014	1.56E+013
3.17E-008	3.57E+014	3.57E+014	1.55E+013
9.51E-007	3.53E+014	3.53E+014	1.49E+013
1.90E-006	3.51E+014	3.51E+014	1.45E+013
9.51E-006	3.43E+014	3.43E+014	1.35E+013
5.70E-005	3.06E+014	3.06E+014	1.24E+013
6.84E-004	2.66E+014	2.66E+014	8.11E+012
2.74E-003	2.27E+014	2.27E+014	6.66E+012
1.92E-002	6.13E+013	6.13E+013	1.60E+012
5.07E-001	1.60E+012	1.59E+012	5.59E+010
9.97E-001	3.20E+011	3.13E+011	1.87E+010
5.00E+000	1.12E+011	1.11E+011	2.13E+009
5.00E+001	1.10E+011	1.10E+011	1.23E+008
1.00E+002	1.06E+011	1.06E+011	2.46E+007
2.00E+002	9.88E+010	9.88E+010	1.70E+007
5.00E+002	8.02E+010	8.02E+010	1.52E+007
1.50E+003	4.49E+010	4.49E+010	1.38E+007

Table B.18: Dose rate of TZM in the inner wall of the vacuum vessel

Time [years]	**TZM dose rate [Sv/h]**	**TZM no imp., dose rate [Sv/h]**	**TZM isotopic tail., dose rate [Sv/h]**
0.00E+000	3.45E+004	3.45E+004	3.39E+003
3.17E-008	3.43E+004	3.43E+004	3.30E+003
9.51E-007	3.35E+004	3.35E+004	3.05E+003
1.90E-006	3.30E+004	3.30E+004	2.92E+003
9.51E-006	2.97E+004	2.97E+004	2.61E+003
5.70E-005	1.87E+004	1.87E+004	2.22E+003
6.84E-004	1.18E+004	1.18E+004	8.49E+002
2.74E-003	9.84E+003	9.84E+003	5.65E+002
1.92E-002	3.92E+003	3.92E+003	1.23E+002
5.07E-001	1.41E+002	1.40E+002	1.50E+001
9.97E-001	2.18E+001	2.09E+001	3.43E+000
5.00E+000	4.37E-001	2.12E-001	1.34E-001
5.00E+001	2.08E-001	2.06E-001	1.36E-003
1.00E+002	2.02E-001	2.01E-001	9.48E-004
2.00E+002	1.92E-001	1.91E-001	8.02E-004
5.00E+002	1.66E-001	1.66E-001	4.89E-004
1.50E+003	1.19E-001	1.19E-001	9.61E-005

Table B.19: Dose rate of TZM in the outer region of the vacuum vessel

Time [years]	**TZM dose rate [Sv/h]**	**TZM no imp., dose rate [Sv/h]**	**TZM isotopic tail., dose rate [Sv/h]**
0.00E+000	2.45E+004	2.45E+004	1.69E+003
3.17E-008	2.45E+004	2.45E+004	1.64E+003
9.51E-007	2.40E+004	2.39E+004	1.51E+003
1.90E-006	2.36E+004	2.36E+004	1.44E+003
9.51E-006	2.11E+004	2.11E+004	1.29E+003
5.70E-005	1.25E+004	1.24E+004	1.10E+003
6.84E-004	7.32E+003	7.32E+003	4.41E+002
2.74E-003	6.17E+003	6.16E+003	3.05E+002
1.92E-002	2.30E+003	2.30E+003	7.06E+001
5.07E-001	6.97E+001	6.87E+001	7.99E+000
9.97E-001	1.09E+001	1.01E+001	1.96E+000
5.00E+000	3.53E-001	1.03E-001	1.51E-001
5.00E+001	1.02E-001	1.01E-001	9.72E-004
1.00E+002	9.88E-002	9.83E-002	5.34E-004
2.00E+002	9.38E-002	9.35E-002	4.52E-004
5.00E+002	8.15E-002	8.13E-002	2.75E-004
1.50E+003	5.86E-002	5.86E-002	5.30E-005

Table B.20: Decay heat of TZM in the inner wall of the vacuum vessel

Time [years]	**TZM decay heat [kW/kg]**	**TZM no imp., decay heat [kW/kg]**	**TZM isotopic tail., decay heat [kW/kg]**
0.00E+000	5.00E-002	5.00E-002	3.58E-003
3.17E-008	4.98E-002	4.98E-002	3.53E-003
9.51E-007	4.82E-002	4.82E-002	3.34E-003
1.90E-006	4.75E-002	4.75E-002	3.25E-003
9.51E-006	4.43E-002	4.42E-002	3.00E-003
5.70E-005	3.22E-002	3.22E-002	2.56E-003
6.84E-004	2.30E-002	2.30E-002	1.00E-003
2.74E-003	1.93E-002	1.93E-002	7.16E-004
1.92E-002	5.63E-003	5.63E-003	1.57E-004
5.07E-001	1.38E-004	1.36E-004	1.05E-005
9.97E-001	2.06E-005	2.00E-005	2.43E-006
5.00E+000	8.97E-007	7.65E-007	8.23E-008
5.00E+001	7.53E-007	7.51E-007	1.72E-009
1.00E+002	7.29E-007	7.28E-007	1.10E-009
2.00E+002	6.83E-007	6.82E-007	9.09E-010
5.00E+002	5.68E-007	5.67E-007	6.26E-010
1.50E+003	3.48E-007	3.48E-007	2.97E-010

Table B.21: Decay heat of TZM in the outer wall of the vacuum vessel

Time [years]	**TZM decay heat [kW/kg]**	**TZM no imp., decay heat [kW/kg]**	**TZM isotopic tail., decay heat [kW/kg]**
0.00E+000	3.55E-002	3.55E-002	1.90E-003
3.17E-008	3.54E-002	3.54E-002	1.87E-003
9.51E-007	3.44E-002	3.44E-002	1.78E-003
1.90E-006	3.39E-002	3.39E-002	1.73E-003
9.51E-006	3.16E-002	3.16E-002	1.61E-003
5.70E-005	2.26E-002	2.26E-002	1.39E-003
6.84E-004	1.58E-002	1.58E-002	6.33E-004
2.74E-003	1.33E-002	1.33E-002	4.74E-004
1.92E-002	3.65E-003	3.65E-003	1.07E-004
5.07E-001	6.78E-005	6.70E-005	5.60E-006
9.97E-001	1.02E-005	9.77E-006	1.37E-006
5.00E+000	5.27E-007	3.84E-007	8.83E-008
5.00E+001	3.89E-007	3.88E-007	1.08E-009
1.00E+002	3.79E-007	3.78E-007	6.68E-010
2.00E+002	3.57E-007	3.56E-007	5.71E-010
5.00E+002	3.00E-007	3.00E-007	4.08E-010
1.50E+003	1.91E-007	1.91E-007	2.19E-010

- **Eurofer97 and Eurofer-ODS**

Table B.22: Specific activity of Eurofer97 and Eurofer-ODS in the inner wall of the vacuum vessel

Time [years]	**Eurofer97 with imp., Specific act. [Bq/kg]**	**Eurofer97 no imp., Specific act. [Bq/kg]**	**Eurofer97 no imp., isotopic tail. Specific act. [Bq/kg]**	**Eurofer-ODS Specific act. [Bq/kg]**
0.00E+000	3.01E+014	3.00E+014	1.94E+014	3.00E+014
3.17E-008	3.00E+014	2.99E+014	1.88E+014	3.00E+014
9.51E-007	2.97E+014	2.97E+014	1.68E+014	2.97E+014
1.90E-006	2.96E+014	2.96E+014	1.59E+014	2.95E+014
9.51E-006	2.89E+014	2.88E+014	1.27E+014	2.88E+014
5.70E-005	2.74E+014	2.74E+014	1.19E+014	2.73E+014
6.84E-004	2.07E+014	2.07E+014	1.08E+014	2.06E+014
2.74E-003	1.86E+014	1.86E+014	9.73E+013	1.85E+014
1.92E-002	1.79E+014	1.79E+014	8.27E+013	1.79E+014
5.07E-001	1.29E+014	1.29E+014	2.38E+013	1.29E+014
9.97E-001	1.09E+014	1.09E+014	8.44E+012	1.09E+014
5.00E+000	3.60E+013	3.60E+013	2.18E+011	3.61E+013
5.00E+001	8.29E+008	7.38E+008	6.68E+008	4.39E+008
1.00E+002	1.27E+008	7.40E+007	4.37E+007	1.32E+007
2.00E+002	8.26E+007	5.69E+007	3.88E+006	1.18E+007
5.00E+002	6.53E+007	5.52E+007	3.60E+006	1.18E+007
1.50E+003	5.51E+007	5.02E+007	3.20E+006	1.18E+007

Table B.23: Specific activity of Eurofer97 and Eurofer-ODS in the outer wall of the vacuum vessel

Time [years]	**Eurofer97, with imp. specific act. [Bq/kg]**	**Eurofer97, no imp. specific act. [Bq/kg]**	**Eurofer97, no imp., isotopic tail., specific act. [Bq/kg]**	**Eurofer-ODS, specific act. [Bq/kg]**
0.00E+000	1.55E+014	1.55E+014	6.87E+013	1.54E+014
3.17E-008	1.55E+014	1.54E+014	6.68E+013	1.54E+014
9.51E-007	1.53E+014	1.53E+014	5.93E+013	1.52E+014
1.90E-006	1.52E+014	1.52E+014	5.44E+013	1.51E+014
9.51E-006	1.49E+014	1.48E+014	3.88E+013	1.47E+014
5.70E-005	1.41E+014	1.41E+014	3.53E+013	1.40E+014
6.84E-004	1.05E+014	1.05E+014	3.07E+013	1.04E+014
2.74E-003	9.32E+013	9.31E+013	2.63E+013	9.22E+013
1.92E-002	8.91E+013	8.91E+013	2.07E+013	8.86E+013
5.07E-001	6.29E+013	6.29E+013	5.70E+012	6.30E+013
9.97E-001	5.26E+013	5.26E+013	1.90E+012	5.28E+013
5.00E+000	1.70E+013	1.70E+013	4.93E+010	1.71E+013
5.00E+001	4.36E+008	3.71E+008	3.22E+008	2.06E+008
1.00E+002	7.45E+007	4.34E+007	2.12E+007	6.22E+006
2.00E+002	4.93E+007	3.42E+007	2.05E+006	5.61E+006
5.00E+002	3.88E+007	3.32E+007	1.92E+006	5.61E+06
1.50E+003	3.29E+007	3.00E+007	1.70E+006	5.61E+006

Table B.24: Contact dose rate of Eurofer97 and Eurofer-ODS in the inner wall of the vacuum vessel

Time [years]	**Eurofer97, with imp., dose rate [Sv/h]**	**Eurofer97, no imp., dose rate [Sv/h]**	**Eurofer97, no imp., isotopic tail., dose rate [Sv/h]**	**Eurofer-ODS, dose rate [Bq/kg]**
0.00E+000	5.91E+004	5.89E+004	1.46E+004	6.05E+004
3.17E-008	5.91E+004	5.89E+004	1.46E+004	6.04E+004
9.51E-007	5.86E+004	5.84E+004	1.41E+004	5.97E+004
1.90E-006	5.81E+004	5.80E+004	1.37E+004	5.92E+004
9.51E-006	5.54E+004	5.54E+004	1.22E+004	5.64E+004
5.70E-005	4.88E+004	4.88E+004	1.12E+004	4.97E+004
6.84E-004	1.55E+004	1.54E+004	7.39E+003	1.63E+004
2.74E-003	5.63E+003	5.58E+003	5.78E+003	6.40E+003
1.92E-002	5.29E+003	5.27E+003	4.81E+003	6.08E+003
5.07E-001	3.28E+003	3.28E+003	2.01E+003	3.55E+003
9.97E-001	2.16E+003	2.16E+003	9.51E+002	2.25E+003
5.00E+000	9.25E+001	9.07E+001	2.14E+001	9.13E+001
5.00E+001	5.53E-003	1.66E-004	2.81E-005	1.67E-004
1.00E+002	2.88E-004	3.51E-006	6.67E-006	3.35E-006
2.00E+002	2.78E-004	2.67E-006	8.27E-007	2.68E-006
5.00E+002	2.74E-004	2.58E-006	1.31E-007	2.61E-006
1.50E+003	2.63E-004	2.58E-006	1.30E-007	2.61E-006

Table B.25: Contact dose rate of Eurofer97 and Eurofer-ODS in the outer wall of the vacuum vessel

Time [years]	**Eurofer97, with imp., dose rate [Sv/h]**	**Eurofer97, no imp., dose rate [Sv/h]**	**Eurofer97, no imp., isotopic tail. dose rate [Sv/h]**	**Eurofer-ODS, dose rate [Bq/kg]**
0.00E+000	3.19E+004	3.18E+004	6.04E+003	3.26E+004
3.17E-008	3.19E+004	3.18E+004	6.02E+003	3.26E+004
9.51E-007	3.16E+004	3.15E+004	5.76E+003	3.22E+004
1.90E-006	3.14E+004	3.13E+004	5.55E+003	3.19E+004
9.51E-006	3.00E+004	2.99E+004	4.79E+003	3.04E+004
5.70E-005	2.65E+004	2.64E+004	4.34E+003	2.69E+004
6.84E-004	8.80E+003	8.76E+003	2.69E+003	9.15E+003
2.74E-003	3.52E+003	3.48E+003	1.97E+003	3.88E+003
1.92E-002	3.26E+003	3.24E+003	1.53E+003	3.66E+003
5.07E-001	1.97E+003	1.97E+003	5.81E+002	2.11E+003
9.97E-001	1.28E+003	1.27E+003	2.44E+002	1.32E+003
5.00E+000	5.40E+001	5.18E+001	3.76E+000	5.21E+001
5.00E+001	6.48E-003	1.18E-004	1.06E-005	1.19E-004
1.00E+002	2.46E-004	1.55E-006	7.34E-007	1.51E-006
2.00E+002	2.35E-004	1.26E-006	1.15E-007	1.26E-006
5.00E+002	2.32E-004	1.24E-006	4.27E-008	1.24E-006
1.50E+003	2.23E-004	1.23E-006	4.25E-008	1.24E-006

Table B.26: Decay heat of Eurofer97 and Eurofer-ODS in the inner wall of the vacuum vessel

Time [years]	**Eurofer97, with imp. decay heat [kW/kg]**	**Eurofer97, no imp. decay heat [kW/kg]**	**Eurofer97, no imp., isotopic tail., decay heat [kW/kg]**	**Eurofer-ODS, decay heat [Bq/kg]**
0.00E+000	4.84E-002	4.82E-002	2.27E-002	4.91E-002
3.17E-008	4.84E-002	4.82E-002	2.25E-002	4.91E-002
9.51E-007	4.78E-002	4.76E-002	2.00E-002	4.84E-002
1.90E-006	4.73E-002	4.72E-002	1.83E-002	4.78E-002
9.51E-006	4.47E-002	4.47E-002	1.25E-002	4.52E-002
5.70E-005	3.91E-002	3.91E-002	1.08E-002	3.95E-002
6.84E-004	1.20E-002	1.19E-002	7.55E-003	1.24E-002
2.74E-003	3.94E-003	3.89E-003	5.86E-003	4.30E-003
1.92E-002	3.61E-003	3.59E-003	4.49E-003	4.00E-003
5.07E-001	2.16E-003	2.16E-003	1.61E-003	2.30E-003
9.97E-001	1.42E-003	1.42E-003	6.94E-004	1.47E-003
5.00E+000	8.38E-005	8.28E-005	1.36E-005	8.31E-005
5.00E+001	4.78E-009	1.03E-009	6.71E-010	4.39E-010
1.00E+002	8.86E-010	3.89E-010	7.95E-011	1.44E-011
2.00E+002	6.66E-010	3.69E-010	3.56E-011	1.11E-011
5.00E+002	5.77E-010	3.55E-010	3.31E-011	1.09E-011
1.50E+003	5.16E-010	3.16E-010	2.98E-011	1.09E-011

Table B.27: Decay heat of Eurofer97 and Eurofer-ODS in the outer wall of the vacuum vessel

Time [years]	**Eurofer97, with imp., decay heat [kW/kg]**	**Eurofer97, no imp., decay heat [kW/kg]**	**Eurofer97, no imp., isotopic tail., decay heat [kW/kg]**	**Eurofer-ODS, decay heat [Bq/kg]**
0.00E+000	2.61E-002	2.60E-002	1.03E-002	2.65E-02
3.17E-008	2.61E-002	2.60E-002	1.02E-002	2.65E-02
9.51E-007	2.58E-002	2.57E-002	8.94E-003	2.61E-02
1.90E-006	2.56E-002	2.55E-002	7.98E-003	2.58E-02
9.51E-006	2.42E-002	2.42E-002	4.91E-003	2.44E-02
5.70E-005	2.12E-002	2.12E-002	4.11E-003	2.14E-02
6.84E-004	6.85E-003	6.81E-003	2.69E-003	6.99E-03
2.74E-003	2.51E-003	2.47E-003	1.94E-003	2.66E-03
1.92E-002	2.23E-003	2.21E-003	1.36E-003	2.43E-03
5.07E-001	1.29E-003	1.29E-003	4.60E-004	1.36E-03
9.97E-001	8.35E-004	8.34E-004	1.79E-004	8.59E-04
5.00E+000	4.59E-005	4.46E-005	2.38E-006	4.48E-05
5.00E+001	4.66E-009	5.82E-010	3.17E-010	2.29E-10
1.00E+002	5.86E-010	2.43E-010	3.54E-011	6.67E-12
2.00E+002	4.57E-010	2.32E-010	1.70E-011	5.35E-12
5.00E+002	4.04E-010	2.24E-010	1.62E-011	5.28E-12
1.50E+003	3.65E-010	1.99E-010	1.45E-011	5.28E-12

- **SS 316 304**

Table B.28: Specific activity SS 316 and 304 in the outer wall of the vacuum vessel

Time [years]	**SS 316 Specific act. [Bq/kg]**	**SS 316, no imp., Specific act. [Bq/kg]**	**SS 316 no imp. iso. tail., Specific act. [Bq/kg]**	**SS 304 Specific act. [Bq/kg]**	**SS 304 iso. tail., Specific act. [Bq/kg]**
0.00E+000	2.11E+014	2.08E+014	7.56E+013	1.86E+014	4.26E+013
3.17E-008	2.11E+014	2.08E+014	7.54E+013	1.86E+014	4.24E+013
9.51E-007	2.10E+014	2.07E+014	7.25E+013	1.85E+014	3.70E+013
1.90E-006	2.09E+014	2.06E+014	7.00E+013	1.83E+014	3.25E+013
9.51E-006	2.02E+014	2.00E+014	6.06E+013	1.76E+014	1.76E+013
5.70E-005	1.90E+014	1.90E+014	5.17E+013	1.66E+014	1.30E+013
6.84E-004	1.53E+014	1.53E+014	2.14E+013	1.32E+014	4.83E+012
2.74E-003	1.36E+014	1.36E+014	1.48E+013	1.19E+014	3.04E+012
1.92E-002	1.24E+014	1.25E+014	1.40E+013	1.13E+014	2.98E+012
5.07E-001	6.78E+013	6.85E+013	9.48E+012	6.36E+013	2.01E+012
9.97E-001	5.15E+013	5.21E+013	6.60E+012	4.98E+013	1.42E+012
5.00E+000	1.37E+013	1.39E+013	7.08E+011	1.41E+013	1.91E+011
5.00E+001	1.77E+010	1.64E+010	2.50E+009	9.47E+009	8.41E+008
1.00E+002	1.23E+010	1.16E+010	6.24E+008	6.23E+009	1.67E+008
2.00E+002	7.44E+009	7.08E+009	3.09E+008	3.20E+009	7.45E+007
5.00E+002	2.90E+009	2.84E+009	5.26E+007	5.39E+008	9.67E+006
1.50E+003	1.41E+009	1.40E+009	1.41E+007	1.52E+008	2.86E+005

Table B.29: Specific activity SS 316 in the inner wall of the vacuum vessel

Time [years]	**SS 316 Specific act. [Bq/kg]**	**SS 316, no imp., Specific act. [Bq/kg]**	**SS 316., no imp., isotopic tail., Specific act. [Bq/kg]**	**SS 316 no imp., elemental sub., Specific act. [Bq/kg]**
0.00E+000	3.97E+014	3.92E+014	1.25E+014	4.12E+014
3.17E-008	3.97E+014	3.92E+014	1.24E+014	4.11E+014
9.51E-007	3.94E+014	3.90E+014	1.18E+014	4.09E+014
1.90E-006	3.91E+014	3.88E+014	1.14E+014	4.06E+014
9.51E-006	3.78E+014	3.77E+014	9.49E+013	3.91E+014
5.70E-005	3.58E+014	3.58E+014	7.98E+013	3.66E+014
6.84E-004	2.95E+014	2.94E+014	3.84E+013	2.71E+014
2.74E-003	2.66E+014	2.66E+014	3.08E+013	2.41E+014
1.92E-002	2.45E+014	2.47E+014	2.95E+013	2.27E+014
5.07E-001	1.38E+014	1.39E+014	1.99E+013	1.46E+014
9.97E-001	1.06E+014	1.07E+014	1.39E+013	1.15E+014
5.00E+000	2.87E+013	2.92E+013	1.56E+012	2.81E+013
5.00E+001	2.78E+010	2.60E+010	4.90E+009	6.48E+009
1.00E+002	1.94E+010	1.82E+010	8.72E+008	5.35E+009
2.00E+002	1.22E+010	1.16E+010	4.27E+008	4.93E+009
5.00E+002	5.21E+009	5.12E+009	8.27E+007	3.97E+009
1.50E+003	2.53E+009	2.52E+009	2.99E+007	2.17E+009

Table B.30: Specific activity of stainless steels 304 in the inner wall of the vacuum vessel

Time [years]	**SS 304 Specific act. [Bq/kg]**	**SS 304 isotopic tail. Specific act. [Bq/kg]**	**SS 304 elemental sub. Specific act. [Bq/kg]**
0.00E+000	3.61E+014	8.03E+013	3.75E+014
3.17E-008	3.61E+014	7.99E+013	3.75E+014
9.51E-007	3.58E+014	6.91E+013	3.71E+014
1.90E-006	3.55E+014	6.02E+013	3.68E+014
9.51E-006	3.41E+014	3.10E+013	3.52E+014
5.70E-005	3.22E+014	2.22E+013	3.28E+014
6.84E-004	2.62E+014	9.28E+012	2.45E+014
2.74E-003	2.38E+014	6.63E+012	2.20E+014
1.92E-002	2.25E+014	6.49E+012	2.12E+014
5.07E-001	1.30E+014	4.39E+012	1.35E+014
9.97E-001	1.03E+014	3.14E+012	1.08E+014
5.00E+000	2.97E+013	4.68E+011	2.90E+013
5.00E+001	1.42E+010	1.72E+009	4.19E+008
1.00E+002	9.11E+009	2.44E+008	1.50E+007
2.00E+002	4.70E+009	1.01E+008	9.25E+006
5.00E+002	8.24E+008	1.38E+007	9.20E+006
1.50E+003	2.60E+008	1.23E+006	9.19E+006

Table B.31: Specific activity of stainless steel 316 in the outer wall of the vacuum vessel

Time [years]	**SS 316 Specific act. [Bq/kg]**	**SS 316 no imp., Specific act. [Bq/kg]**	**SS 316 no imp., isotopic tail., Specific act. [Bq/kg]**	**SS 316 no imp., elemental sub., Specific act. [Bq/kg]**
0.00E+000	2.11E+014	2.08E+014	7.56E+013	2.44E+014
3.17E-008	2.11E+014	2.08E+014	7.54E+013	2.44E+014
9.51E-007	2.10E+014	2.07E+014	7.25E+013	2.42E+014
1.90E-006	2.09E+014	2.06E+014	7.00E+013	2.41E+014
9.51E-006	2.02E+014	2.00E+014	6.06E+013	2.32E+014
5.70E-005	1.90E+014	1.90E+014	5.17E+013	2.15E+014
6.84E-004	1.53E+014	1.53E+014	2.14E+013	1.41E+014
2.74E-003	1.36E+014	1.36E+014	1.48E+013	1.18E+014
1.92E-002	1.24E+014	1.25E+014	1.40E+013	1.10E+014
5.07E-001	6.78E+013	6.85E+013	9.48E+012	7.04E+013
9.97E-001	5.15E+013	5.21E+013	6.60E+012	5.54E+013
5.00E+000	1.37E+013	1.39E+013	7.08E+011	1.33E+013
5.00E+001	1.77E+010	1.64E+010	2.50E+009	3.33E+009
1.00E+002	1.23E+010	1.16E+010	6.24E+008	2.77E+009
2.00E+002	7.44E+009	7.08E+009	3.09E+008	2.56E+009
5.00E+002	2.90E+009	2.84E+009	5.26E+007	2.09E+009
1.50E+003	1.41E+009	1.40E+009	1.41E+007	1.19E+009

Table B.32: Specific activity of stainless steel 304 in the outer wall of the vacuum vessel

Time [years]	**SS 304 Specific act. [Bq/kg]**	**SS 304 isotopic tail., Specific act. [Bq/kg]**	**SS 304 elemental sub., Specific act. [Bq/kg]**
0.00E+000	1.86E+014	4.26E+013	2.11E+014
3.17E-008	1.86E+014	4.24E+013	2.11E+014
9.51E-007	1.85E+014	3.70E+013	2.09E+014
1.90E-006	1.83E+014	3.25E+013	2.08E+014
9.51E-006	1.76E+014	1.76E+013	1.99E+014
5.70E-005	1.66E+014	1.30E+013	1.84E+014
6.84E-004	1.32E+014	4.83E+012	1.24E+014
2.74E-003	1.19E+014	3.04E+012	1.06E+014
1.92E-002	1.13E+014	2.98E+012	1.02E+014
5.07E-001	6.36E+013	2.01E+012	6.49E+013
9.97E-001	4.98E+013	1.42E+012	5.21E+013
5.00E+000	1.41E+013	1.91E+011	1.37E+013
5.00E+001	9.47E+009	8.41E+008	1.93E+008
1.00E+002	6.23E+009	1.67E+008	6.83E+006
2.00E+002	3.20E+009	7.45E+007	4.39E+006
5.00E+002	5.39E+008	9.67E+006	4.37E+006
1.50E+003	1.52E+008	2.86E+005	4.36E+006

Table B.33: Contact dose rate of stainless steel 316 in the inner wall of the vacuum vessel

Time [years]	**SS 316 Dose rate [Sv/h]**	**SS 316 no imp., Dose rate [Sv/h]**	**SS 316 no imp., isotopic tail., Dose rate [Sv/h]**	**SS 316 no imp., elemental sub., Dose rate [Sv/h]**
0.00E+000	6.86E+004	6.66E+004	2.90E+004	9.98E+004
3.17E-008	6.86E+004	6.66E+004	2.89E+004	9.98E+004
9.51E-007	6.75E+004	6.58E+004	2.73E+004	9.88E+004
1.90E-006	6.66E+004	6.51E+004	2.60E+004	9.79E+004
9.51E-006	6.16E+004	6.10E+004	2.10E+004	9.28E+004
5.70E-005	5.39E+004	5.37E+004	1.81E+004	8.20E+004
6.84E-004	2.67E+004	2.62E+004	9.81E+003	3.47E+004
2.74E-003	1.82E+004	1.79E+004	7.43E+003	2.07E+004
1.92E-002	1.65E+004	1.64E+004	7.29E+003	2.01E+004
5.07E-001	6.22E+003	6.19E+003	5.29E+003	1.33E+004
9.97E-001	3.53E+003	3.51E+003	3.92E+003	8.96E+003
5.00E+000	5.34E+002	5.12E+002	8.74E+002	3.56E+002
5.00E+001	1.18E+000	1.11E+000	2.08E+000	4.84E-003
1.00E+002	1.24E-002	6.25E-003	2.51E-003	4.60E-003
2.00E+002	9.43E-003	4.45E-003	2.82E-006	4.38E-003
5.00E+002	7.40E-003	3.92E-003	2.82E-006	3.84E-003
1.50E+003	5.55E-003	2.92E-003	2.80E-006	2.82E-003

Table B.34: Dose rate of stainless steel 304 in the inner wall of the vacuum vessel

Time [years]	**SS 304 Dose rate [Sv/h]**	**SS 304 isotopic tail., Dose rate [Sv/h]**	**SS 304 elemental sub., Dose rate [Sv/h]**
0.00E+000	6.52E+004	1.26E+004	8.86E+004
3.17E-008	6.51E+004	1.26E+004	8.85E+004
9.51E-007	6.38E+004	1.15E+004	8.71E+004
1.90E-006	6.27E+004	1.07E+004	8.58E+004
9.51E-006	5.67E+004	7.47E+003	7.91E+004
5.70E-005	4.87E+004	5.96E+003	6.86E+004
6.84E-004	2.16E+004	2.57E+003	2.75E+004
2.74E-003	1.34E+004	1.59E+003	1.54E+004
1.92E-002	1.24E+004	1.56E+003	1.50E+004
5.07E-001	4.88E+003	1.13E+003	9.91E+003
9.97E-001	2.83E+003	8.54E+002	6.66E+003
5.00E+000	3.78E+002	2.16E+002	2.67E+002
5.00E+001	7.79E-001	5.26E-001	1.35E-004
1.00E+002	1.21E-003	7.79E-004	2.31E-006
2.00E+002	1.01E-004	7.81E-007	2.24E-006
5.00E+002	1.01E-004	7.79E-007	2.24E-006
1.50E+003	1.00E-004	7.75E-007	2.24E-006

Table B.35: Dose rate of stainless steel 316 in the outer wall of the vacuum vessel

Time [years]	**SS 316 Dose rate [Sv/h]**	**SS 316 no imp., Dose rate [Sv/h]**	**SS 316 no imp., isotopic tail., Dose rate [Sv/h]**	**SS 316 no imp., elemental sub., Dose rate [Sv/h]**
0.00E+000	3.92E+004	3.81E+004	2.08E+004	6.99E+004
3.17E-008	3.92E+004	3.81E+004	2.08E+004	6.98E+004
9.51E-007	3.86E+004	3.77E+004	1.99E+004	6.93E+004
1.90E-006	3.81E+004	3.73E+004	1.93E+004	6.88E+004
9.51E-006	3.55E+004	3.51E+004	1.67E+004	6.58E+004
5.70E-005	3.12E+004	3.11E+004	1.46E+004	5.82E+004
6.84E-004	1.55E+004	1.52E+004	6.02E+003	2.13E+004
2.74E-003	1.06E+004	1.04E+004	3.52E+003	1.04E+004
1.92E-002	9.65E+003	9.57E+003	3.44E+003	1.01E+004
5.07E-001	3.51E+003	3.47E+003	2.48E+003	6.64E+003
9.97E-001	1.95E+003	1.92E+003	1.83E+003	4.46E+003
5.00E+000	2.96E+002	2.72E+002	3.89E+002	1.77E+002
5.00E+001	6.57E-001	5.86E-001	9.17E-001	2.39E-003
1.00E+002	7.23E-003	3.15E-003	1.34E-003	2.24E-003
2.00E+002	5.69E-003	2.18E-003	6.72E-007	2.14E-003
5.00E+002	4.64E-003	1.93E-003	6.61E-007	1.87E-003
1.50E+003	3.68E-003	1.44E-003	6.56E-007	1.38E-003

Table B.36: Dose rate of stainless steel 304 in the outer wall of the vacuum vessel

Time [years]	**SS 304 Dose rate [Sv/h]**	**SS 304 isotopic tail., Dose rate [Sv/h]**	**SS 304 elemental sub., Dose rate [Sv/h]**
0.00E+000	3.60E+004	7.41E+003	5.83E+004
3.17E-008	3.59E+004	7.39E+003	5.83E+004
9.51E-007	3.53E+004	6.87E+003	5.76E+004
1.90E-006	3.46E+004	6.43E+003	5.68E+004
9.51E-006	3.15E+004	4.79E+003	5.31E+004
5.70E-005	2.72E+004	3.92E+003	4.64E+004
6.84E-004	1.23E+004	1.47E+003	1.66E+004
2.74E-003	7.79E+003	7.57E+002	7.78E+003
1.92E-002	7.26E+003	7.41E+002	7.58E+003
5.07E-001	2.78E+003	5.30E+002	5.00E+003
9.97E-001	1.57E+003	3.97E+002	3.36E+003
5.00E+000	2.02E+002	9.59E+001	1.34E+002
5.00E+001	4.12E-001	2.32E-001	9.52E-005
1.00E+002	6.29E-004	3.46E-004	1.12E-006
2.00E+002	5.93E-005	1.83E-007	1.04E-006
5.00E+002	5.91E-005	1.83E-007	1.04E-006
1.50E+003	5.86E-005	1.82E-007	1.04E-006

Table B.37: Decay heat of stainless steel 316 in the inner wall of the vacuum vessel

Time [years]	**SS 316 Decay heat [kW/kg]**	**SS 316 no imp., Decay heat [kW/kg]**	**SS 316 isotopic tail., Decay heat [kW/kg]**	**SS 316 elemental sub., Decay heat [kW/kg]**
0.00E+000	5.58E-002	5.40E-002	2.80E-002	7.97E-002
3.17E-008	5.57E-002	5.40E-002	2.78E-002	7.96E-002
9.51E-007	5.47E-002	5.32E-002	2.60E-002	7.86E-002
1.90E-006	5.38E-002	5.24E-002	2.44E-002	7.77E-002
9.51E-006	4.91E-002	4.85E-002	1.88E-002	7.25E-002
5.70E-005	4.21E-002	4.20E-002	1.55E-002	6.29E-002
6.84E-004	1.99E-002	1.96E-002	6.76E-003	2.46E-002
2.74E-003	1.30E-002	1.27E-002	4.60E-003	1.33E-002
1.92E-002	1.15E-002	1.15E-002	4.47E-003	1.27E-002
5.07E-001	4.42E-003	4.40E-003	3.23E-003	8.28E-003
9.97E-001	2.52E-003	2.51E-003	2.38E-003	5.57E-003
5.00E+000	3.42E-004	3.29E-004	5.12E-004	2.39E-004
5.00E+001	7.58E-007	7.11E-007	1.21E-006	2.07E-008
1.00E+002	6.35E-008	5.54E-008	3.94E-009	1.92E-008
2.00E+002	4.14E-008	3.59E-008	1.35E-009	1.80E-008
5.00E+002	2.05E-008	1.77E-008	3.78E-010	1.51E-008
1.50E+003	1.18E-008	9.89E-009	2.16E-010	9.48E-009

Table B.38: Decay heat of stainless steel 304 in the inner region of the vacuum vessel

Time [years]	**SS 304 Decay heat [kW/kg]**	**SS 304 isotopic tail., Decay heat [kW/kg]**	**SS 304 elemental sub., Decay heat [kW/kg]**
0.00E+000	5.30E-002	1.88E-002	7.12E-002
3.17E-008	5.30E-002	1.87E-002	7.11E-002
9.51E-007	5.18E-002	1.62E-002	6.97E-002
1.90E-006	5.06E-002	1.41E-002	6.85E-002
9.51E-006	4.51E-002	7.21E-003	6.21E-002
5.70E-005	3.81E-002	5.08E-003	5.28E-002
6.84E-004	1.59E-002	1.83E-003	1.95E-002
2.74E-003	9.30E-003	9.74E-004	9.71E-003
1.92E-002	8.61E-003	9.55E-004	9.45E-003
5.07E-001	3.44E-003	6.89E-004	6.18E-003
9.97E-001	2.00E-003	5.17E-004	4.17E-003
5.00E+000	2.49E-004	1.26E-004	1.85E-004
5.00E+001	4.88E-007	3.07E-007	4.11E-010
1.00E+002	2.56E-008	1.05E-009	1.76E-011
2.00E+002	1.27E-008	2.81E-010	1.08E-011
5.00E+002	1.87E-009	3.69E-011	9.04E-012
1.50E+003	2.98E-010	1.73E-012	8.58E-012

Table B.39: Decay heat of stainless steel 316 in the outer wall of the vacuum vessel

Time [years]	**SS 316 Decay heat [kW/kg]**	**SS 316 no imp., Decay heat [kW/kg]**	**SS 316 isotopic tail., Decay heat [kW/kg]**	**SS 316 elemental sub., Decay heat [kW/kg]**
0.00E+000	3.18E-002	3.08E-002	1.93E-002	5.61E-002
3.17E-008	3.18E-002	3.08E-002	1.91E-002	5.61E-002
9.51E-007	3.12E-002	3.03E-002	1.82E-002	5.55E-002
1.90E-006	3.07E-002	3.00E-002	1.75E-002	5.50E-002
9.51E-006	2.82E-002	2.79E-002	1.46E-002	5.20E-002
5.70E-005	2.44E-002	2.43E-002	1.24E-002	4.55E-002
6.84E-004	1.15E-002	1.13E-002	4.35E-003	1.55E-002
2.74E-003	7.50E-003	7.36E-003	2.20E-003	6.73E-003
1.92E-002	6.69E-003	6.63E-003	2.12E-003	6.32E-003
5.07E-001	2.45E-003	2.43E-003	1.52E-003	4.12E-003
9.97E-001	1.37E-003	1.35E-003	1.11E-003	2.77E-003
5.00E+000	1.88E-004	1.73E-004	2.28E-004	1.18E-004
5.00E+001	4.29E-007	3.84E-007	5.35E-007	1.08E-008
1.00E+002	4.00E-008	3.48E-008	2.56E-009	1.01E-008
2.00E+002	2.54E-008	2.18E-008	9.45E-010	9.49E-009
5.00E+002	1.20E-008	9.82E-009	2.28E-010	8.05E-009
1.50E+003	7.09E-009	5.49E-009	1.13E-010	5.25E-009

Table B.40: Decay heat of stainless steel 304 in the outer wall of the vacuum vessel

Time [years]	**SS 304 Decay heat [kW/kg]**	**SS 304 isotopic tail., Decay heat [kW/kg]**	**SS 304 elemental sub., Decay heat [kW/kg]**
0.00E+000	2.91E-002	1.04E-002	4.70E-002
3.17E-008	2.91E-002	1.03E-002	4.70E-002
9.51E-007	2.84E-002	9.05E-003	4.62E-002
1.90E-006	2.79E-002	8.01E-003	4.55E-002
9.51E-006	2.49E-002	4.49E-003	4.20E-002
5.70E-005	2.12E-002	3.33E-003	3.62E-002
6.84E-004	9.00E-003	1.07E-003	1.20E-002
2.74E-003	5.35E-003	4.64E-004	4.91E-003
1.92E-002	4.99E-003	4.53E-004	4.77E-003
5.07E-001	1.92E-003	3.23E-004	3.12E-003
9.97E-001	1.09E-003	2.40E-004	2.10E-003
5.00E+000	1.32E-004	5.62E-005	9.25E-005
5.00E+001	2.64E-007	1.36E-007	2.07E-010
1.00E+002	1.75E-008	6.31E-010	7.77E-012
2.00E+002	8.69E-009	2.08E-010	4.93E-012
5.00E+002	1.25E-009	2.67E-011	4.25E-012
1.50E+003	1.74E-010	4.39E-013	4.08E-012

- **FLiBe**

Table B.41: Specific activity of FLiBe, with and without impurities, in the cooling channel (31) and in the tank (40)

Time [years]	**FLiBe with imp., 31 Specific act. [Bq/kg]**	**FLiBe no imp., 31 Specific act. [Bq/kg]**	**FLiBe with imp., 40 Specific act. [Bq/kg]**	**FLiBe no imp., 40 Specific act. [Bq/kg]**
0.00E+000	7.14E+013	7.24E+013	1.03E+013	1.33E+013
3.17E-008	4.79E+013	4.92E+013	8.34E+012	1.08E+013
9.51E-007	3.64E+012	3.74E+012	9.76E+011	1.25E+012
1.90E-006	9.43E+011	9.72E+011	2.98E+011	3.74E+011
9.51E-006	3.19E+010	3.78E+010	8.90E+009	1.42E+010
5.70E-005	2.70E+010	3.29E+010	7.50E+009	1.25E+010
6.84E-004	1.05E+010	1.60E+010	3.16E+009	6.75E+009
2.74E-003	8.15E+009	1.33E+010	2.55E+009	5.91E+009
1.92E-002	8.14E+009	1.33E+010	2.55E+009	5.90E+009
5.07E-001	7.92E+009	1.30E+010	2.48E+009	5.74E+009
9.97E-001	7.71E+009	1.26E+010	2.41E+009	5.58E+009
5.00E+000	6.15E+009	1.01E+010	1.92E+009	4.46E+009
5.00E+001	4.90E+008	7.03E+008	1.53E+008	3.84E+008
1.00E+002	2.95E+007	3.18E+007	9.23E+006	2.82E+007
2.00E+002	1.13E+005	5.34E+004	3.33E+004	1.29E+005
5.00E+002	2.37E+001	5.16E-001	7.46E+000	2.73E-001
1.50E+003	1.03E+001	5.12E-001	3.19E+000	2.41E-001

Table B.42: Dose rate of FLiBe, with and without impurities, in the cooling channel (31) and in the tank (40)

Time [years]	**FLiBe with imp., 31 Dose rate [Sv/h]**	**FLiBe no imp., 31 Dose rate [Sv/h]**	**FLiBe with imp., 40 Dose rate [Sv/h]**	**FLiBe no imp., 40 Dose rate [Sv/h]**
0.00E+000	5.67E+004	5.72E+004	1.22E+004	1.56E+004
3.17E-008	5.15E+004	5.20E+004	1.11E+004	1.42E+004
9.51E-007	3.55E+003	3.61E+003	8.08E+002	1.04E+003
1.90E-006	3.94E+002	4.15E+002	1.08E+002	1.33E+002
9.51E-006	5.02E+000	5.18E+000	1.35E+000	1.76E+000
5.70E-005	3.93E+000	4.06E+000	1.03E+000	1.36E+000
6.84E-004	4.89E-001	5.57E-001	1.28E-001	1.76E-001
2.74E-003	1.01E-003	6.74E-004	3.33E-004	3.04E-004
1.92E-002	3.43E-004	0.00E+000	1.66E-004	0.00E+000
5.07E-001	8.65E-005	0.00E+000	4.04E-005	0.00E+000
9.97E-001	3.47E-005	0.00E+000	1.52E-005	0.00E+000
5.00E+000	4.71E-006	0.00E+000	1.78E-006	0.00E+000
5.00E+001	1.06E-008	0.00E+000	3.90E-009	0.00E+000
1.00E+002	1.00E-010	0.00E+000	3.08E-011	0.00E+000
2.00E+002	7.88E-011	0.00E+000	2.33E-011	0.00E+000
5.00E+002	6.37E-011	0.00E+000	1.89E-011	0.00E+000
1.50E+003	3.57E-011	0.00E+000	1.08E-011	0.00E+000

Table B.43: Decay heat of FLiBe, with and without impurities, in the cooling channel (31) and in the tank (40)

Time [years]	**FLiBe with imp., 31 Decay heat [kW/kg]**	**FLiBe no imp., 31 Decay heat [kW/kg]**	**FLiBe with imp., 40 Decay heat [kW/kg]**	**FLiBe no imp., 40 Decay heat [kW/kg]**
0.00E+000	4.72E-002	4.78E-002	8.88E-003	1.14E-002
3.17E-008	3.86E-002	3.93E-002	7.84E-003	1.01E-002
9.51E-007	2.84E-003	2.90E-003	6.90E-004	8.89E-004
1.90E-006	4.77E-004	4.96E-004	1.43E-004	1.77E-004
9.51E-006	5.07E-006	5.23E-006	1.39E-006	1.80E-006
5.70E-005	3.74E-006	3.86E-006	9.81E-007	1.30E-006
6.84E-004	4.72E-007	5.40E-007	1.24E-007	1.72E-007
2.74E-003	8.31E-009	1.28E-008	2.59E-009	5.69E-009
1.92E-002	7.68E-009	1.22E-008	2.44E-009	5.39E-009
5.07E-001	7.30E-009	1.19E-008	2.29E-009	5.25E-009
9.97E-001	7.07E-009	1.15E-008	2.21E-009	5.11E-009
5.00E+000	5.63E-009	9.20E-009	1.76E-009	4.08E-009
5.00E+001	4.48E-010	6.43E-010	1.40E-010	3.52E-010
1.00E+002	2.70E-011	2.90E-011	8.44E-012	2.58E-011
2.00E+002	1.03E-013	4.89E-014	3.05E-014	1.18E-013
5.00E+002	8.56E-017	2.04E-017	2.71E-017	9.71E-018
1.50E+003	4.63E-017	2.04E-017	1.46E-017	9.67E-018

- **PbLi**

Table B.44: Specific activity of PbLi, with and without impurities, in the cooling channel (31) and in the tank (40)

Time [years]	**PbLi with imp., 31 Specific act. [Bq/kg]**	**PbLi no imp., 31 Specific act. [Bq/kg]**	**PbLi with imp., 40 Specific act. [Bq/kg]**	**PbLi no imp., 40 Specific act. [Bq/kg]**
0.00E+000	1.25E+014	1.24E+014	5.55E+012	5.58E+012
3.17E-008	5.31E+013	5.20E+013	2.39E+012	2.38E+012
9.51E-007	3.63E+010	3.59E+010	5.90E+009	5.61E+009
1.90E-006	4.27E+009	3.96E+009	1.72E+009	1.54E+009
9.51E-006	2.01E+009	1.99E+009	1.10E+009	1.09E+009
5.70E-005	9.23E+008	9.21E+008	6.90E+008	6.91E+008
6.84E-004	5.66E+008	5.67E+008	3.33E+008	3.34E+008
2.74E-003	3.95E+008	3.95E+008	1.77E+008	1.78E+008
1.92E-002	9.92E+007	1.01E+008	6.51E+007	6.51E+007
5.07E-001	4.65E+007	4.64E+007	4.46E+007	4.47E+007
9.97E-001	4.51E+007	4.51E+007	4.34E+007	4.34E+007
5.00E+000	3.60E+007	3.60E+007	3.46E+007	3.47E+007
5.00E+001	2.86E+006	2.87E+006	2.76E+006	2.80E+006
1.00E+002	1.73E+005	1.74E+005	1.66E+005	1.66E+005
2.00E+002	8.08E+002	7.77E+002	7.01E+002	5.42E+002
5.00E+002	2.01E+002	1.86E+002	8.23E+001	7.41E+001
1.50E+003	1.89E+002	1.86E+002	7.61E+001	7.41E+001

Table B.45: Dose rate of PbLi, with and without impurities, in the cooling channel (31) and in the tank (40)

Time [years]	**PbLi with imp., 31 Dose rate [Sv/h]**	**PbLi no imp., 31 Dose rate [Sv/h]**	**PbLi with imp., 40 Dose rate [Sv/h]**	**PbLi no imp., 40 Dose rate [Sv/h]**
0.00E+000	3.61E+004	3.58E+004	1.59E+003	1.60E+003
3.17E-008	1.53E+004	1.49E+004	6.78E+002	6.73E+002
9.51E-007	4.94E+000	4.94E+000	7.43E-001	7.44E-001
1.90E-006	6.32E-001	6.19E-001	1.89E-001	1.89E-001
9.51E-006	2.37E-001	2.37E-001	9.00E-002	9.03E-002
5.70E-005	5.66E-002	5.65E-002	2.76E-002	2.77E-002
6.84E-004	5.57E-003	5.52E-003	2.30E-003	2.32E-003
2.74E-003	3.01E-003	2.99E-003	1.13E-003	1.12E-003
1.92E-002	4.60E-004	4.60E-004	1.78E-004	1.66E-004
5.07E-001	6.98E-006	4.87E-007	6.33E-006	1.72E-007
9.97E-001	3.87E-006	3.48E-008	3.68E-006	1.22E-008
5.00E+000	1.04E-007	3.10E-010	7.96E-008	1.14E-010
5.00E+001	7.47E-009	6.76E-011	3.96E-009	2.70E-011
1.00E+002	6.90E-009	6.76E-011	3.65E-009	2.70E-011
2.00E+002	6.02E-009	6.76E-011	3.16E-009	2.70E-011
5.00E+002	4.11E-009	6.76E-011	2.09E-009	2.70E-011
1.50E+003	1.71E-009	6.76E-011	7.55E-010	2.70E-011

Table B.46: Decay heat of PbLi, with and without impurities, in the cooling channel (31) and in the tank (40)

Time [years]	**PbLi with imp., 31 Decay heat [kW/kg]**	**PbLi no imp., 31 Decay heat [kW/kg]**	**PbLi with imp., 40 Decay heat [kW/kg]**	**PbLi no imp., 40 Decay heat [kW/kg]**
0.00E+000	3.26E-002	3.23E-002	1.44E-003	1.45E-003
3.17E-008	1.38E-002	1.35E-002	6.13E-004	6.09E-004
9.51E-007	4.99E-006	4.93E-006	8.01E-007	7.69E-007
1.90E-006	7.24E-007	6.85E-007	2.41E-007	2.23E-007
9.51E-006	3.04E-007	3.02E-007	1.25E-007	1.24E-007
5.70E-005	8.54E-008	8.51E-008	4.73E-008	4.75E-008
6.84E-004	2.95E-008	2.95E-008	1.42E-008	1.42E-008
2.74E-003	2.02E-008	2.01E-008	7.63E-009	7.64E-009
1.92E-002	3.06E-009	3.14E-009	1.18E-009	1.16E-009
5.07E-001	6.40E-011	4.88E-011	5.46E-011	4.31E-011
9.97E-001	5.06E-011	4.34E-011	4.60E-011	4.05E-011
5.00E+000	3.39E-011	3.38E-011	3.21E-011	3.20E-011
5.00E+001	2.63E-012	2.63E-012	2.53E-012	2.56E-012
1.00E+002	1.67E-013	1.61E-013	1.57E-013	1.53E-013
2.00E+002	8.76E-015	2.57E-015	4.72E-015	1.24E-015
5.00E+002	6.01E-015	2.03E-015	2.92E-015	8.12E-016
1.50E+003	3.29E-015	2.03E-015	1.41E-015	8.12E-016